DATGAN: Integrating expert knowledge into deep learning for synthetic tabular data

Gael Lederrey
Transport and Mobility Laboratory,
École Polytechnique Fédérale de Lausanne,
Lausanne, Switzerland
gael.lederrey@epfl.ch

Tim Hillel
Transport and Mobility Laboratory,
École Polytechnique Fédérale de Lausanne,
Lausanne, Switzerland
tim.hillel@epfl.ch

Michel Bierlaire
Transport and Mobility Laboratory,
École Polytechnique Fédérale de Lausanne,
Lausanne, Switzerland
michel.bierlaire@epfl.ch

ABSTRACT

Synthetic data can be used in various applications, such as correcting bias datasets or replacing scarce original data for simulation purposes. Generative Adversarial Networks (GANs) are considered state-of-the-art for developing generative models. However, these deep learning models are data-driven, and it is, thus, difficult to control the generation process. It can, therefore, lead to the following issues: lack of representativity in the generated data, the introduction of bias, and the possibility of overfitting the sample's noise. This article presents the Directed Acyclic Tabular GAN (DATGAN) to address these limitations by integrating expert knowledge in deep learning models for synthetic tabular data generation. This approach allows the interactions between variables to be specified explicitly using a Directed Acyclic Graph (DAG). The DAG is then converted to a network of modified Long Short-Term Memory (LSTM) cells to accept multiple inputs. Multiple DATGAN versions are systematically tested on multiple assessment metrics. We show that the best versions of the DATGAN outperform state-of-the-art generative models on multiple case studies. Finally, we show how the DAG can create hypothetical synthetic datasets.

Keywords Tabular Data Synthesis · Generative Adversarial Networks · Expert Knowledge

Contents

1 Introduction

A massive increase in data availability has created tremendous opportunities for targeted modeling and a greater understanding of systems, particularly those involving human behavior. However, reliance on data creates a division based on data. For example, leading international cities in developed nations produce rich data about population movements and interactions with infrastructures. On the other hand, undeveloped nations have much lower data availability. The collection of such data, particularly socio-economic, can be prohibitively expensive. It can, thus, prevent non-data-rich areas from modeling. Furthermore, data can be controlled by certain groups (companies, government, or public agencies), who may be unwilling or unable to make full data publicly available. In addition, the sharing of detailed disaggregated socio-economic data has become increasingly complex with the current focus on data privacy (GDPR). Thus, synthetic data generation, *i.e.* the creation of synthetic data samples which are consistent with the true population, has the opportunity to address many of these limitations.

There are multiple use cases for synthetic tabular data: (i) The most common use-case is dataset augmentation. It can allow researchers and modelers to approximate a large population from a smaller sample, thus reducing the cost of data collection. (ii) Secondly, synthetic data can be used for privacy preservation. It can, then, enable the sharing of detailed disaggregate populations without contravening GDPR and other data privacy laws. (iii) Another use case is bias correction. Synthetic data can correct bias in existing samples, allowing for reliable modeling of marginal and minority groups and behavior. (iv) Finally, synthetic data generation models can be used as transfer learning methods. They can thus be used to transfer data from one city or context to a new context, allowing for detailed modeling where existing high-quality data is not available. In this paper, we focus mainly on synthetic population generation. Such populations are generally used for simulation in agent-based models, particularly for activity-based transport models. However, the techniques proposed and reviewed in this article can be used in any context where there is a need for detailed tabular datasets.

Many methods have been developed to generate such synthetic populations in existing studies. The two main approaches are statistical techniques such as Iterative Proportional Fitting (IPF) (Deming and Stephan, 1940) or simulation using Gibbs sampling (Geman and Geman, 1984), and machine learning techniques. While the first approaches have been well studied within the transportation community, the latter comes from the Machine Learning community and generally focuses on general synthetic data. These deep learning methods, such as Generative Adversarial Networks (GANs) (Goodfellow et al., 2014), have already been tested against standard statistical techniques and outperform them while generating correlations in synthetic datasets. However, these methods are data-driven. They, therefore, lack control over the generation process. Without controlling the latter, it is impossible to know how well the deep learning models have understood the original sample, *i.e.* which correlations between the variables in the original dataset the models have learned. It can, thus, lead to spurious correlations or propagation of existing bias in the sample. In addition, there is generally no focus on the representativity of the output, which is crucial for the accurate understanding of socio-economic characteristics.

This article, thus, proposes a novel model that controls the generation process of such synthetic tabular data. We propose to let the researcher or modeler design a network to represent the interactions between the variables with a Directed Acyclic Graph (DAG). This DAG is then used to model the structure of the model that will generate such a population. Allowing researchers to control the process has three main advantages: they can tinker with the data generation process, create hypothetical datasets, and control the dependencies for forecasting. In this article, we thus present our new GAN model named Directed Acyclic Table GAN (DATGAN). We show that it outperforms state-of-the-art synthetic data generators on multiple metrics. These metrics have been created to allow for systematic testing both using formal statistical analysis and supervised learning-based approaches. We also provide a sensitivity analysis on the DAG to show its effect on the data generation process. Finally, we show how the DAG can create hypothetical situations and generate a synthetic dataset based on the new rules.

The rest of this article is laid as follows. In the next section, we present the Literature Review. We first introduce the existing approaches for population synthesis and then discuss the different research axes. Finally, we conclude the literature review with the opportunities and limitations of existing research. In Section 3, we present the whole methodology for the DATGAN. We discuss how to preprocess the data, what models are used for the generator and the discriminator, and how to use the DAG to create the generator's structure using LSTM cells. Section 4 presents the case studies and Section 5 shows the results. We conclude this article in Section 6 and give ideas for future work. In addition to this article, we provide supplementary materials containing a notation table for the methodology, a comparison of multiple DATGAN versions, and all the detailed results used in Section 5.

2 Literature Review

There are five main research axes for synthetic tabular data generation: simulation/activity-based modeling, Machine Learning efficacy, bias correction, privacy preservation, and transfer learning. These research axes are discussed in detail in Section 2.2. The literature review first focuses on population synthesis with older methods such as Iterative Proportional Fitting (IPF) and Gibbs sampling. Then, we look at more general Machine Learning techniques for synthetic tabular data generation. These techniques are discussed in detail in Section 2.1. Then, in Section 2.3, we discuss in more detail some state-of-the-art models that we selected to compare to the model presented in this article. Next, Section 2.4 is dedicated to model evaluation and shows how the transportation and Machine Learning communities are evaluating generated synthetic datasets. Finally, in Section 2.5, we discuss the opportunities and limitations of these techniques linked to the five research axes.

2.1 Existing approaches for synthetic tabular data generation

One of the primary uses of synthetic tabular data has been for the creation of synthetic populations, in particular for transportation research. As a result, many research contributions focus specifically on this topic, using different techniques. Therefore, we focus this review first on synthetic population generation and then introduce more general-purpose Machine Learning algorithms that have been proposed in the literature, which could also be applied for this purpose.

We can identify two main categories of techniques for synthetic tabular data generation: Statistical techniques such as resampling methods and simulation-based methods (see Section 2.1.1), and Machine Learning methods (see Section 2.1.2). In the following sections, we discuss these different methods in detail. Table 1 gives a summary of the main methods in each category with a list of references, advantages, and disadvantages.

2.1.1 Statistical techniques

There are two main methods to generate synthetic populations within the transportation community: resampling and simulation-based approaches. The first one is based on Iterative Proportional Fitting methods (IPF) (Deming and Stephan, 1940). It consists of proportionally adjusting a matrix to produce a new table such that the specified marginals are individually conserved. Beckman et al. (1996), first, use this methodology to create a synthetic population based on the SF3 (San Francisco area) census data. Auld et al. (2009) and Barthelemy and Toint (2013) both propose to improve the IPF methodology using a multi-step procedures. While IPF methods are simple to implement, this technique has multiple significant limitations in generating highly detailed and realistic synthetic tabular data. Firstly, there is no interaction between the variables with the basic algorithm. It is possible to add these interactions by adding more dimensions to the table. However, for each level of interaction, one more dimension has to be added to the table. It, thus, quickly becomes a computationally expensive algorithm. In addition, IPF cannot differentiate between structural and sampling zeros. Multiple methods have been suggested to avoid sampling zero issues in the literature, such as Auld et al. (2009). Finally, IPF cannot differentiate between the different data types (categorical and continuous). Thus, researchers have developed new techniques to generate synthetic populations, such as Markov Chain Monte Carlo (MCMC) simulation.

Farooq et al. (2013) proposes to use a Markov Chain Monte Carlo (MCMC) simulation using Gibbs sampling to generate synthetic populations. The idea is to draw from an (unknown) multi-dimensional random variable characterizing the distribution of individuals in the population using a Gibbs sampler. The marginal distributions used by the Gibbs sampler are generated from real data. Since the full-conditionals are rarely available for all the attributes in the original data, the authors use a parametric model to construct the missing conditional distributions. The authors show that this simulation technique outperforms IPF methods using multiple statistical metrics such as R^2 and Standardized Root Mean Squared Error (SRMSE) (Müller and Axhausen, 2010). Multiple improvements have been made on the original method (Casati et al., 2015; Kim and Lee, 2016; Philips et al., 2017). However, while simulation-based techniques outperform IPF techniques, these methods still have limitations in the context of synthetic population generation. The main issue is that the models are working with conditionals only. This can be an advantage if only this information is available. However, since MCMC methods must assume the type of probability distributions that the variables follow, wrong assumptions can lead to fundamentally incorrect distributions.

While these statistical methods have been widely used in the transportation community, they are outdated compared to Machine Learning techniques. For example, Borysov et al. (2019) show that their Machine Learning-based approaches outperform MCMC-based approaches on multiple criteria. Therefore, in this article, we concentrate on testing our methodology against state-of-the-art Machine Learning methods.

Table 1: Main methods for synthetic tabular data generation found in the transportation literature and in the Machine Learning community.

Categories	Methods	Description	References	Advantages	Disadvantages
Statistical techniques	IPF	Iterative method using marginals to create a synthetic table.	Auld et al. (2009); Barthelemy and Toint (2013); Rich (2018)	• Efficient in its basic form • Simple to implement	• No interactions between variables • Computationally expensive if more complexity added • Prone to sampling zero issue • No differences between data types
	Gibbs sampling	Gibbs sampler trained until reaching stationary state on prepared conditionals.	Farooq et al. (2013); Casati et al. (2015); Kim and Lee (2016)	• Learn from marginals • Outperforms IPF • Can be linked to other methods	• No interactions between variables • Computationally expensive • Probability distributions are an assumption
Machine Learning techniques	Bayesian networks	Probabilistic graphical model used to determine probabilistic inferences between the variables.	Sun and Erath (2015); Zhang et al. (2019)	• Dependencies of variables defined prior to training • Probabilistic model	• Requires prior information on the dataset • Computationally expensive when dealing with large and sparse datasets
	VAE	Pair of neural networks composed of an encoder and a decoder. Transforms data in a latent space to reduce its dimensionality. Encoding-decoding scheme has to be learned.	Garrido et al. (2019); Xu et al. (2019)	• Aims at learning a latent representation of the variables • Latent space is suitable for inference and completion of data	• Might not be able to learn the true posterior distribution • Usually outperformed by GANs
	GAN	Pair of neural networks composed of a generator and a discriminator. The generator is trained to fool the discriminator. Learning process is a two players minimax game.	Goodfellow et al. (2014); Xu and Veeramachaneni (2018); Xu et al. (2019); Zhao et al. (2021)	• Generator never sees true data (privacy ensured) • Architectures of both neural networks are flexible • Current state-of-the-art generative model	• Equilibrium between both neural networks difficult to achieve • Dependencies of variables cannot be controlled

2.1.2 Machine Learning techniques

Recent advances in Machine Learning and data generation techniques have enabled new approaches for generating synthetic populations. We identify three primary Machine Learning-based approaches that have been used for this purpose: Bayesian networks, Variational AutoEncoder (VAE), and Generative Adversarial Networks (GANs).

(2021) use Bayesian networks to generate such populations. Bayesian networks are graphical models used to encode probability distributions for a set of variables. They use a Directed Acyclic Graph (DAG) to represent the dependencies between the variables and a set of local probability distributions for each variable in the original table and given conditional probabilities. The authors show that their model outperforms both IPF and Gibbs sampling. Zhang et al. (2019) extended this concept further by using a three-step procedure to generate a population and its social network. They use a Bayesian network to create a synthetic population of households, an integer problem with Langrangian relaxation for the assignment problem, and an Exponential Random Graph Model (ERGM) for the social network simulation.

Variational AutoEncoders (VAEs) (Kingma and Welling, 2014) aim to reduce the dimensionality of the data into an encoded vector in the latent space. Data can then be generated more easily in this latent space since it is smaller in dimensionality. For example, Borysov et al. (2019) have used a VAE to generate a synthetic population. They demonstrated that their VAE model outperforms both IPF and Gibbs sampling for generating complex data. However, this type of method has quickly been outperformed by the current state-of-the-art method for generating synthetic data: Generative Adversarial Networks (GANs).

Generative Adversarial Networks (GANs) (Goodfellow et al., 2014) make use of two neural networks, the *generator* and the *discriminator*, which compete against each other on independent, unsupervised tasks. The generator processes random noise to produce synthetic data. The discriminator (or critic) then evaluates the synthetic data against original data to provide a classification or continuous score on each data point on whether the data is original or synthetic. The generator is then trained through backpropagation. Figure 1 shows the schematic representation of a GAN.
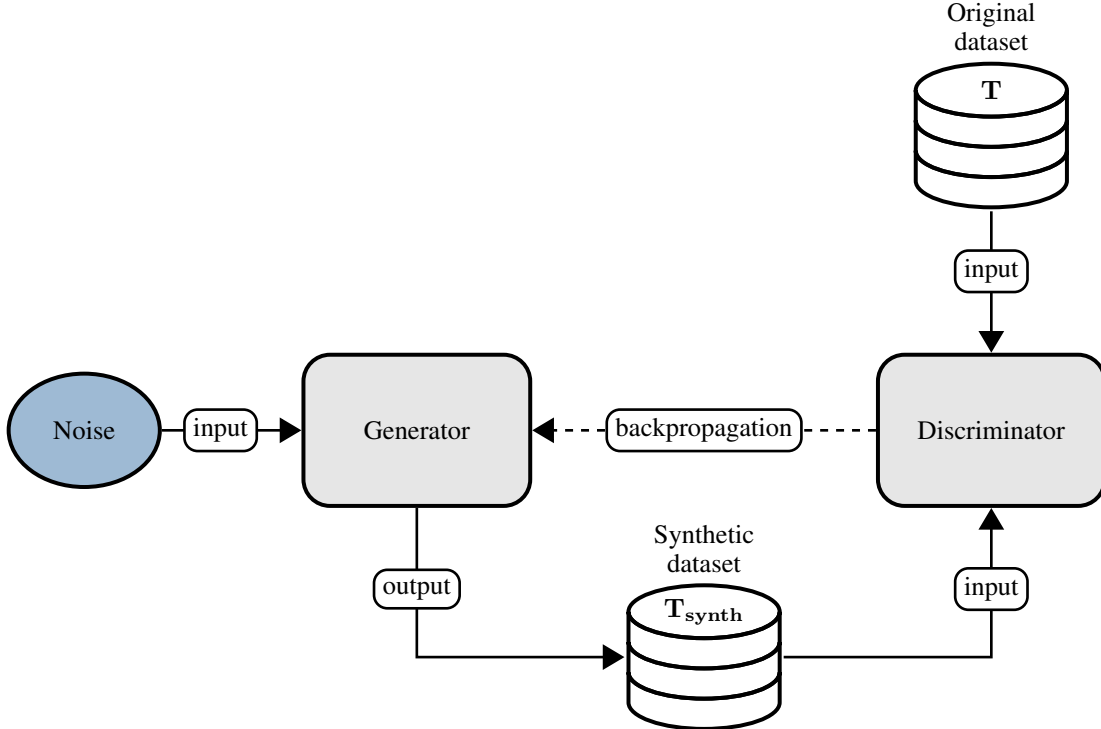
Figure 1: Schematic representation of the standard GAN structure.

GANs have quickly evolved to become more specialized. For example, Arjovsky et al. (2017) demonstrate that the use of a discrete loss function results in issues such as vanishing gradients. They thus propose an alternative continuous loss function based on the Wasserstein distance. This GAN is therefore named Wasserstein GAN (WGAN). Further key developments in GAN research include the introduction of a penalty on the gradient during model training (Gulrajani

et al., 2017) or the addition of conditionality (Mirza and Osindero, 2014). While the primary application of GANs has been the generation of image data, with a particular focus on human faces (Alqahtani et al., 2021), researchers have also developed specific architectures for tabular data. It, thus, allowed researchers to switch their focus to more general synthetic tabular data generation rather than synthetic population generation.

TableGAN (Park et al., 2018) and TGAN (Xu and Veeramachaneni, 2018) are two specific GANs models for tabular data. TableGAN has been developed with privacy-preservation techniques in mind. This model is based on Deep Convolutional GAN (DCGAN) (Radford et al., 2016). On the other hand, TGAN has been developed to reproduce tabular data as realistically as possible using Long Short Term Memory (LSTM) cells for the generator (Hochreiter and Schmidhuber, 1997). The authors demonstrated that TGAN outperforms tableGAN. Researchers have also developed their own GAN structures to generate synthetic populations in the transportation community. For example, Garrido et al. (2019) develop their own GAN structure based on the WGAN to use tabular data. They show that this new model was statistically better than IPF techniques, Gibbs sampling, and the VAE of Borysov et al. (2019). Finally, Badu-Marfo et al. (2020) created a new GAN named Composite Travel GAN (CTGAN). Their GAN is based on the Coupled GAN (CoGAN) (Liu and Tuzel, 2016) and is used to generate the table of attributes for the population and the sequence of Origin-Destination segments. They show that the CTGAN outperforms the VAE statistically. While these models are showing outstanding performances compared to previous methods, the switch to data-driven methods has hindered the control of the researchers or modelers on the generation process. The lack of control during this process can hinder the final results depending on the research axis. Thus, in the next section, we discuss multiple axes found in the literature, some requiring high control on the generated synthetic data.

2.2 Research axes

The primary focus of existing population synthesis in the transportation domain has been for direct use in simulation models. On the other hand, the deep learning community motivates their research by stating that using more data improves the efficacy of Machine Learning models. For example, Jha et al. (2019) show that a larger and more complete dataset leads to better validation and fewer uncertainties. Other examples discussing the dataset size can be found in the literature (Barbedo, 2018; Linjordet and Balog, 2019). However, this does not represent the only research axis for synthetic tabular data generation. In the remainder of this section, we present and discuss five different research axes for synthetic generation in the literature.

2.2.1 Simulation and agent-based modeling

Agent-based models (Bonabeau, 2002) are used to simulate the actions and interactions of autonomous agents in order to understand the behavior of a system. These models are extensively used in the transportation community (Kagho et al., 2020) and require a large amount of data to be adequately trained. Synthetic data are, thus, often used to replace scarce and expensive original data.

In the transportation community, the predominant focus for the population synthesis papers introduced in Section 2.1 is for direct use in simulation. For example, Beckman et al. (1996), Barthelemy and Toint (2013), Farooq et al. (2013), Borysov et al. (2019), and Garrido et al. (2019) all motivate their work by discussing the generation of synthetic population for (agent-based) simulation models.

2.2.2 Privacy preservation

Privacy preservation techniques ensure that any private information is not disclosed using data or Machine Learning models. Synthetic data can, thus, replace highly sensitive original data when privacy is of concern. Methods using only the conditionals, such as IPF or Gibbs sampling, are especially effective since the methods never use the original data to generate the synthetic data.

For example, Barthelemy and Toint (2013) motivate their model (a three-step procedure based on simulation techniques) to improve the privacy preservation of the standard IPF methods. They state that the standard method tends to repeat observations, and thus it is possible to retrieve information from the original dataset. More recently, the tableGAN (Park et al., 2018) has been specifically designed to preserve the original datasets' privacy. Multiple GAN models have been created in computer vision, with privacy preservation as the core motivation. For example, Liu et al. (2019) created the Privacy-Preserving GAN (PPGAN). This GAN uses differential privacy by adding specifically designed noise to the gradient during the learning procedure. Yin and Yang (2018), on the other hand, directly generated protected data within the generator of their GAN by removing some sensible information and encoding them in the generated data. They tested their synthetic data against attack models to show that their GAN could generate more complex data to be deciphered. More recently, Zhao et al. (2021) motivate and test their model on privacy preservation.

2.2.3 Machine Learning efficacy

The generation of synthetic populations also enables the augmentation of existing real-world datasets with synthetic individuals, therefore increasing the size and variability of the dataset. Several studies have investigated the estimation of Machine Learning techniques on augmented or fully synthetic data. This concept is already widely used on images (Shorten and Khoshgoftaar, 2019). While simple techniques such as rotating or scaling images can be used in Computer Vision, applying such simple tricks on tabular data is impossible. Thus, researchers have been developing models aiming at augmenting tabular data.

For example, Xu and Veeramachaneni (2018) motivate the development of the TGAN because organizations are using Machine Learning on relational tabular data to augment process workflows carried out by humans. Furthermore, they state that these synthetic datasets can either be used as an augmentation for the existing datasets or as a means to preserve privacy, which is discussed in Section 2.2.2. On the other hand, Xu et al. (2019) do not give a clear motivation on the usage of synthetic datasets. However, they test their models on Machine Learning efficacy by replacing the training data with the generated synthetic data. More recently, both Wen et al. (2021) and Zhao et al. (2021) motivate their models using Machine Learning efficacy as the core method to assess their generated synthetic datasets.

2.2.4 Bias correction

Synthetic data can also be applied to correct bias in existing datasets by controlling the data generation process. It builds on standard resampling methods (Rubin, 1973) to rebalance the dataset, which reduces the signal-to-noise ratio of the existing data (by removing oversampled data or resampling undersampled data). Indeed, data generation techniques can also be used to augment an existing dataset and rebalance it.

For example, Conditional GANs (Mirza and Osindero, 2014) have been created to tackle such imbalance issues. The idea of such GANs is to generate synthetic data using prior information. They, thus, increase the probability of generating synthetic data with the given information. Xu et al. (2019) have adapted this methodology to tabular data with the Conditional Table GAN (CTGAN). They show that the conditionality is truly efficient for Machine Learning models when the data is highly imbalanced. They create synthetic datasets addressing the imbalance and trained Machine Learning models on this synthetic and the original dataset. The models trained on the synthetic datasets perform better than those trained on the original dataset. Previously, Farooq et al. (2013) motivate their research on population synthesis with Gibbs sampling using the fact that it can complete datasets. However, the authors have not formally evaluated this use of synthetic data.

2.2.5 Transfer learning

The use of Conditional GANs, and other conditional data generation approaches, enables the possibility for transfer learning, where knowledge from one context with large data availability can be transferred to another context with lower data availability.

For example, Noguchi and Harada (2019) propose a new method using the BigGAN to transfer the knowledge learned on large datasets and apply this knowledge to a dataset with only 25 images. They show that they can add a new class to a pre-trained generator without disturbing the performance of the original domain. Wang et al. (2020) propose to use a miner network that identifies which distribution of multiple pre-trained GANs is the most beneficial for a specific target. This mining pushed the sampling towards more suitable regions in the latent space. Therefore, the MineGAN can transfer the knowledge of multiple GANs such as the BigGAN and the Progressive GAN to a domain with fewer images. Other relevant methods for transfer knowledge can be found in the articles of Jeon et al. (2020) and Frégier and Gouray (2020).

While this research axis has already been explored in the computer vision community, it has not been explored in population synthesis. Indeed, while the transfer of knowledge between two tabular datasets might not make sense, it could be used for tabular data of populations. For example, census data are often collected regularly, *e.g.* every two of five years. We could, thus, imagine using GANs trained on data from previous years to transfer their knowledge to the most recent years.

2.3 State-of-the-art models

We present a detailed overview of four different approaches demonstrated to achieve the best performance when generating synthetic tabular data. As such, these approaches represent the state-of-the-art in this field. The four approaches, which all make use of deep learning algorithms, are introduced across three key articles: Xu and Veeramachaneni (2018), Xu et al. (2019), and Zhao et al. (2021). A summary of the models is given in Table 2.

Table 2: Summary of the state-of-the-art models selected for comparison with the DATGAN.

Model	Article	Information
TGAN	Xu and Veera-machaneni (2018)	• *Generator:* LSTM cells in linear arrangement • *Discriminator:* Fully-connected neural network • *Data preprocessing:* Continuous vs categorical • *Loss function:* Cross-entropy loss • *Conditionality:* None
CTGAN	Xu et al. (2019)	• *Generator:* Fully-connected neural network • *Discriminator:* Fully connected neural network • *Data preprocessing:* Continuous vs categorical • *Loss function:* Wasserstein loss with gradient-penalty • *Conditionality:* On categorical variables
TVAE	Xu et al. (2019)	• *Encoder:* Updated structure for preprocessed data • *Decoder:* Similar to conventional VAE • *Data preprocessing:* Continuous vs categorical • *Loss function:* Evidence lower-bound (ELBO) loss • *Conditionality:* None
CTAB-GAN	Zhao et al. (2021)	• *Generator:* Convolutional neural network • *Discriminator:* Convolutional neural network • *Classifier:* Multi-layer perceptron • *Data preprocessing:* Continuous vs categorical vs mixed • *Loss function:* Cross-entropy, information and classification losses • *Conditionality:* On categorical variables

While some GANs have been developed for privacy preservation, TGAN (Xu and Veeramachaneni, 2018) focuses on learning the marginal distributions using recurrent neural networks. Since our focus is on creating representative synthetic data, we thus selected TGAN as the first model to be compared. It uses Long Short-Term Memory (LSTM) cells (Hochreiter and Schmidhuber, 1997) to generate each variable in the table. The LSTM cells are arranged linearly following the order of the variables in the dataset. The authors make the difference between categorical and continuous variables. Both variable types are encoded differently: (i) continuous variables are encoded using Gaussian mixtures; (ii) categorical variables are one-hot encoded. Finally, the TGAN is trained using the standard minimax loss function (Goodfellow et al., 2014), and it is compared to other data synthesizers such as Gaussian Copula and Bayesian Networks. The authors show that TGAN outperforms all these methods.

CTGAN (Xu et al., 2019) uses a fully-connected neural network for both the generator and the critic. Like TGAN, the variables are differentiated between categorical and continuous variables. CTGAN uses the same encoding procedure for both variable types with a slight difference for continuous variables: a Variational Gaussian Mixture (VGM) is used instead of standard Gaussian mixtures. In addition, this model uses conditionality by adding a conditional vector on categorical variables. Finally, CTGAN is trained using the Wasserstein loss with gradient-penalty (Gulrajani et al., 2017).

The Tabular VAE (TVAE) (Xu et al., 2019) is an adaptation of a standard Variational AutoEncoder (VAE) by modifying the loss function and preprocessing the data. The variables are encoded using the same procedure as in CTGAN. TVAE uses the evidence lower-bounder (ELBO) loss (Kingma and Welling, 2014). While the encoder is slightly updated compared to conventional VAEs, the decoder keeps a usual structure. The authors have compared TVAE, CTGAN, and other methods for synthesizing tabular data such as tableGAN. They show that both TVAE and CTGAN outperform other methods. On multiple metrics, TVAE performs better than CTGAN. However, as stated by the authors, CTGAN achieves differential privacy (Jordon et al., 2018) easier than TVAE since the generator never sees the original data.

Finally, the particularity of CTAB-GAN (Zhao et al., 2021) compared to the previous models is that it aims at fixing issues with skewed continuous distributions. Indeed, continuous distributions can take many forms, such as long-tailed, exponential, or mixed distributions. Therefore, this model implements multiple data preprocessing methods for different

distributions. CTAB-GAN comprises three neural networks: a generator, a discriminator, and an additional classifier. The latter is used to learn the semantic integrity of the original data and predict the synthetic data classes. This helps produce more accurate labeled synthetic data. The generator and discriminator are convolutional neural networks, while the classifier is a multi-layer perceptron. In addition, CTAB-GAN uses conditionality to counter the imbalance in the training dataset to improve the learning process. Finally, CTAB-GAN is trained using the standard cross-entropy loss function with the addition of an information loss and a classification loss. The authors have tested their model against other state-of-the-art models such as tableGAN and CTGAN. They have shown that their model outperforms all the other models using Machine Learning efficacy and statistical similarity metrics.

2.4 Model evaluation

Model evaluation is intrinsically linked to the research axis for which a model was developed. Indeed, a generator developed to correct bias should not be tested on the same characteristics as a model developed for privacy preservation. Thus, researchers have come up with different methods for assessing generated synthetic datasets. In this section, we discuss two types of methods that are primarily used to assess the representativity of a synthetic dataset compared to its original counterpart: statistical methods (in Section 2.4.1) and Machine Learning methods (in Section 2.4.2).

2.4.1 Statistical assessments

Multiple statistical tests can be used to compare two distributions, such as the Ξ^2 test or the Student's t-test. While these tests can provide good information when comparing the distributions of each variable separately, it does not consider the correlation between the variables. Since this aspect is essential for creating representative synthetic populations, researchers in the transportation community have been developing new statistical tests to address this issue. The Standardized Root Mean Squared Error (SRMSE) (Müller and Axhausen, 2010) is used in most transportation articles working on population synthesis to assess the generated datasets. The test consists in selecting one or multiple variables in a dataset and creating a frequency list based on the appearance of each unique value. We can, then, apply the SRMSE (see Equation 41) formulation on this frequency list. While this technique has been shown to work well compared to other statistical methods, it has two main flaws: (i) the frequency lists are computed by counting the unique values (or combinations of unique values). Therefore, it is preferably used on discrete values. (ii) The choice of variables (or combination of variables) is up to the researcher or modeler. Thus, articles using this methodology tend only to test a couple of combinations. In order to address the first flaws, we can transform the continuous values into discrete values by assigning them to specific buckets. This is a relatively simple fix, but if the discretization is done correctly, SRMSE should still provide valid results. However, the second flaw is more problematic. Indeed, when generating a synthetic dataset, we want to make sure that all the correlations are correctly generated. Therefore, it is required to update the methodology of the SRMSE to do systematic testing on all the variables and their possible combinations.

2.4.2 Machine Learning techniques

In Machine Learning, many datasets are considered classification datasets. Thus, they are used with a Machine Learning model to predict future instances of a unique variable. Therefore, researchers developing generators to improve the efficacy of such models usually only test the synthetic datasets using the predictive power of Machine Learning models on a single variable. While this technique works well in this specific case, it does not provide enough information if one is trying to assess the representativity of a synthetic dataset compared to an original one. Indeed, there might be missing correlations between the other variables in the dataset that the Machine Learning models will overlook. It is, thus, possible to update this technique such that a Machine Learning model is used to predict each variable in the dataset instead of a single one. If there are issues with correlations between the variables, the efficacy of the Machine Learning models will drop while predicting the other variables, thus providing more information.

2.5 Opportunities and limitations

The role of the generator in a GAN is to produce batches of synthetic data, taking only noise as an input. As such, the structure of the generator network should be closely matched to the underlying structure of the data being replicated. For instance, in images, each variable represents a pixel whose meaning is image-specific and only defined relative to other pixels in the image. In other words, the meaning of a pixel in an image is dependent on its relative position and value, not its absolute position and value, and the meaning of a single pixel in one image is (largely) independent from the meaning of the corresponding pixel in another image in the same dataset. It is therefore typical for generators used in image generation to make use of convolutional neural networks (Radford et al., 2016; Isola et al., 2017; Zhu et al., 2018), which model the relative definitions of the pixel values learned over thousands or millions of images in a dataset.

Unlike images, the variables in tabular data typically have a specific meaning and can be understood by their absolute positions and values (within a single dataset). For example, a column representing an individual's age in socio-economic data defines the age of every instance (row) in the table. Furthermore, the age value of each row can be understood without needing to know the values of the other variables. While the variables in a dataset have a fixed position-specific meaning, their values are dependent on the other variables in the dataset. As such, the generator must capture the interdependencies between these variables.

There are several different approaches to this in the literature. The first approach mimics what is done with images. Indeed, several models are built using fully connected networks (Xu et al., 2019) or convolutional neural networks (Park et al., 2018; Zhao et al., 2021). The generator has to learn the structure from the data during the learning process using backpropagation. This can be rather cumbersome for the generator since it never has access to the original data. Therefore, another approach is to fix the structure of the data. For example, the TGAN (Xu and Veeramachaneni, 2018) uses a sequential order based on the columns' order. The structure is implicitly learned using attention vectors used with each variable in the dataset.

In both approaches, the generator learns the relationships between the variables from the available data via backpropagation of the discriminator loss. However, there are two primary limitations of this approach. Firstly, the generator, which needs to be highly flexible, can overfit the noise in the data and generalize to relationships between the columns which do not actually exist in unseen data. Secondly, the generator has to use the limited signal in the data to learn the core structure of the data, which is often already known to some degree by the modeler. Both can cause issues when the signal-to-noise ratio is high, as is often the case with socio-economic datasets of limited size.

Therefore, there is an opportunity to develop techniques that address these flaws and use the learning power of GANs. Indeed, by defining the relationships between the variables beforehand using expert knowledge, we can force the generator only to learn specific correlations. In addition, if the researcher or modeler provides these relationships, the model starts its learning process with more information than a fully connected network that has to learn all these connections. Therefore, we can overcome the issues with GANs while keeping their strengths.

3 Methodology

Following several previous works in the literature, our approach for synthetic tabular data generation makes use of a GAN (Goodfellow et al., 2014) to generate synthetic data. Our primary contribution is to closely match the generator structure to the underlying structure of the data through a Directed Acyclic Graph (DAG) specified by the modeler. According to their prior expert knowledge of the data structure, the DAG allows the modeler to define the structure of the correlations between variables in the dataset as a series of directed links between nodes in a graph. Each link in the DAG represents a causal link that the generator can capture, and if no links (either direct or indirect) exist between two variables, then the generator treats those variables independently. This has two primary advantages over the existing approaches within the context of the limitations identified in the literature review. Firstly, by restricting the set of permissible links between the variables in the datasets, the DAG represents an expert regularisation of the model and restricts the ability of the GAN to overfit noise in the training sample. Secondly, giving the generator a headstart in knowing the underlying structure of the data allows the GAN to make more efficient use of the training sample when learning to generate data. These benefits could enable the DATGAN to use limited available original data more efficiently when learning to produce realistic and representative synthetic data samples.

Figure 2 provides a high-level overview of the DATGAN data generation process. As is typical with GANs, the generator in the DATGAN (described in Section 3.1) never sees the original data. It generates data purely from a random noise input. The generator's structure is determined according to a DAG which specifies the structural relationships between the variables in the data (*i.e.* the expert knowledge), as defined by the modeler. We present the DAG in Section 3.1.1 and the process to automatically create the generator structure from the DAG in Section 3.1.2. At the same time, the discriminator (described in Section 3.2) is trained to classify/critique the original and synthetic data. Therefore, it can be considered a competitive game between two adversaries (the generator and the discriminator). The loss functions used to optimize both models are presented in Section 3.3. Since tabular data can contain attributes of different types (*e.g.* continuous, nominal, and ordinal), original and synthetic data have to be processed before being used. We, thus, introduce several new data processing steps specific to the DATAGAN model in Section 3.4. At the end of this section, we present the result assessments methods used to compare the synthetic datasets in Section 3.5. We conclude the methodology by providing some implementation notes in Section 3.6. The supplementary materials include a notation table summarizing all the notations used in the methodology and a summary of the possible DATGAN versions using the different components presented here.

Formally, we consider a table $\mathbf{T}$ containing N_V columns. Each column in the table $\mathbf{T}$ is represented by $\boldsymbol{v}_t$ for $t = 1, \ldots, N_V$. We, thus, have $\mathbf{T} = \{\boldsymbol{v}_{1:N_V}\}$. These columns have been drawn from an unknown joint distribution
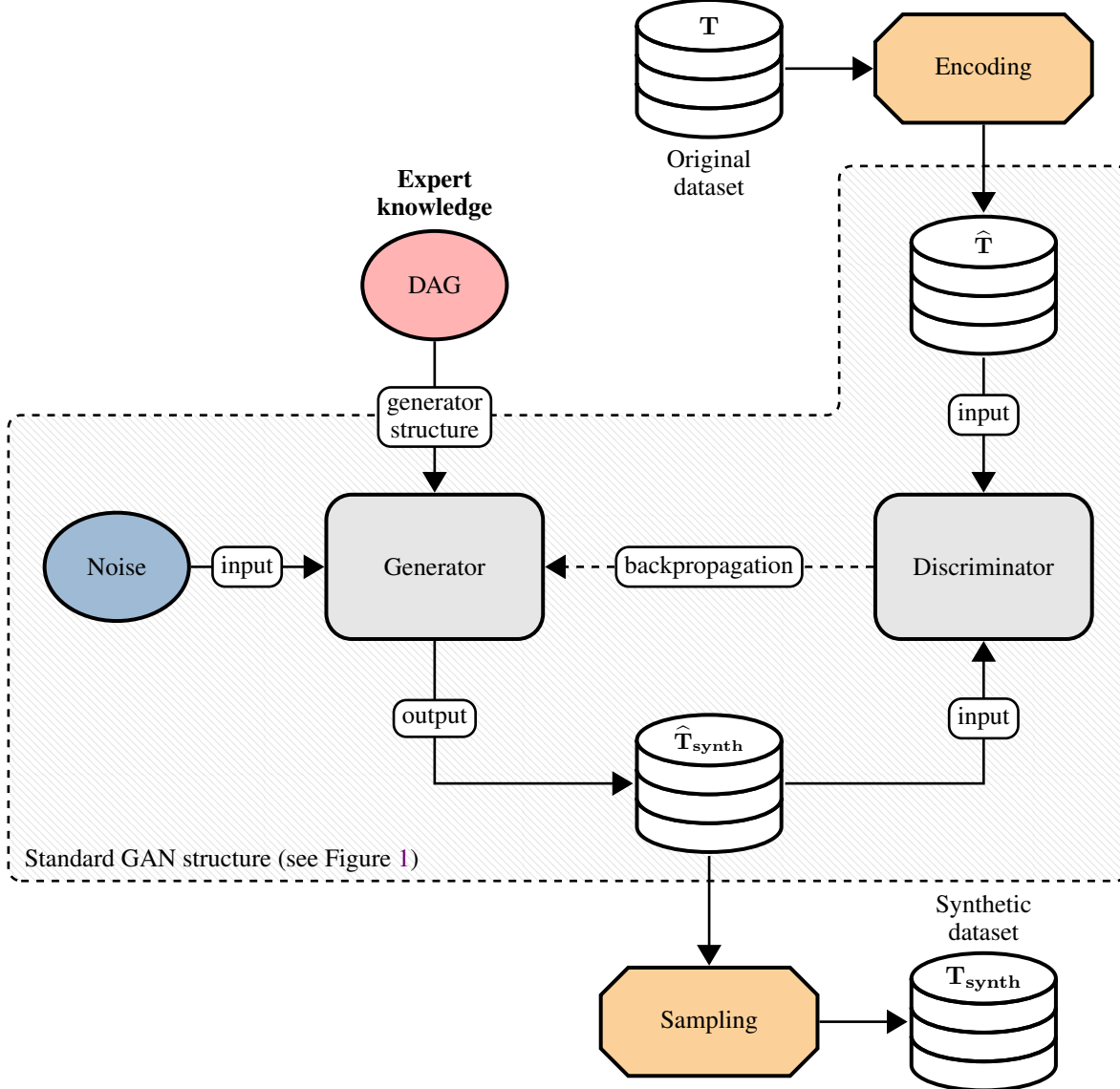
Figure 2: Global schematic representation of the DATGAN. The different element in this figure are presented in the following sections: the Generator is presented in Section 3.1, the DAG in Section 3.1.1, the Discriminator in Section 3.2, the Encoding in Section 3.4.1, and the Sampling in Section 3.4.4.

of random variables V_t, *i.e.* the values in $\mathbf{T}$ are drawn from $\mathbb{P}\left(V_{1:N_V}\right)$. We, thus, usally refer to the variables in $\mathbf{T}$ using V_t. We represent the rows of $\mathbf{T}$ by $\{v_{1:N_V,i}\}$ for $i = 1, \ldots, N_{\text{rows}}$ where N_{rows} corresponds to the number of rows in $\mathbf{T}$. We assume that each row of $\mathbf{T}$ is sampled independently, *i.e.* it is cross-sectional and does not contain panel or sequential data. Our goal is to learn a generative model $G(\boldsymbol{z})$, where $\boldsymbol{z}$ is a tensor of random noise, such that the samples generated from G create a synthetic table $\mathbf{T}_{\text{synth}}$. For neural networks, we work in standardized space consisting of values between -1 and 1. We, thus, denote processed datasets with the character $\widehat{\cdot}$, as shown in Figure 2. In the meantime, the discriminator D is trained to differentiate between original data $\widehat{\mathbf{T}}$ and synthetic data $\widehat{\mathbf{T}}_{\text{synth}}$.

3.1 Generator

The role of the generator is to produce batches of synthetic data, taking only noise as an input. Within DATGAN, the generator structure is defined using a Directed Acyclic Graph (DAG), which specifies the interdependencies between each variable V_t in the original dataset $\mathbf{T}$. We first present the DAG, including how the modeler should construct it, in Section 3.1.1. We then demonstrate how the DAG is used to automatically create the generator network in Section 3.1.2,

through the use of Long Short Term Memory (LSTM) cells (Gers et al., 2000). This includes defining a new multi-input LSTM cell required to capture complex correlations specified in the DAG.

3.1.1 Directed Acyclic Graph (DAG)

The DAG $\mathcal{G}$ is specified by the modeler to define the correlations between the variables in the data. However, similarly to Bayesian networks, a DAG must represent causal links between variables. Indeed, correlations do not have a direction, while causal links do. The main reason to use a directed graph instead of an undirected one is due to the nature of the representation of the variables in the Generator. As explained in Section 3.1.2, each variable v_t in $\mathbf{T}$ is represented by a single LSTM cell. These cells communicate with each other in a directed manner, *i.e.* the previous cell sends information to the next one. Therefore, to better reflect this behavior, a directed graph is required.

The mathematical definition of a directed acyclic graph is given by:

- The graph $\mathcal{G}$ must be directed, *i.e.* each edge in the graph has only direction.
- The graph $\mathcal{G}$ must not contain any cycle, *i.e.* the starting vertex of any given path cannot be the same as the ending vertex.

These two properties ensure that the DAG is a topological sorting. It means that we can extract a linear ordering of the vertices such that for every directed edge $v_{t_1} \to v_{t_2}$ from vertex v_{t_1} to vertex v_{t_2}, v_{t_1} comes before v_{t_2} in the ordering.

With these rules in mind, the modeler can define the DAG for the DATGAN. It is possible to get inspiration from Bayesian networks and how their respective DAG is created manually (Lucas et al., 2004). However, there are some slight differences between the two DAGs. Therefore, we provide some insights about the components of our DAG:

- Each variable v_t in the table $\mathbf{T}$ must be associated to a node in the graph $\mathcal{G}$.
- A directed edge between two vertices, *i.e.* $v_{t_1} \to v_{t_2}$, means that the generation of the first variable v_{t_1} will influence the generation of the second variable v_{t_2}. Usually, the direction of the edge is a matter of judgement and should not influence the final result.
- The absence of a link between two variables means that their correlation is not *directly* learned by the Generator. However, it is possible to obtain some correlation in the final synthetic dataset if these two variables have a common ancestor in the graph $\mathcal{G}$. Therefore, two variables will not show any correlations in the synthetic dataset if they do not have any common ancestors or links between them in the DAG.
- The graph $\mathcal{G}$ can be composed of multiple DAGs as long as the first rule is respected. By creating multiple DAGs, the modeler ensures that the different parts of the dataset are not correlated. While this approach is not common, it could be used in a dataset containing variables about multiple unrelated topics.

As for Bayesian networks, there is no unique way to create a DAG for a given dataset. Using the example shown in Figure 3, we present different possibilities. The first one consists of following the variables' order in the datasets. This creates a simple ordered list of the variables. For example, the TGAN (Xu and Veeramachaneni, 2018) uses this specific list to link each of its LSTM cells. The advantage of such a DAG is its simplicity since no prior knowledge of the data is required. However, this DAG defines causal links based on an arbitrary order. It, thus, does not make use of expert knowledge and results in poorer results. Another possibility is to create a DAG centered around predicting a given variable. For example, in the case of Table 3a, one could want to predict the variable mode choice. Therefore, a possible structure for the DAG is to link all the other nodes in the table to a single sink node representing the variable that we want to predict. However, while this DAG would capture all possible correlations between each variable and the one that needs to be predicted, it will not capture other correlations. Therefore, a population generated using this DAG would fail basic correlation tests.

While the two possibilities presented above allow creating a DAG without prior knowledge of the data, they will fail to deliver a synthetic dataset that correctly models the correlations between the variables in a table $\mathbf{T}$. We recommend building a DAG containing as many links as possible. It is always possible to perform a transitive reduction of $\mathcal{G}$, *i.e.* removing paths such that for all vertices v_{t_1} and v_{t_2} there exists only a unique path that goes from v_{t_1} to v_{t_2}, after its definition. There are no strict rules to decide whether one should add a causal link between two variables. It is a matter of judgment, and multiple trials and errors will be needed. However, we provide a set of instructions that can help the modeler define such a DAG:

- If the dataset is used to predict one variable, define this variable as a sink node in $\mathcal{G}$. For example, in Figure 3, the dataset can be used to predict the variable mode choice. It is, thus, the sink node of the graph. It is also possible to define multiple sink nodes.

14

- Usually, datasets contain different categories of variables. For example, a travel survey dataset might contain trips, individuals, and households variables. It is, thus, generally easier to define the causal links between variables belonging to similar semantic groups.

- The next step consists in defining the source nodes. However, there are no specific rules for this. It is entirely up to the modeler.

- Finally, the modeler has to choose the direction of the causal links. Again, there are no rules for this. In the example of Figure 3b, one could decide that the variables `driving license` and `age` have an inverted causal link. This would slightly change the DAG but should not fundamentally change the results.

As shown in Figure 3, we present a mock dataset (see Figure 3a) and one possible DAG (see Figure 3b) representing the causal links between the variables. This dataset is a travel survey dataset. We thus define the mode choice as the sink node. We can define the following category of variables: (i) trip-related variables: `mode choice` and `trip purpose`; (ii) individual-related variables: `age` and `driving license`; (iii) household-related variables: `nbr cars household`; (iv) survey-related variables: `type of survey`. For each of these categories, we want to make sure that the variables are linked together. Since `mode choice` is the sink node, we can create an edge from `trip purpose` to `mode choice`. For the individual-related variables, the direction of the causal link can be either direction. For the source nodes, we decide to set the variables `age` and `nbr cars household` as the source nodes. Finally, we can add some more links to complete the DAG. We decided, on purpose, to let the variable `type of survey` out of the DAG not to influence the data generation. One could argue that it could be linked to the age since older individuals are less familiar with internet technologies. However, as stated earlier, the modeler has to make choices while constructing the DAG, requiring trials and errors.

age	driving license	trip purpose	type of survey	nbr cars household	mode choice
continuous	**boolean**	**nominal**	**nominal**	**ordinal**	**nominal**
0-100	True False	Work Leisure ...	Internet Phone ...	0 1 2 ...	Driving Soft Modes ...

(a) Example of a mock dataset
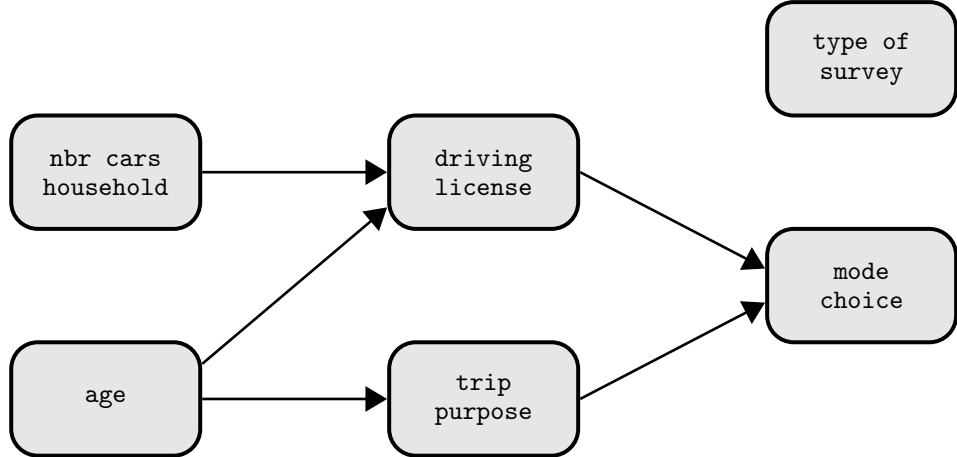
(b) Example of a DAG used to represent the structure of the variables

Figure 3: Example of the structure of the data. Figure 3a shows the structure of a table with six variables. Figure 3b shows one possible DAG used to represent the variables in Figure 3a.

Once the DAG $\mathcal{G}$ has been created, we can define several valuable sets. These sets are used later when representing the structure of the DAG in the generator.

- $\mathcal{A}(V_t)$: the set of ancestors of the variable V_t.

- $\mathcal{D}(V_t)$: the set of direct ancestors of the variable V_t.

- $\mathcal{S}(V_t)$: the set of sources nodes leading to the variable V_t.

- $\mathcal{E}(V_t)$: the set of in-edges of the variable V_t.

If we use the variable `mode choice` from Figure 3b as an example, we can define these different sets:

- $\mathcal{A}(\texttt{mode choice}) = \{\texttt{nbr cars households; age; driving license; trip purpose}\}$

- $\mathcal{D}(\texttt{mode choice}) = \{\texttt{driving license; trip purpose}\}$

- $\mathcal{S}(\texttt{mode choice}) = \{\texttt{nbr cars households; age}\}$

- $\mathcal{E}(\texttt{mode choice}) = \{\texttt{driving license} \rightarrow \texttt{mode choice; trip purpose} \rightarrow \texttt{mode choice}\}$

3.1.2 Representation of the DAG

As explained in the introduction of this section, the DAG is used to represent the causal links between the variables. Thus, we want to develop an architecture for the generator similar to the specified DAG. Tabular data cannot be considered sequential data since the order of the variables in a dataset is usually random. However, the DAG allows us to have a sequence of variables with a specific order. We can, thus, use Neural Networks models that have been to work well with this type of data. More specifically, we use Long Short Term Memory (LSTM) cells (Hochreiter and Schmidhuber, 1997), a type of recurrent neural network, to generate synthetic values for each variable V_t. We denote the LSTM cell associated to the variable V_t by $\mathbf{LSTM_t}$. The advantage of using recurrent neural networks is that the previous output affects the current state of the neural network. Using the sequence defined by the DAG $\mathcal{G}$, we can, thus, use previous outputs, *i.e.* synthetic values of previous variables, to influence the generation process of a given variable V_t.

The key elements to an LSTM cell are the cell state and the multiple gates used to protect and control the cell state, as shown in Figure 4. For conciseness, we do not present a detailed overview of the mathematical operations of an LSTM cell. For a full description, we direct the reader to Gers et al. (2000). In Figure 4, the input cell state is characterized by C_{t-1} and the output cell state by C_t. The cell will receive an input that is the concatenation between the output of the previous cell ($\boldsymbol{h}_{t-1}$) and an input vector ($\boldsymbol{x}_t$). It is thus given by:

$$\boldsymbol{i}_t = \boldsymbol{h}_{t-1} \oplus \boldsymbol{x}_t \tag{1}$$

This input vector will pass through three different gates to transform the cell state as it is necessary:

1. **the forget gate** is used to decide which old information is forgotten in the cell state.

2. **the input gate** is used to decide which new information is stored kept in the new cell state

3. **the output gate** is used to decide the output of the cell using information from both the input $\boldsymbol{i}_t$ and the new cell state C_t.

The modeler has to define the size of the hidden layers N_h in the LSTM cell and the batch size N_b. The first defines the size of the output vector $\boldsymbol{h}_t$ as well as the cell state C_t. The latter corresponds to the number of data points fed in the network. Therefore, we usually define the output $\boldsymbol{h}_t$ and cell state C_t as tensors of size $N_h \times N_b$. The input x_t usually takes a different size and is thus characterized by a tensor of size $N_x \times N_b$ (the batch size has to remain the same between all the tensors).
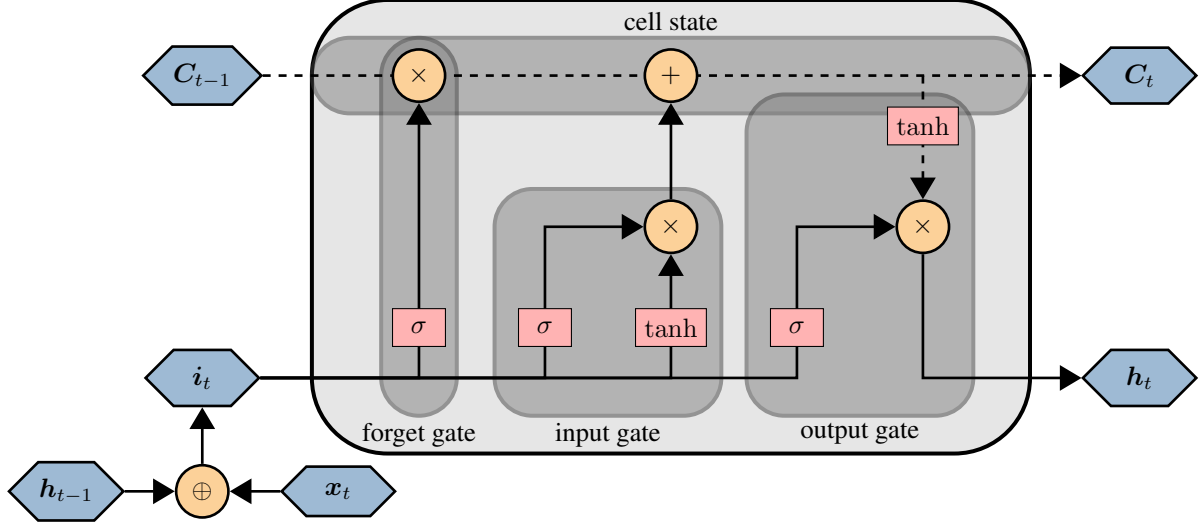
Figure 4: Main components of a LSTM cell following Gers et al. (2000). The blue hexagons represent variables, the red rectangles neural network layers, and the orange circles mathematical operations. The different gates used to transform the input and the cell state are shown in dark gray.

In the case of the DATGAN, we have to modify the inputs and outputs of the LSTM cell according to the principles of GANs. Figure 5 provides a schema of the LSTM structure in the DATGAN. The insides of the LSTM cell $\mathbf{LSTM_t}$ are the same as the one shown in Figure 4. The first main modification concerns the inputs. Indeed, the generator in a GAN takes random noise as an input instead of an input vector such as $\boldsymbol{x}_t$. In addition, we add an attention vector to the input tensor $\boldsymbol{i}_t$. The idea behind the attention vector is to keep information of intermediate encoders and pass it to a new encoder. This mimics cognitive attention and, thus, helps with the long-term memory of the LSTM cells. Therefore, the input tensor $\boldsymbol{i}_t$ corresponds to the concatenation of three tensors:

- $\boldsymbol{z}_t$ is a tensor of Gaussian noise with dimension $N_z \times N_b$. For each source node in the DAG $\mathcal{G}$, we randomly draw values from $\mathcal{N}(0,1)$. For all the other variables V_t, the noise vector is a concatenation of the noise from the source nodes passed through a fully connected layer without any activation function, *i.e.*

$$\boldsymbol{z}_t = \texttt{FC}\left(\bigoplus_{k \in \mathcal{S}(V_t)} \boldsymbol{z}_k, N_z\right) \tag{2}$$

  If two different variables V_{t_1} and V_{t_2} have the same source nodes, *i.e.* $\mathcal{S}(V_{t_1}) = \mathcal{S}(V_{t_2})$, the noise tensor is the same for both variables, *i.e.* $\boldsymbol{z}_{t_1} = \boldsymbol{z}_{t_2}$. There are two reasons to apply such a rule: (i) it removes pointless computation by creating new variables; (ii) if two variables have a unique source node, they will receive the same noise as an input. We must, therefore, follow this rule if there is more than one source node.

- $\boldsymbol{f}_{t-1}$ can be compared to the previous output tensor $\boldsymbol{h}_{t-1}$ in Figure 4. However, one of the differences between the DATGAN and a usual LSTM network is that we do not directly use the output tensor of the LSTM $\boldsymbol{h}_t$. Indeed, as shown in Figure 5, we transform it into the encoded synthetic variable $\widehat{\boldsymbol{v}}_t^{\mathbf{synth}}$. Since $\widehat{\boldsymbol{v}}_t^{\mathbf{synth}}$ do not have a standard size, we thus need to transform it in order to obtain the usable tensor $\boldsymbol{f}_t$ of dimension $N_h \times N_b$. We can thus say that $\boldsymbol{f}_t$ corresponds to the transformed output of the LSTM cell $\mathbf{LSTM_t}$. If the variable V_t is a source node, this tensor is randomly initialized and learned during the optimization process.

- $\boldsymbol{a}_t$ is an attention tensor that allows the cell to learn which previous cell outputs are relevant to the input. It is defined as a weighted average over all the LSTM outputs. If the current variable V_t has at least one ancestor, we learn an attention weight vector $\alpha_t \in \mathbb{R}^{|\mathcal{A}(t)|}$. The context vector is thus computed as:

$$\boldsymbol{a}_t = \sum_{k \in \mathcal{A}(t)} \frac{\exp \alpha_t^{(k)}}{\sum_j \exp \alpha_t^{(j)}} \boldsymbol{h}_k \tag{3}$$

  This context tensor has a dimension $N_h \times N_b$. If variable V_t is a source node, we define $\boldsymbol{a}_t$ as a zero-vector of dimension $N_h \times N_b$.

17

LSTMs cells are initially designed to work in sequence, *i.e.* each cell is linked to a unique following cell. However, as shown in the DAG in Figure 3b, some variables can have multiple direct ancestors. For example, the variable `mode choice` has two ancestors: `driving license` and `trip purpose`. We, thus, need a way to connect multiple LSTM
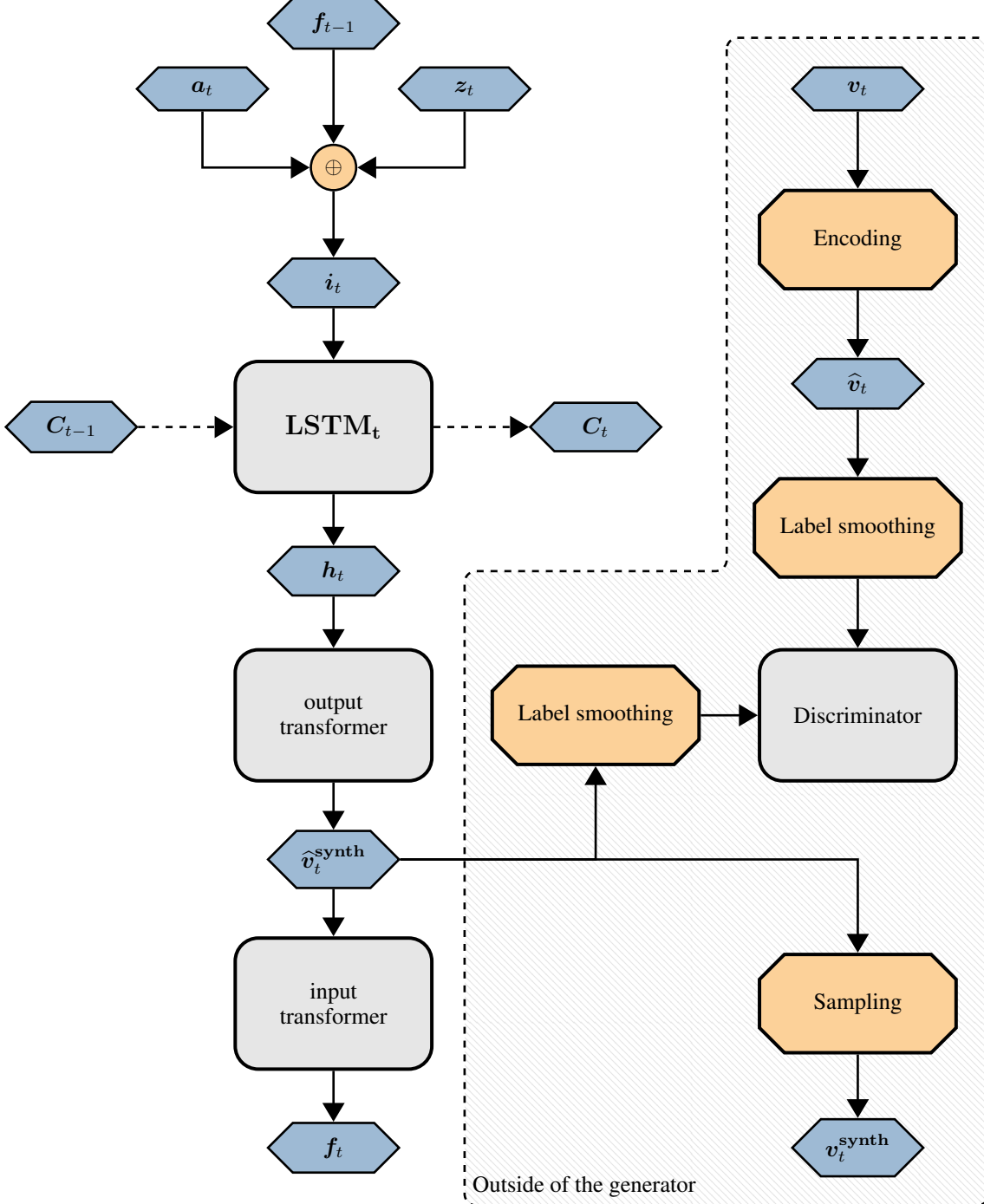
Figure 5: Schematic representation of how the LSTM cells are used withing the DATGAN to generate the synthetic variable $\widehat{v}_t^{\mathbf{synth}}$. In Section 3.1.2, we mainly discuss the left part of the diagram. The right part shows how the new generated variable is passed to the discriminator and sampled. These different elements are presented in the following sections: the Discriminator is presented in Section 3.2, the Encoding in Section 3.4.1, the Label smoothing in Section 3.4.3, and the Sampling in Section 3.4.4.

18

cells. If one cell has multiple outputs, we send the output of the cell to the next cells, *e.g.* the inputs of the cells for the variables `driving license` and `trip purpose` coming from the variable `age` are the same. The main issue lies in having multiple cell inputs. The attention tensor a_t and the noise tensor z_t are defined based on all the ancestors of the current variable. Therefore, we do not have to change these definitions. On the other, the previous cell state C_{t-1} and the transformed output f_{t-1} are defined to work in sequence. Therefore, we define the multi-input cell state and multi-input transformed output by concatenating the cell states and transformed outputs from the direct ancestors and passing them through a fully connected layer to resize them:

$$C_{t-1} = \text{FC}\left(\bigoplus_{k \in \mathcal{D}(V_t)} C_k, N_h\right) \tag{4}$$

$$f_{t-1} = \text{FC}\left(\bigoplus_{k \in \mathcal{D}(V_t)} f_k, N_h\right) \tag{5}$$

During the training process, the weights of the two layers have to be learned. We can, thus, feed the LSTM cell with homogeneous inputs.

Algorithm 1 Ordering of the variables using a DAG

Input: DAG: $\mathcal{G}$
Output: ordered list of variables: `treated`
 1: Compute a dictionary `in_edges` with V_t as the key and $\mathcal{E}(V_t)$ as the value for all $t = 1, \ldots, N_V$.
 2: Initialize `untreated` as a set with all the variables names and `treated` an empty list
 3: Initialize `to_treat` as a list containing all the variables with 0 in-edges
 4: **while** $|\text{untreated}| > 0$ **do**
 5:     **for all** $n \in \text{to\_treat}$ **do**
 6:         Remove n from `untreated` and add it to `treated`
 7:     Set `to_treat` as an empty list
 8:     **for all** $e \in \mathcal{G}.E$ **do**   ▷ e is an edge and it is a tuple with 2 values: the out-vertex and the in-vertex
 9:         Initialize boolean `all_ancestors_treated` to True
10:         **for all** $\ell \in \text{in\_edges}[e[1]]$ **do**
11:             **if** $\ell \notin \text{treated}$ **then**
12:                 Set `all_ancestors_treated` to False
13:         **if** $e[0] \in \text{treated}$ **and** `all_ancestors_treated` is True **and** $e[1] \notin \text{treated}$ **and** $e[1] \notin \text{to\_treat}$ **then**
14:             Add $e[1]$ to the list `to_treat`
15: **return** `treated`

One final issue remains in constructing the structure of the generator. Indeed, we know how to generate each variable separately and connect them using the DAG and the multi-input LSTM cells. However, while building the generator's structure, we cannot start with any random variable in the DAG. Indeed, as per the definition of the inputs of the LSTM cell, the ancestors $\mathcal{A}(V_t)$ must have already been built first. For example, the attention tensor uses the outputs of all the ancestors' cells. Therefore, we need an algorithm that creates an ordered list based on the provided DAG $\mathcal{G}$. This algorithm is given in Algorithm 1. The goal of this algorithm is to take the DAG $\mathcal{G}$ and return an ordered list of the variables V_t such that all the ancestors of a given variable have a smaller index in the list, *i.e.* they appear first in the list. The algorithm is built recursively. The idea is to define two lists, one with untreated nodes `untreated`, containing all the nodes at the beginning of the algorithm, and one with treated nodes `treated`, empty at the beginning. We, then, start by selecting all source nodes and adding to a list named `to_treat`. Then, while the list of untreated nodes is not empty, *i.e.* while there are still nodes to be added to the final list, we start by assigning all nodes in the list `to_treat` in the `treated` list. Then, we check each edge in the DAG $\mathcal{G}$ and check if all the ancestors of the out-vertex have been treated. If it is the case, we can add this node to the `to_treat` list and assign it later to the final list. The algorithm stops when all the nodes have been added to the `treated` list.

Now that every component has been defined for the generator, we can build it following the ordered list provided by Algorithm 1. Each time that we create a LSTM cell for the variable V_t, as in Figure 5, we check the direct ancestors $\mathcal{D}(V_t)$. If more than one direct ancestor, we apply the multi-input technique to the LSTM cell. The generator is finished once one LSTM cell has been created for each variable in the ordered list.

3.2 Discriminator

As seen in Figure 2, the generator is used to create the synthetic dataset $\widehat{\mathbf{T}}_{\mathbf{synth}}$. The role of the discriminator is to compare this dataset with the encoded original dataset $\widehat{\mathbf{T}}$. We, thus, want to train the discriminator to be able to identify original and synthetic data. That way, the generator will have to produce better synthetic data if it wants to fool the discriminator.

Following Xu and Veeramachaneni (2018), we use a fully connected neural network with N_L-layers for the discriminator, where the internal layers, for $i = 1, \ldots, N_L$, are given by:

$$\widehat{l}_i = \texttt{FC}\left(l_{i-1}, N_l\right) \tag{6}$$

$$l_i = \texttt{LeakyReLU}\left(\texttt{BN}\left(\widehat{l}_i \oplus \texttt{div}\left(\widehat{l}_i\right)\right)\right) \tag{7}$$

where (i) $\texttt{div}(\cdot)$ represents the mini-batch discrimination vector presented by Salimans et al. (2016); (ii) $\texttt{BN}(\cdot)$ corresponds to the batch normalization; (iii) $\texttt{LeakyReLU}(\cdot)$ is the leaky reflect linear activation function. The output of the discriminator is computed using a fully connected layer with a size of 1 to return an unbounded scalar:

$$l_D = \texttt{FC}\left(l_{N_L}, 1\right) \tag{8}$$

The input vector l_0 of the discriminator is different depending on the data it is using:

- For the original dataset, l_0 corresponds to the concatenation of all the column vectors $\{\widehat{v}_{1:N_V}\}$ after an encoding step, as shown in Figure 2.

- For the synthetic dataset, l_0 corresponds to the concatenation of all the usable outputs $\left\{\widehat{v}_{1:N_V}^{\mathbf{synth}}\right\}$ given by the generator, as shown in Figure 5.

However, as seen in Figure 5, a label smoothing step has to be performed before feeding these matrices to the discriminator. This step is discussed in Section 3.4.3.

3.3 Loss function

The loss function sets up the game between the discriminator and the generator. The discriminator D aims to maximize the loss function when comparing the synthetic data produced by the generator against the original data. Meanwhile, the generator G aims to minimize the same loss function by generating synthetic data, fooling the discriminator. The generator thus learns from the discriminator in this process by backpropagating the discriminator loss.

Since the loss function drives the optimization process to obtain the best possible model, we argue that our model does not have to be characterized by a single loss function. Therefore, we systematically test three different loss functions. The first one is the standard cross-entropy loss defined by Goodfellow et al. (2014), the second one is the Wasserstein or Earth-Mover distance defined by Arjovsky et al. (2017), and the third one is the Wasserstein distance with Gradient-Penalty defined by Gulrajani et al. (2017).

Standard loss The first loss function is the standard loss function used in the original GAN by Goodfellow et al. (2014). We name it $\mathcal{L}^{\texttt{SGAN}}$ with SGAN standing for Standard GAN. It is given by:

$$\min_G \max_D \mathcal{L}^{\texttt{SGAN}}(D, G) = \mathop{\mathbb{E}}_{\{\widehat{v}_{1:N_V}\} \sim \mathbb{P}(\widehat{\mathbf{T}})} \log D\left(\widehat{v}_{1:N_V}\right) + \mathop{\mathbb{E}}_{z \sim \mathcal{N}(0,1)} \log\left(1 - D(G(z))\right) \tag{9}$$

This loss function requires the discriminator to produce a probability for each data point to be either original or synthetic. However, as it has been defined in Section 3.2, the discriminator outputs an unbounded scalar and not a probability. In order to use this discriminator with this loss function, we thus pass the output through an additional sigmoid layer to produce bounded $[0, 1]$ probabilities.

As explained by Goodfellow et al. (2014), $\log\left(1 - D(G(z))\right)$ tends to saturate during the training process. Therefore, instead of training G to minimize the full loss function, we can instead train it to maximize $\log D(G(z))$. We can thus define the loss function for both networks separately. The goal is to minimize both losses simultaneously during the training process. They are given by:

$$\mathcal{L}_G^{\texttt{SGAN}} = - \mathop{\mathbb{E}}_{z \sim \mathcal{N}(0,1)} \log D(G(z)) \tag{10}$$

$$\mathcal{L}_D^{\texttt{SGAN}} = - \mathop{\mathbb{E}}_{\{\widehat{v}_{1:N_V}\} \sim \mathbb{P}(\widehat{\mathbf{T}})} \log D\left(\widehat{v}_{1:N_V}\right) + \mathop{\mathbb{E}}_{z \sim \mathcal{N}(0,1)} \log D(G(z)) \tag{11}$$

As suggested by the authors, we train our models using the Adam optimizer (Kingma and Ba, 2014).

Wasserstein loss The second loss function has been implemented in the Wasserstein GAN (WGAN) by Arjovsky et al. (2017). It is defined using the Earth-Mover distance:

$$\min_G \max_D \mathcal{L}^{\text{WGAN}}(D, G) = \mathop{\mathbb{E}}_{\{\widehat{\boldsymbol{v}}_{1:N_V}\} \sim \mathbb{P}(\widehat{\mathbf{T}})} D\left(\widehat{\boldsymbol{v}}_{1:N_V}\right) - \mathop{\mathbb{E}}_{\boldsymbol{z} \sim \mathcal{N}(0,1)} D(G(\boldsymbol{z})) \tag{12}$$

There are multiple advantages to use this loss function instead of the standard loss: (i) the main advantage is the fact that the discriminator becomes a critic since it does not need to produce a 0-1 output anymore. Indeed, we can use the output of the discriminator l_D as it is defined. It thus results in less vanishing gradients and an easier learning process for the generator G; (ii) the loss function correlates with the quality of the sample, contrary to the SGAN loss. It is, thus, possible to determine when the GAN has converged.

We can, now, define the separate loss functions for both networks as:

$$\mathcal{L}_G^{\text{WGAN}} = -\mathop{\mathbb{E}}_{\boldsymbol{z} \sim \mathcal{N}(0,1)} D(G(\boldsymbol{z})) \tag{13}$$

$$\mathcal{L}_D^{\text{WGAN}} = -\mathop{\mathbb{E}}_{\{\widehat{\boldsymbol{v}}_{1:N_V}\} \sim \mathbb{P}(\widehat{\mathbf{T}})} D\left(\widehat{\boldsymbol{v}}_{1:N_V}\right) + \mathop{\mathbb{E}}_{\boldsymbol{z} \sim \mathcal{N}(0,1)} D(G(\boldsymbol{z})) \tag{14}$$

As suggested by the authors, we train our models using the RMSProp optimizer (Tieleman and Hinton, 2012).

Wasserstein loss with gradient penalty The loss for the WGAN-GP is the same as the Wasserstein loss with the addition of a gradient penalty (Gulrajani et al., 2017). It is given by:

$$\min_G \max_D \mathcal{L}^{\text{WGGP}}(D, G) = \mathop{\mathbb{E}}_{\{\widehat{\boldsymbol{v}}_{1:N_V}\} \sim \mathbb{P}(\widehat{\mathbf{T}})} D\left(\widehat{\boldsymbol{v}}_{1:N_V}\right) - \mathop{\mathbb{E}}_{\boldsymbol{z} \sim \mathcal{N}(0,1)} D(G(\boldsymbol{z})) + \lambda \mathop{\mathbb{E}}_{\widehat{\boldsymbol{v}} \sim \mathbb{P}(\widehat{\mathbf{T}}, G(\boldsymbol{z}))} \left(\|\nabla_{\widetilde{\boldsymbol{v}}} D(\widetilde{\boldsymbol{v}})\|_2 - 1\right)^2 \tag{15}$$

where λ is a parameter defined by the modeler. The main issue with the WGAN is that it needs to enforce the Lipschitz contsraint on the critic. It does that by clipping the weights of the critic. Gulrajani et al. (2017) show that it leads undesired behaviour in the generator samples. We can, thus, fix this issue by adding a gradient penalty on the critic. In Equation 15, the mid-value $\widetilde{\boldsymbol{v}}$ is sampled uniformly along straight lines between pair of points sampled from the original dataset $\mathbf{T}$ $(\widehat{v})$ and generated data $G(\boldsymbol{z})$ $(\widehat{v}^{\text{synth}})$.

The separate loss functions for each networks are, therefore, defined as:

$$\mathcal{L}_G^{\text{WGGP}} = -\mathop{\mathbb{E}}_{\boldsymbol{z} \sim \mathcal{N}(0,1)} D(G(\boldsymbol{z})) \tag{16}$$

$$\mathcal{L}_D^{\text{WGGP}} = -\mathop{\mathbb{E}}_{\{\widehat{\boldsymbol{v}}_{1:N_V}\} \sim \mathbb{P}(\widehat{\mathbf{T}})} D\left(\widehat{\boldsymbol{v}}_{1:N_V}\right) + \mathop{\mathbb{E}}_{\boldsymbol{z} \sim \mathcal{N}(0,1)} D(G(\boldsymbol{z})) + \lambda \mathop{\mathbb{E}}_{\widehat{\boldsymbol{v}} \sim \mathbb{P}(\widehat{\mathbf{T}}, G(\boldsymbol{z}))} \left(\|\nabla_{\widehat{\boldsymbol{v}}} D(\widehat{\boldsymbol{v}})\|_2 - 1\right)^2 \tag{17}$$

Following Gulrajani et al. (2017), we replace the batch normalization in the discriminator with a layer normalization (Ba et al., 2016), we set $\lambda = 10$, and we train both models using the Adam optimizer (Kingma and Ba, 2014).

Following Xu and Veeramachaneni (2018), we include a Kullback-Leibler (KL) divergence term to all the generator losses. For two discrete probability distributions P and Q defined on the same probability space $\mathcal{X}$, the KL divergence is given by:

$$\text{KL}(P, Q) = \sum_{x \in \mathcal{X}} P(x) \log\left(\frac{P(x)}{Q(x)}\right) \tag{18}$$

Therefore, we can use this divergence for any discrete probability distributions in the original and synthetic datasets. The use of this divergence has two main consequences: (i) it gives a boost when starting the training of the generator since it is trying to make discrete probability distributions as close as possible; (ii) it makes the model more stable under training. We discuss which variables are concerned by this divergence in Section 3.4.1 for the original dataset $\widehat{\mathbf{T}}$ and in Section 3.4.2 for the synthetic dataset $\widehat{\mathbf{T}}_{\text{synth}}$.

3.4 Data processing

Tabular data are generally composed of multiple data types, as seen in Figure 3a. In the context of this article, we consider two different variable types:

Continuous data corresponds to a random variable following a continuous distribution (*e.g.* the distance to travel to a destination). The variable can then be rounded to obtain discrete values, as is usually the case with an individual's age.

Categorical data corresponds to all other types of data such as:
- binary random variables (*e.g.* whether someone is retired or not).
- nominal random variables, *i.e.* discrete random variable with three or more possible values, where there is no order nor notion of distance between the different values (*e.g.* a color).
- ordinal random variables, *i.e.* discrete random variables with three or more possible values with a defined order (and possibly also distance) between each possible value (*e.g.* education level). Contrary to nominal data, we can define an order (and possibly a distance) between the different categories.

Typically, in Machine Learning, neural networks work with data ranging from -1 to 1 or 0 to 1. However, these four types of data are not designed in such a way. We thus need to encode the original dataset $\mathbf{T}$ in a dataset $\widehat{\mathbf{T}}$, as shown in Figure 2, that transforms the different data types into more homogeneous types.

The table $\mathbf{T}$ contains N_C continuous random variables $\{C_1, \ldots, C_{N_C}\}$ and N_D categorical random variables $\{D_1, \ldots, D_{N_D}\}$ such that $N_C + N_D = N_V$. We can thus define the table $\mathbf{T}$ using vectors of continuous and categorical variables, *i.e.* $\mathbf{T} = \{\boldsymbol{c}_{1:N_C}, \boldsymbol{d}_{1:N_D}\}$. Similarly, the synthetic dataset is defined as $\mathbf{T_{synth}} = \left\{\boldsymbol{c}_{1:N_C}^{\mathbf{synth}}, \boldsymbol{d}_{1:N_D}^{\mathbf{synth}}\right\}$.

Since we are considering two different data types in the table $\mathbf{T}$, we cannot process them the same way. Thus, Section 3.4.1 explains how the encoding is done for each type. Section 3.4.2 explains how these types of data are generated. Section 3.4.3 discusses how the synthetic data and the original data are passed to the discriminator. Finally, Section 3.4.4 shows how the data is sampled from the generator's output to create the final synthetic dataset.

3.4.1 Encoding

The DATGAN model takes as input only $[-1, 1]$ or $[0, 1]$ bounded vectors. Therefore, we need to encode unbounded continuous variables and categorical variables to be processed by the GAN. Continuous data tend to follow multimodal distributions. We thus build on the previous methodology of Xu et al. (2019) who apply a Variational Gaussian Mixture (VGM) model (Bishop, 2006) to cluster continuous values into a discrete number of Gaussian mixtures. In this work, we develop this further by automatically determining the number of components from the data.

Algorithm 2 Continuous variables preprocessing

Input: List of float values ($\boldsymbol{c}_t$)
Output: Matrix of probabilities ($\boldsymbol{p}_t$) and values ($\boldsymbol{w}_t$)
1: Set the initial number of modes $N_{m,t} = 10$
2: **while** True **do**
3:     Sample $\boldsymbol{s}_t$ from $\boldsymbol{c}_t$ and fit the `BayesianGaussianMixture` to $\boldsymbol{s}_t$ with $N_{m,t}$ modes
4:     Predict the class on $\boldsymbol{s}_t$ and compute N_{pred} the number of unique classes predicted by the VGM
5:     Define N_{weights}, the number of weights of the model above a threshold $\varepsilon_w = 0.01$
6:     **if** $N_{\text{pred}} < N_{m,t}$ **or** $N_{\text{weights}} < N_{m,t}$ **then**
7:         $N_{m,t} = \min\left(N_{\text{pred}}, N_{\text{weights}}\right)$
8:     **else**
9:         break
10: Fit the `BayesianGaussianMixture` to $\boldsymbol{c}_t$ with $N_{m,t}$ modes.
11: Means and standard deviations of the $N_{m,t}$ Gaussian mixtures are given by

$$\boldsymbol{\eta}_t = \left(\eta_t^{(1)}, \ldots, \eta_t^{(N_{m,t})}\right) \text{ and } \boldsymbol{\sigma}_t = \left(\sigma_t^{(1)}, \ldots, \sigma_t^{(N_{m,i})}\right)$$

12: Compute the posterior probability of $c_{t,j}$ coming from each of the $N_{m,t}$ mixtures as a vector $\boldsymbol{p}_{t,j} = \left(p_{t,j}^{(1)}, \ldots, p_{t,j}^{(N_{m,t})}\right)$. It corresponds to a normalized probability distributions over the $n_{m,i}$ Gaussian distributions.
13: Normalize $c_{t,j}$ for each Gaussian mixture using Equation 19.
14: Clip each value $w_{t,j}^{(k)}$ between -0.99 and 0.99 and set $\boldsymbol{w}_{t,j} = \left(w_{t,j}^{(1)}, \ldots, w_{t,j}^{(N_{m,t})}\right)$.
15: **return** $\boldsymbol{p}_t$ and $\boldsymbol{w}_t$

For each continuous variable C_t in the dataset, we first train a VGM on a random subset of the data with a high number of components ($N_{m,t} = 10$). We then determine how many components are needed to capture the distribution by comparing the component weights against a threshold and the number of predicted components N_{pred} with the original number of components $N_{m,t}$. We repeat this process until convergence. Finally, we retrain the model on the entire

column vector $\boldsymbol{c}_t$ using only the number of significant components. From this trained model, we extract the means $\boldsymbol{\eta}_t$ and standard deviations $\boldsymbol{\sigma}_t$ from the VGM. We can then normalize the values $c_{t,j}$ using the following formula:

$$w_{t,j}^{(k)} = \frac{c_{t,j} - \eta_t^{(k)}}{\delta \sigma_t^{(k)}} \quad \text{for } k = 1, \dots, N_{m,t}, \tag{19}$$

where δ is a parameter specified by the modeller. Following Xu and Veeramachaneni (2018), we use a value of $\delta = 2$ and clip the values of $w_{t,j}^{(k)}$ between -0.99 and 0.99. At the same time, we compute the posterior probability vectors $\boldsymbol{p}_{t,j}$ that the value $c_{t,j}$ belongs to each of the $N_{m,t}$ mixtures. Thus, each value $c_{t,j}$ in $\boldsymbol{c}_t$ are represented by the vector of probabilities $\boldsymbol{p}_{t,j} \in [0,1]^{N_{m,t}}$ and the vector of values $\boldsymbol{w}_{t,j} \in [-0.99, 0.99]^{N_{m,t}}$. Algorithm 2 shows a summary of the procedure used to preprocess continuous variables.

For categorical variables[1], we transform them using one-hot encoding. We consider $\boldsymbol{d}_t$ the realizations of the random variable D_t. $\boldsymbol{d}_t$ is transformed using $|D_t|$-dimensional one-hot vector $\boldsymbol{o}_t$ where $|D_t|$ corresponds to the number of unique categories in D_t.

We can thus convert the initial table $\mathbf{T}$ into an intermediate table $\widehat{\mathbf{T}} = \{\boldsymbol{w}_1, \boldsymbol{p}_1, \dots, \boldsymbol{w}_{N_C}, \boldsymbol{p}_{N_C}, \boldsymbol{o}_1, \dots, \boldsymbol{o}_{N_D}\}$. As a simplification, we write $\widehat{\mathbf{T}} = \{\boldsymbol{w}_{1:N_C}, \boldsymbol{p}_{1:N_C}, \boldsymbol{o}_{1:N_D}\}$. The dimension of this new table is given by $\sum_{t=1}^{N_C} 2N_{m,t} + \sum_{t=1}^{N_D} |D_t|$. While this new encoded table is larger than the original table, we can now use define the KL divergence on multiple variables. Indeed, the vector $\boldsymbol{p}_{t,j}$ corresponds to a discrete probability distribution for a given row. We can, thus, apply the KL divergence on this term. In addition, the one-hot encoded vector $\boldsymbol{o}_{t,j}$ also corresponds to a discrete probability distributions. The only difference is that this distribution is composed of only 1s and 0s. Nevertheless, the KL divergence is also applicable on this variable.

3.4.2 Generator output

In Figure 5, we show how the LSTM cell $\mathbf{LSTM_t}$ produces an output $\boldsymbol{h}_t$ before it is transformed into the encoded synthetic variable $\widehat{\boldsymbol{v}}_t^{\mathbf{synth}}$. However, in Section 3.4.1, we show that we distinguish between two variable types. Thus, the output transformer in Figure 5 differs depending on if we are working with a continuous or a categorical variable. Nevertheless, the first step for the output transformer is similar in both cases. Indeed, the goal is to use some semblance of convolution on the LSTM output $\boldsymbol{h}_t$ to improve the results. We, thus, transform this output through a hidden layer:

$$\boldsymbol{h}_t' = \texttt{tanh}\,(\boldsymbol{h}_t, N_{\text{conv}}) \tag{20}$$

The final transformation into the synthetic encoded variable depends on the variable type. For continuous variables, we thus pass the reduced output $\boldsymbol{h}_t'$ through two different fully connected layers to extract both the vector of probabilities $\boldsymbol{p}_t^{\mathbf{synth}}$ and the vector of corresponding values $\boldsymbol{w}_t^{\mathbf{synth}}$:

$$\boldsymbol{w}_t^{\mathbf{synth}} = \texttt{tanh}(\boldsymbol{h}_t', N_{m,t}) \tag{21}$$

$$\boldsymbol{p}_t^{\mathbf{synth}} = \texttt{softmax}(\boldsymbol{h}_t', N_{m,t}) \tag{22}$$

For the categorical variables, we pass the reduced output $\boldsymbol{h}_t'$ through a single fully connected layer to extract the output probabilities $\boldsymbol{o}_t^{\mathbf{synth}}$ belonging to each class:

$$\boldsymbol{o}_t^{\mathbf{synth}} = \texttt{softmax}(\boldsymbol{h}_t', |D_t|) \tag{23}$$

Both matrices of discrete probabilities $\boldsymbol{p}_t^{\mathbf{synth}}$ and $\boldsymbol{o}_t^{\mathbf{synth}}$ are using a softmax activation function in order to ensure that the sum along the rows is equal to one. This ensures that the rows of these matrices correspond to discrete probability vectors. The matrix $\boldsymbol{w}_t^{\mathbf{synth}}$ uses a $\texttt{tanh}$ activation function since we are allowing this matrix to take values between -1 and 1.

Since these encoded synthetic variables do not have homogeneous sizes, we cannot use them directly as the input of the next LSTM cell. This, thus, explains why we are passing the encoded synthetic values $\widehat{\boldsymbol{v}}_t^{\mathbf{synth}}$ through an input transformer. The goal of this transformer is to take $\widehat{\boldsymbol{v}}_t^{\mathbf{synth}}$ and transform it back to the same tensor for all the different variables V_t. Therefore, we have to distinguish between continuous and categorical variables again. For the continuous variables, we concatenate the transformed synthetic variables together and pass them through a fully connected layer to obtain $\boldsymbol{f}_t$:

$$\boldsymbol{f}_t = \texttt{FC}(\boldsymbol{w}_t^{\mathbf{synth}} \oplus \boldsymbol{p}_t^{\mathbf{synth}}, N_h) \tag{24}$$

---

[1]The same treatment is applied to categorical and boolean variables due to the label smoothing explained in Section 3.4.3.

For the categorical variables, we just pass $\boldsymbol{o}_t^{\mathbf{synth}}$ through a fully connected layer:

$$\boldsymbol{f}_t = \mathtt{FC}(\boldsymbol{o}_t^{\mathbf{synth}}, N_h) \tag{25}$$

Finally, the tensors $\boldsymbol{w}_t^{\mathbf{synth}}$, $\boldsymbol{p}_t^{\mathbf{synth}}$, and $\boldsymbol{o}_t^{\mathbf{synth}}$ are combined to form the encoded synthetic table $\widehat{\mathbf{T}}_{\mathbf{synth}} = \left\{ \boldsymbol{w}_{1:n_C}^{\mathbf{synth}}, \boldsymbol{p}_{1:n_C}^{\mathbf{synth}}, \boldsymbol{o}_{1:n_D}^{\mathbf{synth}} \right\}$. This synthetic table is passed to the discriminator as an input for the optimization process. We thus directly compare it to the encoded table $\widehat{\mathbf{T}}$ defined in Section 3.4.1.

3.4.3 Discriminator input

As explained in Section 3.2, the input tensor $\boldsymbol{l}_0$ corresponds to the concatenation of all the variables in $\widehat{\mathbf{T}}$ for the original data or $\widehat{\mathbf{T}}_{\mathbf{synth}}$ for the synthetic data.

For categorical variables, where the original data are one-hot encoded, it would be trivial for a discriminator to differentiate between the original and synthetic values (as the generator produces probabilities over each class, which will not be $\{0, 1\}$ vectors). In addition, as explained by Goodfellow (2017), deep networks tend to produce overconfident results when adversarially constructed. The author thus suggests using one-sided label smoothing for the standard loss function, as defined in Section 3.3. It means that we perturb the $\{0, 1\}$ vectors with additive uniform noise and rescale them to produce $[0, 1]$ bound vectors. Formally, label smoothing is defined as follows:

$$\begin{aligned} \widetilde{o}_{t,j}^{(k)} &= o_{t,j}^{(k)} + \mathcal{U}_{[0,\gamma]}, \quad k = 0, \ldots, |D_t| \\ \widetilde{\boldsymbol{o}}_t &= \widetilde{\boldsymbol{o}}_t / \|\widetilde{\boldsymbol{o}}_t\| \end{aligned} \tag{26}$$

where γ is a parameter defined by the modeler. $\widetilde{\boldsymbol{o}}_t$ now corresponds to a noisy version of the original one-hot encoded vector $\boldsymbol{o}_t$.

An issue with applying label smoothing is that the generator output tries to match the distorted representation of the data, and so the generator probability outputs will be biased towards low proability values. To address this, we propose here to apply equivalent smoothing to the generator output before passing it to the discriminator:

$$\begin{aligned} \widetilde{o}_{t,j}^{\mathbf{synth},(k)} &= o_{t,j}^{\mathbf{synth},(k)} + \mathcal{U}_{[0,\gamma]}, \quad k = 0, \ldots, |D_t| \\ \widetilde{\boldsymbol{o}}_t^{\mathbf{synth}} &= \widetilde{\boldsymbol{o}}_t^{\mathbf{synth}} / \|\widetilde{\boldsymbol{o}}_t^{\mathbf{synth}}\| \end{aligned} \tag{27}$$

where γ should match the parameter used for the input smoothing. It removes the bias in the generator output and, thus, it is effectively trying to learn the original $[0, 1]$ representations. Therefore, it produces unbiased probabilities. We refer to this as two-sided label smoothing.

To investigate the benefits of label smoothing, we systematically investigate three possible strategies for categorical variables:

$$\text{no label smoothing:} \quad \boldsymbol{l}_0^{\mathtt{NO}} = \begin{cases} \boldsymbol{w}_{1:N_C} \oplus \boldsymbol{p}_{1:N_C} \oplus \boldsymbol{o}_{1:N_D} & \text{for original data} \\ \boldsymbol{w}_{1:N_C}^{\mathbf{synth}} \oplus \boldsymbol{p}_{1:N_C}^{\mathbf{synth}} \oplus \boldsymbol{o}_{1:N_D}^{\mathbf{synth}} & \text{for synthetic data} \end{cases} \tag{28}$$

$$\text{one-sided label smoothing:} \quad \boldsymbol{l}_0^{\mathtt{OS}} = \begin{cases} \boldsymbol{w}_{1:N_C} \oplus \boldsymbol{p}_{1:N_C} \oplus \widetilde{\boldsymbol{o}}_{1:N_D} & \text{for original data} \\ \boldsymbol{w}_{1:N_C}^{\mathbf{synth}} \oplus \boldsymbol{p}_{1:N_C}^{\mathbf{synth}} \oplus \boldsymbol{o}_{1:N_D}^{\mathbf{synth}} & \text{for synthetic data} \end{cases} \tag{29}$$

$$\text{two-sided label smoothing:} \quad \boldsymbol{l}_0^{\mathtt{TS}} = \begin{cases} \boldsymbol{w}_{1:N_C} \oplus \boldsymbol{p}_{1:N_C} \oplus \widetilde{\boldsymbol{o}}_{1:N_D} & \text{for original data} \\ \boldsymbol{w}_{1:N_C}^{\mathbf{synth}} \oplus \boldsymbol{p}_{1:N_C}^{\mathbf{synth}} \oplus \widetilde{\boldsymbol{o}}_{1:N_D}^{\mathbf{synth}} & \text{for synthetic data} \end{cases} \tag{30}$$

3.4.4 Sampling

Once the generator has been trained against the discriminator, we need to be able to generate the final synthetic dataset $\mathbf{T}_{\mathbf{synth}}$. However, the dataset created by the generator $\widehat{\mathbf{T}}_{\mathbf{synth}}$ corresponds to the encoded dataset $\widehat{\mathbf{T}}$. Therefore, we need to decode $\widehat{\mathbf{T}}_{\mathbf{synth}}$ to obtain the final synthetic dataset.

In previous works (Xu and Veeramachaneni, 2018; Xu et al., 2019), the synthetic value is sampled from the probability distribution by simply assigning the value to the highest probability class (*i.e.* $\arg\max$ assignment). However, this approach does not result in representative mode shares. Instead, as is typical in choice modeling scenarios (Ben-Akiva

and Lerman, 1985), we propose to sample the synthetic value through simulation, *i.e.* drawing according to the output probability values (without any label smoothing applied). Thus, for categorical variables, we have two different ways to obtain the final value:

$$d_{t,j}^{\mathbf{synth},\arg\max} = \arg\max \boldsymbol{o}_{t,j}^{\mathbf{synth}} \tag{31}$$

$$d_{t,j}^{\mathbf{synth},\texttt{simul}} = \texttt{simulation}\left[\boldsymbol{o}_{t,j}^{\mathbf{synth}}\right] \tag{32}$$

Similary, by inverting Equation 19, we have for continuous variables:

$$c_{t,j}^{\mathbf{synth},\arg\max} = \delta w_{t,j}^{\mathbf{synth},(k)}\sigma_t^{(k)} + \eta_t^{(k)} \qquad \text{where } k = \arg\max \boldsymbol{p}_{t,j}^{\mathbf{synth}} \tag{33}$$

$$c_{t,j}^{\mathbf{synth},\texttt{simul}} = \delta w_{t,j}^{\mathbf{synth},(k)}\sigma_t^{(k)} + \eta_t^{(k)} \qquad \text{where } k = \texttt{simulation}\left[\boldsymbol{p}_{t,j}^{\mathbf{synth}}\right] \tag{34}$$

where δ corresponds to the same values used to encode the continuous variables $\boldsymbol{c}_t$ in Section 3.4.1.

In order to test the impacts of simulation versus maximum probability assignment for the categorical and continuous variables, we systematically test four different sampling strategies:

$$\text{Only } \arg\max: \quad \mathbf{T}_{\mathbf{synth}}^{\texttt{AA}} = \left\{\boldsymbol{c}_{1:N_C}^{\mathbf{synth},\arg\max}, \boldsymbol{d}_{1:N_D}^{\mathbf{synth},\arg\max}\right\} \tag{35}$$

$$\texttt{simulation} \text{ for continuous and } \arg\max \text{ for categorical}: \quad \mathbf{T}_{\mathbf{synth}}^{\texttt{SA}} = \left\{\boldsymbol{c}_{1:N_C}^{\mathbf{synth},\texttt{simul}}, \boldsymbol{d}_{1:N_D}^{\mathbf{synth},\arg\max}\right\} \tag{36}$$

$$\arg\max \text{ for continuous and } \texttt{simulation} \text{ for categorical}: \quad \mathbf{T}_{\mathbf{synth}}^{\texttt{AS}} = \left\{\boldsymbol{c}_{1:N_C}^{\mathbf{synth},\arg\max}, \boldsymbol{d}_{1:N_D}^{\mathbf{synth},\texttt{simul}}\right\} \tag{37}$$

$$\text{Only } \texttt{simulation}: \quad \mathbf{T}_{\mathbf{synth}}^{\texttt{SS}} = \left\{\boldsymbol{c}_{1:N_C}^{\mathbf{synth},\texttt{simul}}, \boldsymbol{d}_{1:N_D}^{\mathbf{synth},\texttt{simul}}\right\} \tag{38}$$

As a side note, we would like to add that the sampling process is entirely independent of the optimization process of both the generator and the discriminator. It is, therefore, possible to train a single model and test the different sampling methods afterward.

The supplementary materials summarize the possible DATGAN versions using the proposed loss functions, label smoothing strategies, and sampling strategies. In addition, we compare these versions against each other in order to select the best-performing one.

3.5 Result assessments

For assessing the quality of synthetic datasets, compared to the original datasets, we use two main methods: (i) a statistical method; (ii) a machine learning-based method. The goal of the first method (see Section 3.5.1) is to verify that the synthetic datasets display the same statistical properties compared to the original dataset. In order to do this, we compare the distributions of each column individually between the synthetic datasets and the original datasets. We then test combinations of multiple columns to study if the models can grasp more complex correlations between the variables. The second method (see Section 3.5.2) is closer to a real-world problem one can face. Indeed, the goal is to study if the synthetic datasets can be used in classification/regression context in Machine Learning.

3.5.1 Statistical tests

For the statistical tests, we build on existing approaches in the transportation literature (Garrido et al., 2019; Borysov et al., 2019; Badu-Marfo et al., 2020). The idea is to compute frequency lists (i.e. frequency count of each unique value) for each column on both the original dataset $\boldsymbol{\pi}$ and the synthetic dataset $\boldsymbol{\pi}^{\mathbf{synth}}$. In the literature, authors typically only calculate the frequency lists for single columns (i.e. marginal distributions) for a few relevant variables and test them against each other. In this paper, we build on this in two ways: (i) calculating joint frequency lists for n columns simultaneously (therefore assessing joint distributions of order n) and (ii) systematically testing all possible combinations of columns at each aggregation level.

If we only compute only the frequency lists for single variables, we will only assess the marginal distribution of each variable independently. Whilst this verifies whether each column of the synthetic data matches distribution of the corresponding column in the original data, it does not provide any information of the correlations between the columns in either the synthetic or original data (i.e. it assesses each column independently of all other columns). To assess whether relationships between variables in the the synthetic data matches that of the original data, it is necessary to investigate the joint distributions of multiple columns simultaneously. To address this, we calculate the joint frequency

25

lists for multiple columns simultaneously. Furthermore, at each aggregation level (i.e. number of columns), we calculate the frequency lists for all possible combinations of columns.

Since the number of possible combinations is at each aggregation level increases factorially, we limit the level of aggregation to one, two, or three columns as follows:

First order: Columns are compared to each other separately. It returns N_V different aggregated lists.

Second order: Columns are aggregated two-by-two, giving $\binom{N_V}{2}$ different aggregated lists.

Third order: Columns are aggregated three-by-three, giving $\binom{N_V}{3}$ different aggregated lists.

Note that continuous variables must be binned to calculate frequency lists. We arbitrarily set the number of bins for each continuous column to 10, such that the second order and third order frequency lists of continuous columns will have 100 and 1000 unique values respectively.

Once these frequency lists have been computed, we can compare them using standard statistic metrics defined in the literature. We select five different metrics:

- Mean Absolute Error:

$$\text{MAE}\left(\boldsymbol{\pi}^{\textbf{synth}}, \boldsymbol{\pi}\right) = \frac{\sum_{i=1}^{N_{\text{cnt}}} |\pi_i^{\textbf{synth}} - \pi_i|}{N_{\boldsymbol{pi}}} \tag{39}$$

  where $N_{\boldsymbol{\pi}}$ corresponds to the size of the frequency list $\boldsymbol{\pi}$.

- Root Mean Square Error:

$$\text{RMSE}\left(\boldsymbol{\pi}^{\textbf{synth}}, \boldsymbol{\pi}\right) = \left(\frac{\sum_{i=1}^{N_{\text{cnt}}} \left(\pi_i^{\textbf{synth}} - \pi_i\right)^2}{N_{\text{cnt}}}\right)^{1/2} \tag{40}$$

- Standardized Root Mean Square Error (Müller and Axhausen, 2011):

$$\text{SRMSE}\left(\boldsymbol{\pi}^{\textbf{synth}}, \boldsymbol{\pi}\right) = \frac{\text{RMSE}\left(\boldsymbol{\pi}^{\textbf{synth}}, \boldsymbol{\pi}\right)}{\overline{\boldsymbol{\pi}}} \tag{41}$$

  where $\overline{\boldsymbol{\pi}}$ corresponds to the average value of $\boldsymbol{\pi}$.

- Coefficient of determination:

$$R^2\left(\boldsymbol{\pi}^{\textbf{synth}}, \boldsymbol{\pi}\right) = 1 - \frac{\sum_{i=1}^{N_{\text{cnt}}} \left(\pi_i^{\textbf{synth}} - \pi_i\right)^2}{\sum_{i=1}^{N_{\text{cnt}}} \left(\overline{\pi}_i - \pi_i\right)^2} \tag{42}$$

- Pearson's correlation:

$$\rho_{\text{Pearson}}\left(\boldsymbol{\pi}^{\textbf{synth}}, \boldsymbol{\pi}\right) = \frac{\text{cov}\left(\boldsymbol{\pi}^{\textbf{synth}}, \boldsymbol{\pi}\right)}{\sigma_{\boldsymbol{\pi}}\sigma_{\boldsymbol{\pi}^{\textbf{synth}}}} \tag{43}$$

  where cov corresponds to the covariance matrix and $\sigma_{\boldsymbol{X}}$ the standard deviation of a given vector $\boldsymbol{X}$.

Finally, the results can be averaged over all combinations to obtain a single number per synthetic dataset, statistic, and aggregation level.

3.5.2 Supervised learning-based validation

We propose in this paper a new supervised learning-based validation method for synthetic data which makes use of supervised classification and regression models to approximate the full conditional distributions of each variable, given all other variables in the dataset. The general approach is to estimate two regression or classification models for each variable $\boldsymbol{v}_t$. The first model (m_t) is estimated on a training portion of the original data, and the second ($m_t^{\textbf{synth}}$) is estimated on a corresponding training portion of the synthetic data. In each case, the model tries to predict the values in the corresponding column conditional on all other columns in the dataset.

Each model is then validated on the same test portion of the original data, providing two loss scores. The expected value of the loss of the model estimated on the synthetic data (which approximates the conditionals in the synthetic dataset) should be greater than or equal to the expected loss of the model estimated on the original data (which approximates the

---
Algorithm 3 Supervised learning-based validation

Input: Original data $\mathbf{T}$, synthetic data $\mathbf{T_{synth}}$
Output: Similarity score for each variable $\boldsymbol{v}_t \in \mathbf{T}$
1: **for all** $\boldsymbol{v}_t \in \mathbf{T}$ **do**
2:      $\boldsymbol{y}_t = \boldsymbol{v}_t$
3:      $\boldsymbol{X}_t = \mathbf{T} \setminus \boldsymbol{v}_t$
4:      Divide $\boldsymbol{y}_t$ and $\boldsymbol{X}_t$ into training set $(\boldsymbol{y}_{t,\text{train}}, \boldsymbol{X}_{t,\text{train}})$ and test set $(\boldsymbol{y}_{t,\text{test}}, \boldsymbol{X}_{t,\text{test}})$
5:      $\boldsymbol{y}_t^{\mathbf{synth}} = \boldsymbol{v}_t^{\mathbf{synth}}$
6:      $\boldsymbol{X}_t^{\mathbf{synth}} = \mathbf{T_{synth}} \setminus \boldsymbol{v}_t^{\mathbf{synth}}$
7:      Sample training set $(\boldsymbol{y}_{t,\text{train}}^{\mathbf{synth}}, \boldsymbol{X}_{t,\text{train}}^{\mathbf{synth}})$ from $\boldsymbol{y}_t^{\mathbf{synth}}$ and $\boldsymbol{X}_t^{\mathbf{synth}}$, with the same dimensions as $(\boldsymbol{y}_{t,\text{train}}, \boldsymbol{X}_{t,\text{train}})$.
8:      **if** $\boldsymbol{v}_t \in \boldsymbol{c}_{1:N_C}$ **then**
9:          Estimate regression model $m_{t,\text{reg}}$ on $(\boldsymbol{y}_{t,\text{train}}, \boldsymbol{X}_{t,\text{train}})$
10:          Estimate regression model $m_{t,\text{reg}}^{\mathbf{synth}}$ on $(\boldsymbol{y}_{t,\text{train}}^{\mathbf{synth}}, \boldsymbol{X}_{t,\text{train}}^{\mathbf{synth}})$
11:          $g_t^{\text{reg}} = \mathcal{L}_{\text{MSE}}(\boldsymbol{y}_{t,\text{test}}, m_{t,\text{reg}}^{\mathbf{synth}}(\boldsymbol{X}_{t,\text{test}})) / \mathcal{L}_{\text{MSE}}(\boldsymbol{y}_{t,\text{test}}^{\mathbf{synth}}, m_{t,\text{reg}}(\boldsymbol{X}_{t,\text{test}}^{\mathbf{synth}}))$
12:          **return** g_t^{reg}
13:      **else**
14:          Estimate probabilistic classification model $m_{t,\text{class}}$ on $(\boldsymbol{y}_{t,\text{train}}, \boldsymbol{X}_{t,\text{train}})$
15:          Estimate probabilistic classification model $m_{t,\text{class}}^{\mathbf{synth}}$ on $(\boldsymbol{y}_{t,\text{train}}^{\mathbf{synth}}, \boldsymbol{X}_{t,\text{train}}^{\mathbf{synth}})$
16:          $g_t^{\text{class}} = \mathcal{L}_{\text{log-loss}}(\boldsymbol{y}_{t,\text{test}}, m_{t,\text{class}}^{\mathbf{synth}}(\boldsymbol{X}_{t,\text{test}})) - \mathcal{L}_{\text{log-loss}}(\boldsymbol{y}_{t,\text{test}}^{\mathbf{synth}}, m_{t,\text{class}}(\boldsymbol{X}_{t,\text{test}}^{\mathbf{synth}}))$
17:          **return** g_t^{class}
---

true conditionals in the original data). The closer the loss scores of the models estimated on the synthetic and original data, the more closely the synthetic data has captured the conditional distributions of the original data. The approach is detailed in Algorithm 3.

We make use of gradient boosting ensembles of decision trees for both $m_{\text{reg},t}$ and $m_{\text{class},t}$ as (i) they can be easily applied to both regression and probabilistic classification problems; (ii) are computationally efficient to estimate; (iii) have been shown to have high predictive performance on a wide variety of supervised learning tasks; (iv) can determine appropriate regularisation automatically using early stopping. We specifically make use of the LightGBM library (Ke et al., 2017) which inherently handles categorical input features, thus avoiding the need for one-hot encoding of categorical variables.

For continuous variables, the score g_t^{reg} is the ratio of the mean-squared error of the model estimated on the synthetic dataset to the mean-squared error of the model estimated on the original dataset, with a score of 1 indicating a perfect match, and a higher score representing a worse fit. For categorical variables, the score g_t^{class} is the absolute difference between the normalized log-loss of the model estimated on the synthetic dataset and the normalized log-loss of the model estimated on the original dataset, with a score of 0 indicating a perfect match, and a higher score representing a worse fit. The scores can be summed over all columns to give aggregate scores for all continuous and categorical variables, respectively.

While Algorithm 3 describes a single train-test split, the same algorithm can be used with k-fold cross-validation to obtain more accurate estimates of the model losses. We use 5-fold cross-validation and stratified sampling to select training folds for the categorical data.

3.6   Implementation notes

The code for the DATGAN has been implemented using Python 3.7.9. We use the libraries `tensorflow` (v1.15.5) (Abadi et al., 2016) and `tensorpack` (v0.9.4) (Yuxin, 2016) for the main components of the neural networks. In addition, we use the library `networkx` (v2.5) (Hagberg et al., 2008) for specifying the DAG $\mathcal{G}$ discussed in Section 3.1.1. This library already has built-in functions to verify that a user-specified graph is a directed acyclic graph.

For the optimization process using the different loss functions presented in Section 3.3, we follow the instructions of the authors of the different articles for the hyperparameters. During initial tests, we investigated different values of the learning rate and decided on the following learning rates for each loss, which appeared to work best in these initial tests:

Standard loss learning rate of $1 \cdot 10^{-3}$

Wasserstein loss learning rate of $2 \cdot 10^{-4}$

Wasserstein loss with gradient-penalty learning rate of $1 \cdot 10^{-4}$

We do not provide any specific results for this hyperparameter since it is not the main focus of our article. Finally, the sizes of the different components presented in the methodology are directly given in the notation table in the supplementary materials.

The complete code for this project, including the different versions of the DATGAN, the case studies, and the results, can be found on Github: https://github.com/glederrey/SynthPop. A Python library has been created with the original DATGAN model as well as an updated version written with `tensorflow` (v2.8.0). The code can be found here: https://github.com/glederrey/DATGAN.

4 Case studies

In this section, we present the case study for this article. First, we introduce the datasets in Section 4.1. For each dataset, we provide a short description of the dataset, a summary of the variables, and the DAG used in the DATGAN. Then, in Section 3.5, we present the new methods used to assess the quality of the synthetic datasets generated by all the models presented in this article. Finally, Section 4.2 gives a detailed overview of the training method used with all the models in order to bring as much fairness as possible in the comparison of the models.

4.1 Datasets

The first dataset is a travel survey made by the Chicago Metropolitan Agency for Planning. We named this dataset CMAP. The original dataset is a household travel survey of the Chicago metropolitan area, conducted from January 2007 to February 2008. The trips are given as one and two-day travel diaries, provided by all the members of the households. The data is therefore hierarchical. The dataset has first been cleaned to remove incomplete entries. Then, we selected one unique trip per individual per household for the final dataset to remove data leakage. It thus contains a total of 8'929 trips with 15 columns. A complete description of this dataset is given in Table 8 in the appendix. The DAG used for the DATGAN with this dataset can also be found in the appendix; see Figure 7.

The second dataset is the London Passenger Mode Choice (LPMC) dataset (Hillel et al., 2018). It combines the London Travel Demand Survey (LTDS) records with matched trip trajectories and corresponding mode alternatives. The LTDS has been conducted between April 2012 and March 2015 and records trips made by individuals residing within Greater London. The trip trajectories are extrapolated from Google Maps API. The final dataset has been processed to not lead to data leakage. Similar to the CMAP dataset, we selected only one trip per household. The final dataset contains a total of 17'616 trips with 27 columns. A complete description of this dataset is given in Table 9 in the appendix. The DAG used for the DATGAN with this dataset can also be found in the appendix; see Figure 8. In addition, we created a smaller version of the LPMC dataset by randomly selecting 50% of the rows for testing the DATGAN versions. This dataset is conveniently named LPMC_half. We mainly use it to understand the effect of the number of rows on the performance of the models.

The third and final dataset is the ADULT dataset (Kohavi, 1996), also known as the Census-Income dataset. This dataset contains socio-economic variables on multiple individuals to predict if their income is below or above $50k/yr. From the original dataset, we removed all the rows with unknown values. A complete description of this dataset is given in Table 10 in the appendix. The DAG used for the DATGAN with this dataset can also be found in the appendix; see Figure 9. Due to its larger size compared to the other datasets, the ADULT dataset is only used when comparing the DATGAN with state-of-the-art models.

Table 3: Summary of the datasets used in the case studies. Full description of the datasets can be found in the Appendix.

Name	#columns	#continuous	#categorical	#rows
CMAP	15	3	12	8'929
LPMC	27	13	14	17'616
LPMC_half	27	13	14	8'808
ADULT	14	4	10	45'222

4.2 Training process

This article aims to propose a new way to generate synthetic data. However, for fairness towards state-of-the-art methods in the literature, we need to test all these generative models on a similar playground. We, thus, decide to train every model on 1'000 epochs with a batch size N_b of 500, even if the optimization process could be stopped earlier. In addition, we decided to keep the original hyperparameters provided in the articles. While optimizing these parameters would most likely lead to better results, most users would use the models as the authors provide them. In addition, each model is trained five times on each dataset, and each of the five models generates five synthetic datasets with the same number of rows as the original dataset. This means that each test is performed on a total of 25 synthetic datasets. Thus, the results provided in Section 5 correspond to the average value of the performed tests.

The training process is slightly different for the DATGAN versions (summary given in the supplementary materials). Indeed, the sampling can be done independently after the training process. Therefore, we only have to train a total of nine different models (combinations of loss functions and label smoothing). Each of these models is trained five times. Then, for each of these 45 models, we use the four different sampling methods to produce five synthetic datasets for each method. Therefore, we get a total of 900 synthetic datasets to be compared, *i.e.* 25 synthetic datasets for each model presented in the summary table in the supplementary materials for each case study presented in Section 4.1.

5 Results

In this section, we present the results obtained using the assessment methods presented in Section 3.5 on the different case studies presented in Section 4. The first section, see Section 5.1, compares the DATGAN against state-of-the-art models found in the literature. The second section, see Section 5.2, performs a sensitivity analysis on the DAG used for the DATGAN in order to understand its effect on the performance of the model.

In the supplementary materials, we analyze the results of the possible DATGAN versions. We provide here the conclusions of this analysis. The reader may refer to this document for more information. Across all case studies, the DATGAN performs better when using the two-sided label smoothing and the simulation sampling strategy for both continuous and categorical variables. However, we have found that using the WGAN loss function leads to better results on datasets with fewer variables, such as the CMAP dataset. On the other hand, the WGGP loss performs better on the LPMC dataset. Since the comparison of DATGAN version was not performed on the ADULT dataset (due to its larger size compared to the other case studies), we will test both the WGAN and the WGGP loss functions for this case study. Results on the other case studies indicate that the WGAN loss should outperform the WGGP loss.

5.1 Comparison with state-of-the-art models

At this point of the article, we have presented our new model for generating synthetic datasets and have selected the best version depending on the type of case study. In addition, we have studied the effect of the DAG on the generated synthetic data. However, we now want to compare our model against state-of-the-art models presented in the literature. We, thus, test our DATGAN model against the four models presented in the literature (see Section 2.3) on the four different case studies. We use the same assessment methods as previously to compare all the models. We have compiled all the results in Table 4. It shows the average rankings on both assessment methods for the four different case studies. We see that the DATGAN model outperforms all the other models in the first three case studies. For example, it is consistently the best model when using the Machine Learning efficacy method. For the ADULT case study, we decided to test the DATGAN with the WGAN and the WGGP loss functions. Since the ADULT dataset contains more categorical variables than continuous, we expect the WGAN loss to perform better, as it is shown in Table 4. It performs the best on the statistical assessments. However, it seems to struggle with the Machine Learning efficacy method. While the results are quite close on the continuous variables, the two DATGAN models are the only models that do not fail the test on the categorical variables. Indeed, it seems that the other models tend not to produce enough of the low probability categories. Thus, these models tend to oversimplify the generated synthetic data compared to the DATGAN models. One of the reasons why such a thing happens might come from the sampling process. Indeed, using simulation to get the final categories allows for more representation of the low probability values than using the maximum probability estimator.

Since we compared models across multiple articles, it is interesting to look at their conclusions. For example, Xu et al. (2019) show that their CTGAN model is consistently outperforming the TVAE model. We see the same ranking between the two models except for the ADULT case study. Therefore, we can draw the same conclusion on these two models as the authors. However, Zhao et al. (2021) claim that the CTAB-GAN outperforms the CTGAN across all their assessments. In our case, we see that the CTAB-GAN outperforms the CTGAN only when the case studies contain a small number of data points. While we have used both models as intended to be used by their authors, we only changed

Table 4: Average rankings of the state-of-the-art models against the DATGAN on the four case studies.

Name	Avg. rank stats	Avg. rank ML	rank
CMAP case study			
DATGAN (WGAN)	**1.00**	**1.0**	**1.00**
CTAB-GAN	2.92	2.5	2.71
TGAN	2.60	3.0	2.80
CTGAN	4.24	4.0	4.12
TVAE	4.24	4.5	4.37
LPMC case study			
DATGAN (WGGP)	**1.00**	**1.0**	**1.00**
TGAN	2.36	2.5	2.43
CTGAN	3.04	3.0	3.02
CTAB-GAN	4.08	3.5	3.79
TVAE	4.52	5.0	4.76
LPMC_half case study			
DATGAN (WGGP)	**1.08**	**1.0**	**1.04**
TGAN	2.60	2.5	2.55
CTAB-GAN	3.04	4.0	3.52
CTGAN	3.64	3.5	3.57
TVAE	4.64	4.0	4.32
ADULT case study			
DATGAN (WGAN)	**1.08**	**3.0**	**2.04**
TGAN	1.92	3.5	2.71
DATGAN (WGGP)	3.32	3.5	3.41
TVAE	3.80	3.5	3.65
CTGAN	4.88	**3.0**	3.94
CTAB-GAN	6.00	4.5	5.25

the final number of epochs. In their article, Zhao et al. (2021) have trained both models on 150 epochs. Therefore, the CTAB-GAN may be providing a better early optimization process than the CTGAN. However, further work would be required to analyze this result, and it is out of the scope of this article.

In addition, we have tested both models presented by Garrido et al. (2019): a WGAN and a VAE. Unfortunately, results are not shown in the article because both models failed to produce adequate continuous variables. Indeed, the encoding of continuous variables is done such that they are binned based on their original distributions, thus treating them as categorical variables. This, therefore, lead to especially poor results when comparing continuous distributions.

5.2 Sensitivity analysis of the DAG

In this section, we want to analyze how the DAG can affect the performances of the DATGAN and how it can be used to modify the generation of synthetic datasets. Section 5.2.1 performs the analysis on the DAG using different versions of the latter, and Section 5.2.2 explains how we can alter the DAG to generate hypothetical synthetic datasets.

5.2.1 Structure of the DAG

In the previous section, we have analyzed all the different versions of the DATGAN to select the best one. However, in this section, we want to investigate how the DAG will influence the results. Thus, we only use the best possible model for each case study. The idea is to start with the DAG presented in the appendix for each case study and make variations of it to study the generated datasets. Therefore, we created five different DAGs for each case study:

- `full`: Complete DAG presented in the appendix for each case study.
- `trans. red.`: Transitive reduction of the `full` DAG. The transitive reduction consists in removing as many edges as possible in a DAG such that there exists only one path between two vertices in the graph.
- `linear`: This DAG consists in taking the variables in the order provided by the dataset and linking them to each other linearly. Thus, there are no multi-inputs within the DAG. This is similar to the technique used in the TGAN (Xu and Veeramachaneni, 2018).
- `prediction`: This DAG consists of only one sink node. All the other nodes are considered source nodes linked to the sink node. The source nodes are not linked to each other. The sink nodes are the `choice` for the CMAP case study and the `travel_mode` for the LPMC case studies.
- `no links`: This DAG consists of only nodes without any edges. This, thus, cuts all the links between the variables.

At first glance, we can already predict that the last two DAGs should all perform badly since the connections between them are either badly implemented or absent. However, we are mostly interested in the first three DAGs. Indeed, if the DAG can help the model to generate more representative synthetic data, the `full` DAG or the `trans. red.` DAG should outperform the `linear` DAG. As for the previous section, the details of the results are given in the supplementary materials. Table 5 shows the rankings of the DAGs on the CMAP case study. As expected, the best two DAGs are the two complete ones. It is interesting to note that the `full` DAG provides better results on the Machine Learning efficacy assessment while the `trans. red.` provides better results on the statistical assessments. Since the model with the `full` DAG contains more edges than the other DAGs, it is, therefore, larger and more complex to train. Thus, this can hurt the LSTM cells' performance when creating the synthetic variables. However, the correlations between the variables are better with the complete DAG since it always performs best compared to the other DAGs.

Table 5: Average rankings of the different DAGs on the CMAP dataset

Name	Avg. rank stats	Avg. rank ML	rank
`trans. red.`	**1.96**	2.0	**1.98**
`full`	3.04	**1.0**	2.02
`linear`	2.80	3.0	2.90
`prediction`	3.80	4.0	3.90
`no links`	3.40	5.0	4.20

The CMAP dataset is relatively small. Therefore, learning the correlations between the variables can be pretty difficult. The LPMC dataset, on the other hand, is twice as big. It is thus interesting if the DAG can still provide the same kind of help on a larger dataset. Table 6 shows the rankings of the DAG on the LPMC case study. We see that this time, the `linear` DAG is the best one, closely followed by the two complete DAGs. While the `full` DAG has some issues with the statistical assessments, it remains the best on the Machine Learning efficacy method. Therefore, it seems that if one wants to generate a synthetic dataset with column data as close as possible to the original dataset, a smaller dataset leads to better results. However, if one wants to keep as much correlation as possible, one should opt for a complete DAG.

Table 6: Average rankings of the different DAGs on the LPMC dataset

Name	Avg. rank stats	Avg. rank ML	rank
`linear`	**2.08**	2.0	**2.04**
`full`	2.80	**1.5**	2.15
`trans. red.`	2.16	2.5	2.33
`prediction`	4.00	4.0	4.00
`no links`	3.96	5.0	4.48

Finally, we want to confirm our hypothesis that the completeness of the DAG is less important with more data points. We, thus, make the same tests on the smaller LPMC case study. Table 7 shows the rankings of the DAG on the

LPMC_half case study. Results show that the `linear` DAG performs better than the `full` DAG on both metrics. At first glance, this result can be quite surprising. However, when we look at the DAG for both the CMAP and the LPMC case study, we see that the LPMC DAG is much more complex than the CMAP DAG. Indeed, the CMAP DAG contains a total of 25 edges for 15 nodes for an average of $1.\bar{6}$ edges per node. On the other hand, the LPMC DAG contains a total of 63 edges for 27 nodes for an average of $2.\bar{3}$ edges per node. It is, thus, possible that the model struggles to train correctly with a more complex DAG. However, we see that the `trans. red.` version of the LPMC DAG leads to even worse results than the `full` DAG. Therefore, it might also be possible that this DAG is not well constructed for this particular case study. It, thus, requires further investigation to fully understand how the DAG affects the results of this case study.

Table 7: Average rankings of the different DAGs on the LPMC_half dataset

Name	Avg. rank stats	Avg. rank ML	rank
linear	**1.84**	**1.0**	**1.42**
full	2.04	2.0	2.02
trans. red.	3.76	3.0	3.38
prediction	4.08	4.0	4.04
no links	3.28	5.0	4.14

5.2.2 Effect of the DAG on the synthetic dataset

The final section of the results shows what can be achieved with the DAG depending on the desire of the modeler. Indeed, we have shown that using a complete DAG allows generating the best possible synthetic datasets compared to state-of-the-art models. However, the DAG can also be used to create hypothetical synthetic datasets. Since the DAG controls the causal links between the variables, removing any relationships between two or more variables is simple. For example, in the CMAP case study, we could imagine a hypothetical population with no minimum age requirement to get a driving license. In order to achieve this, we can simply remove the link between the variables `age` and `license` in the DAG presented in Figure 7. If the modeler wants to ensure that two variables do not interact, these variables should be defined as source nodes in the DAG. Figure 6 shows the age distributions for the original CMAP dataset, for a synthetic dataset generated with a complete DAG, and for a synthetic dataset generated with the altered DAG. The top figure distribution shows the distribution of the variable `age` in all of the datasets. As we can see, the synthetic probability distributions are quite similar to the original probability distributions. However, if we look at the age distribution when the individual owns a driving license (middle figure), we see that the synthetic dataset with the altered DAG still produces individuals of age lower than 18 owning a driving license. It is also the case with the synthetic dataset generated from a complete DAG. However, the number of minors with a driving license is marginally less than the data generated with the altered DAG. The effect of the altered DAG can be seen even better when looking at the age distribution of individuals not owning a driving license (bottom figure). Indeed, both the original and synthetic datasets with a complete DAG show most young individuals who do not own a driving license. However, the altered DAG produces the same type of distributions compared to the previous two. This, thus, shows that we eliminated the correlation between age and owning a driving license with the altered DAG.

Since the DAG can remove the correlations between variables altogether, the modeler must ensure that the source nodes used in the DAG do not have any correlations in the original dataset. This can be done by analyzing the data before creating the DAG. However, this is a small price to pay in order to be able to have more control on the dependencies between the variables.

6 Conclusion

This article presents a novel GAN architecture, the DATGAN, that integrates expert knowledge to control the causal links between the variables. In the methodology, we show how a Directed Acyclic Graph (DAG) can model the generator's structure and how synthetic variables are generated using Long-Short Term Memory (LSTM) cells. In addition, we provide an efficient way to encode categorical and continuous variables. While the core mechanics of the DATGAN remain the same, we explore different loss functions for training the DATGAN, the use of label smoothing on categorical variables, and multiple sampling methods. In order to compare the results as fairly as possible, we provide two new systematic assessment methods for comparing synthetic datasets: a statistical method and a Machine Learning efficacy method. Using these two methods, we show that two-sided label smoothing and using simulation
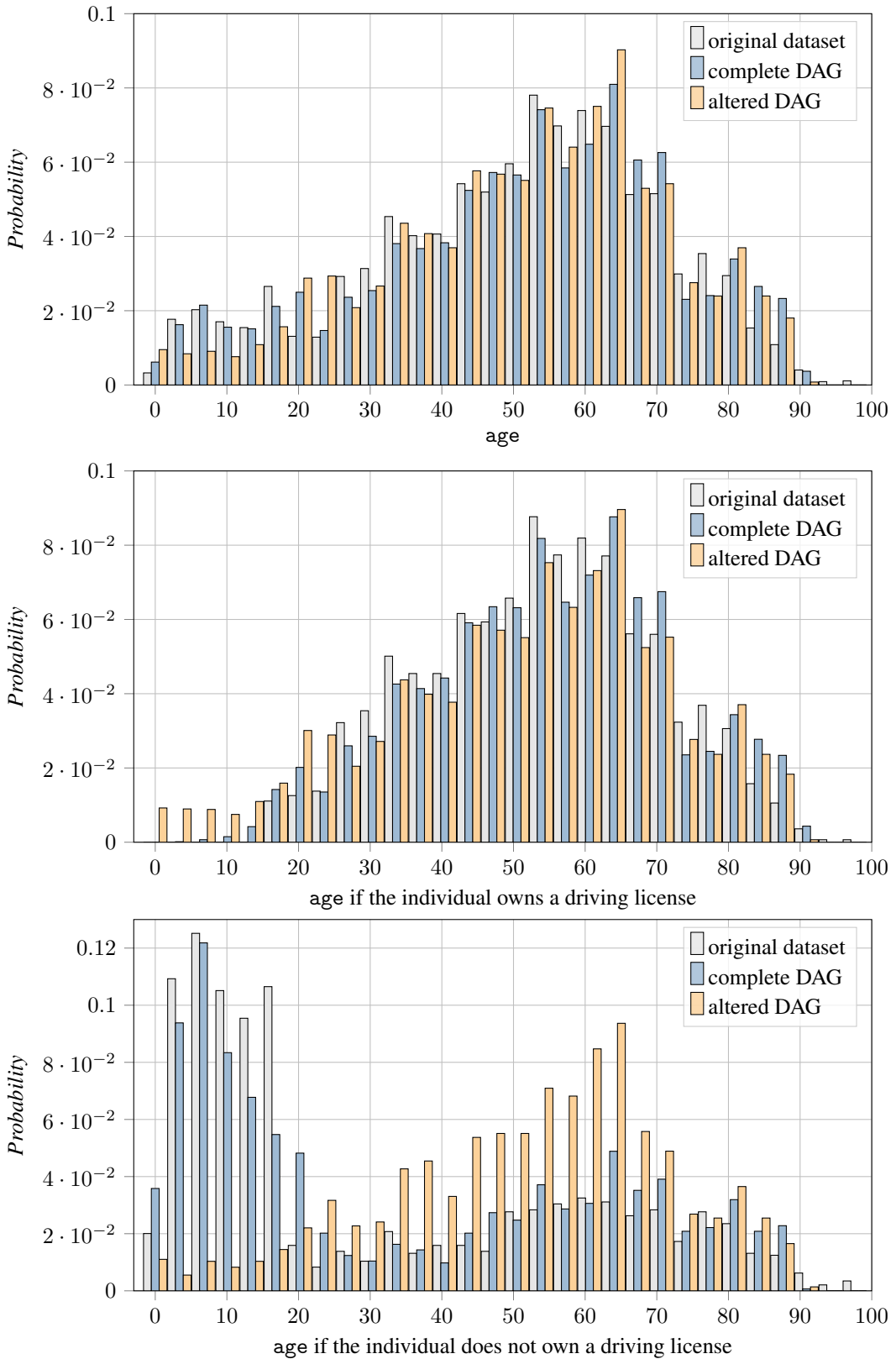
Figure 6: Age distributions for the original CMAP dataset, for a synthetic CMAP dataset with a complete DAG, and for a synthetic CMAP dataset with an altered DAG.

to sample the final synthetic variables lead to the best performances. The most optimal loss function, on the other hand, depends on the ratio of continuous and categorical variables. Indeed, if a dataset contains primarily categorical variables, we recommend using a `WGAN` loss function. On the contrary, if the dataset contains more continuous variables than categorical variables, we recommend using a `WGGP` loss function. We then show that using a complete DAG leads to better correlations in the final synthetic dataset than a stripped one. The optimal DATGAN models are then compared against state-of-the-art models. We show that the DATGAN models outperform all the other models on all the case studies using both assessment methods. Finally, we show how the DATGAN can create hypothetical synthetic populations.

The DATGAN architecture has been developed to improve the representativity of its generated synthetic data. Such datasets can then be used in simulations and might improve the latter's results since it has shown better results than other synthetic datasets generated by state-of-the-art models found in the literature. However, it might be possible to improve the DATGAN even further by upgrading the encoding of the tabular data. In the DATGAN, we have only considered two types of variables: continuous and categorical. However, Zhao et al. (2021) consider four different types of variables: continuous, categorical, mixed data, and integers. Therefore, a straightforward improvement to the DATGAN would be to add more data types in the encoding process. Indeed, if the encoding of the data is improved, the generated synthetic data will most likely improve as well. In addition, the DATGAN, as every other GAN, achieves differential privacy (Jordon et al., 2018) since the generator never sees the original data. Therefore, privacy preservation is generally not a concern for GANs. For the Machine Learning efficacy research axis, the DATGAN is already showing improvements thanks to the Machine Learning evaluation metric results. However, the DATGAN does not consider bias in the original data. Therefore, it also generates biased data. Thus, improving the bias correction of the DATGAN will also improve the Machine Learning efficacy. A simple fix that already exists in the literature is the use of conditionality on GANs. We could, thus, update the DATGAN such that it can conditionally generate synthetic data to reduce the bias in the data. Furthermore, one of the difficult tasks with the DATGAN is to create a good DAG to hinder the models' performances. While the relationship between some variables might be easy to find, it is more subtle for others. Therefore, it would be interesting to add a feature to combine multiple variables in a cluster such that they all influence each other without having to decide in which specific order. However, such an improvement might not work with the current design of the DATGAN using LSTM cells since each cell is assigned to a single variable. Therefore, a complete redesign of the DATGAN might be needed to implement such an improvement. Finally, we have discussed four of the five research axes presented in the literature review. The final axis is transfer learning. Researchers have already been working on this topic with synthetic image generators. Therefore, one of the future steps for synthetic tabular data generators is to follow this trend and start implementing models that can transfer knowledge between multiple datasets.

References

Abadi, Martín, Agarwal, Ashish, Barham, Paul, Brevdo, Eugene, Chen, Zhifeng, Citro, Craig, Corrado, Greg S., Davis, Andy, Dean, Jeffrey, Devin, Matthieu, Ghemawat, Sanjay, Goodfellow, Ian, Harp, Andrew, Irving, Geoffrey, Isard, Michael, Jia, Yangqing, Jozefowicz, Rafal, Kaiser, Lukasz, Kudlur, Manjunath, Levenberg, Josh, Mane, Dan, Monga, Rajat, Moore, Sherry, Murray, Derek, Olah, Chris, Schuster, Mike, Shlens, Jonathon, Steiner, Benoit, Sutskever, Ilya, Talwar, Kunal, Tucker, Paul, Vanhoucke, Vincent, Vasudevan, Vijay, Viegas, Fernanda, Vinyals, Oriol, Warden, Pete, Wattenberg, Martin, Wicke, Martin, Yu, Yuan, and Zheng, Xiaoqiang. TensorFlow: Large-Scale Machine Learning on Heterogeneous Distributed Systems. *arXiv:1603.04467 [cs]*, March 2016. URL http://arxiv.org/abs/1603.04467. arXiv: 1603.04467.

Alqahtani, Hamed, Kavakli-Thorne, Manolya, and Kumar, Gulshan. Applications of Generative Adversarial Networks (GANs): An Updated Review. *Archives of Computational Methods in Engineering*, 28(2):525–552, March 2021. ISSN 1886-1784. doi: 10.1007/s11831-019-09388-y. URL https://doi.org/10.1007/s11831-019-09388-y.

Arjovsky, Martin, Chintala, Soumith, and Bottou, Léon. Wasserstein GAN. *arXiv:1701.07875 [cs, stat]*, December 2017. URL http://arxiv.org/abs/1701.07875. arXiv: 1701.07875.

Auld, Joshua A., Mohammadian, Abolfazl (Kouros), and Wies, Kermit. Population Synthesis with Subregion-Level Control Variable Aggregation. *Journal of Transportation Engineering*, 135(9):632–639, September 2009. ISSN 0733-947X. doi: 10.1061/(ASCE)TE.1943-5436.0000040. URL https://ascelibrary.org/doi/abs/10.1061/%28ASCE%29TE.1943-5436.0000040. Publisher: American Society of Civil Engineers.

Ba, Jimmy Lei, Kiros, Jamie Ryan, and Hinton, Geoffrey E. Layer Normalization. *arXiv:1607.06450 [cs, stat]*, July 2016. URL http://arxiv.org/abs/1607.06450. arXiv: 1607.06450.

Badu-Marfo, Godwin, Farooq, Bilal, and Paterson, Zachary. Composite Travel Generative Adversarial Networks for Tabular and Sequential Population Synthesis. *arXiv:2004.06838 [cs, stat]*, April 2020. URL http://arxiv.org/abs/2004.06838. arXiv: 2004.06838.

Barbedo, Jayme Garcia Arnal. Impact of dataset size and variety on the effectiveness of deep learning and transfer learning for plant disease classification. *Computers and Electronics in Agriculture*, 153:46–53, October 2018. ISSN 0168-1699. doi: 10.1016/j.compag.2018.08.013. URL https://www.sciencedirect.com/science/article/pii/S0168169918304617.

Barthelemy, Johan and Toint, Philippe L. Synthetic Population Generation Without a Sample. *Transportation Science*, 47 (2):266–279, 2013. ISSN 0041-1655. URL https://www.jstor.org/stable/43666649. Publisher: INFORMS.

Beckman, Richard J., Baggerly, Keith A., and McKay, Michael D. Creating synthetic baseline populations. *Transportation Research Part A: Policy and Practice*, 30(6):415–429, November 1996. ISSN 0965-8564. doi: 10.1016/0965-8564(96)00004-3. URL http://www.sciencedirect.com/science/article/pii/0965856496000043.

Ben-Akiva, Moshe E. and Lerman, Steven R. *Discrete Choice Analysis: Theory and Application to Travel Demand*. MIT Press, 1985. ISBN 978-0-262-02217-0. Google-Books-ID: oLC6ZYPs9UoC.

Bishop, Christopher M. *Pattern Recognition and Machine Learning*. Springer: New York, 2006.

Bonabeau, Eric. Agent-based modeling: Methods and techniques for simulating human systems. *Proceedings of the National Academy of Sciences*, 99(suppl 3):7280–7287, May 2002. ISSN 0027-8424, 1091-6490. doi: 10.1073/pnas.082080899. URL https://www.pnas.org/content/99/suppl_3/7280. Publisher: National Academy of Sciences Section: Colloquium Paper.

Borysov, Stanislav S., Rich, Jeppe, and Pereira, Francisco C. How to generate micro-agents? A deep generative modeling approach to population synthesis. *Transportation Research Part C: Emerging Technologies*, 106:73–97, September 2019. ISSN 0968-090X. doi: 10.1016/j.trc.2019.07.006. URL http://www.sciencedirect.com/science/article/pii/S0968090X1831180X.

Casati, Daniele, Müller, Kirill, Fourie, Pieter J., Erath, Alexander, and Axhausen, Kay W. Synthetic Population Generation by Combining a Hierarchical, Simulation-Based Approach with Reweighting by Generalized Raking. *Transportation Research Record: Journal of the Transportation Research Board*, (2493), 2015. ISSN 0361-1981. URL https://trid.trb.org/view.aspx?id=1339142. ISBN: 9780309369633 Number: 15-5284.

Deming, W. Edwards and Stephan, Frederick F. On a Least Squares Adjustment of a Sampled Frequency Table When the Expected Marginal Totals are Known. *Annals of Mathematical Statistics*, 11(4):427–444, December 1940. ISSN 0003-4851, 2168-8990. doi: 10.1214/aoms/1177731829. URL https://projecteuclid.org/euclid.aoms/1177731829. Publisher: Institute of Mathematical Statistics.

Farooq, Bilal, Bierlaire, Michel, Hurtubia, Ricardo, and Flötteröd, Gunnar. Simulation based population synthesis. *Transportation Research Part B: Methodological*, 58:243–263, December 2013. ISSN 0191-2615. doi: 10.1016/j.trb.2013.09.012. URL http://www.sciencedirect.com/science/article/pii/S0191261513001720.

Frégier, Yaël and Gouray, Jean-Baptiste. Mind2Mind : transfer learning for GANs. *arXiv:1906.11613 [cs, stat]*, October 2020. URL http://arxiv.org/abs/1906.11613. arXiv: 1906.11613.

Garrido, Sergio, Borysov, Stanislav S., Pereira, Francisco C., and Rich, Jeppe. Prediction of rare feature combinations in population synthesis: Application of deep generative modelling. *arXiv:1909.07689 [cs, stat]*, September 2019. URL http://arxiv.org/abs/1909.07689. arXiv: 1909.07689.

Geman, Stuart and Geman, Donald. Stochastic Relaxation, Gibbs Distributions, and the Bayesian Restoration of Images. *IEEE Transactions on Pattern Analysis and Machine Intelligence*, PAMI-6(6):721–741, November 1984. ISSN 1939-3539. doi: 10.1109/TPAMI.1984.4767596. Conference Name: IEEE Transactions on Pattern Analysis and Machine Intelligence.

Gers, Felix A., Schmidhuber, Jürgen, and Cummins, Fred. Learning to Forget: Continual Prediction with LSTM. *Neural Computation*, 12(10):2451–2471, October 2000. ISSN 0899-7667. doi: 10.1162/089976600300015015. URL https://ieeexplore.ieee.org/document/818041. Conference Name: Neural Computation.

Goodfellow, Ian. NIPS 2016 Tutorial: Generative Adversarial Networks. *arXiv:1701.00160 [cs]*, April 2017. URL http://arxiv.org/abs/1701.00160. arXiv: 1701.00160.

Goodfellow, Ian J., Pouget-Abadie, Jean, Mirza, Mehdi, Xu, Bing, Warde-Farley, David, Ozair, Sherjil, Courville, Aaron, and Bengio, Yoshua. Generative Adversarial Networks. *arXiv:1406.2661 [cs, stat]*, June 2014. URL http://arxiv.org/abs/1406.2661. arXiv: 1406.2661.

Gulrajani, Ishaan, Ahmed, Faruk, Arjovsky, Martin, Dumoulin, Vincent, and Courville, Aaron. Improved Training of Wasserstein GANs. *arXiv:1704.00028 [cs, stat]*, December 2017. URL http://arxiv.org/abs/1704.00028. arXiv: 1704.00028.

Hagberg, Aric, Swart, Pieter, and Schult, Daniel. Exploring Network Structure, Dynamics, and Function Using NetworkX. In *Proceedings of the 7th Python in Science Conference*, United States, January 2008. URL https://www.researchgate.net/publication/236407765_Exploring_Network_Structure_Dynamics_and_Function_Using_NetworkX.

Hillel, Tim, Elshafie, Mohammed Z E B, and Jin, Ying. Recreating passenger mode choice-sets for transport simulation: A case study of London, UK. *Proceedings of the Institution of Civil Engineers - Smart Infrastructure and Construction*, 171(1):29–42, March 2018. doi: 10.1680/jsmic.17.00018. URL https://www.icevirtuallibrary.com/doi/full/10.1680/jsmic.17.00018.

Hochreiter, Sepp and Schmidhuber, Jürgen. Long Short-Term Memory. *Neural Computation*, 9(8):1735–1780, November 1997. ISSN 0899-7667. doi: 10.1162/neco.1997.9.8.1735. URL https://ieeexplore.ieee.org/abstract/document/6795963. Conference Name: Neural Computation.

Isola, Phillip, Zhu, Jun-Yan, Zhou, Tinghui, and Efros, Alexei A. Image-To-Image Translation With Conditional Adversarial Networks. pages 1125–1134, 2017. URL https://openaccess.thecvf.com/content_cvpr_2017/html/Isola_Image-To-Image_Translation_With_CVPR_2017_paper.html.

Jeon, Hyeonseong, Bang, Youngoh, Kim, Junyaup, and Woo, Simon S. T-GD: Transferable GAN-generated Images Detection Framework. *arXiv:2008.04115 [cs]*, August 2020. URL http://arxiv.org/abs/2008.04115. arXiv: 2008.04115.

Jha, Anurag, Chandrasekaran, Anand, Kim, Chiho, and Ramprasad, Rampi. Impact of dataset uncertainties on machine learning model predictions: the example of polymer glass transition temperatures. *Modelling and Simulation in Materials Science and Engineering*, 27(2):024002, January 2019. ISSN 0965-0393. doi: 10.1088/1361-651X/aaf8ca. URL https://doi.org/10.1088/1361-651x/aaf8ca. Publisher: IOP Publishing.

Jordon, James, Yoon, Jinsung, and Schaar, Mihaela van der. PATE-GAN: Generating Synthetic Data with Differential Privacy Guarantees. September 2018. URL https://openreview.net/forum?id=S1zk9iRqF7.

Kagho, Grace O., Balac, Milos, and Axhausen, Kay W. Agent-Based Models in Transport Planning: Current State, Issues, and Expectations. *Procedia Computer Science*, 170:726–732, January 2020. ISSN 1877-0509. doi: 10.1016/j.procs.2020.03.164. URL https://www.sciencedirect.com/science/article/pii/S187705092030627X.

Ke, Guolin, Meng, Qi, Finley, Thomas, Wang, Taifeng, Chen, Wei, Ma, Weidong, Ye, Qiwei, and Liu, Tie-Yan. LightGBM: A Highly Efficient Gradient Boosting Decision Tree. In *Advances in Neural Information Processing Systems*, volume 30. Curran Associates, Inc., 2017. URL https://proceedings.neurips.cc/paper/2017/hash/6449f44a102fde848669bdd9eb6b76fa-Abstract.html.

Kim, Jooyoung and Lee, Seungjae. A simulated annealing algorithm for the creation of synthetic population in activity-based travel demand model. *KSCE Journal of Civil Engineering*, 20(6):2513–2523, September 2016. ISSN 1976-3808. doi: 10.1007/s12205-015-0691-7. URL https://doi.org/10.1007/s12205-015-0691-7.

Kingma, Diederik P. and Ba, Jimmy. Adam: A Method for Stochastic Optimization. *arXiv:1412.6980 [cs]*, December 2014. URL http://arxiv.org/abs/1412.6980. arXiv: 1412.6980.

Kingma, Diederik P. and Welling, Max. Auto-Encoding Variational Bayes. *arXiv:1312.6114 [cs, stat]*, May 2014. URL http://arxiv.org/abs/1312.6114. arXiv: 1312.6114.

Kohavi, Ron. Scaling up the accuracy of Naive-Bayes classifiers: a decision-tree hybrid. In *Proceedings of the Second International Conference on Knowledge Discovery and Data Mining*, KDD'96, pages 202–207, Portland, Oregon, August 1996. AAAI Press. URL https://www.aaai.org/Papers/KDD/1996/KDD96-033.pdf.

Linjordet, Trond and Balog, Krisztian. Impact of Training Dataset Size on Neural Answer Selection Models. In Azzopardi, Leif, Stein, Benno, Fuhr, Norbert, Mayr, Philipp, Hauff, Claudia, and Hiemstra, Djoerd, editors, *Advances in Information Retrieval*, Lecture Notes in Computer Science, pages 828–835, Cham, 2019. Springer International Publishing. ISBN 978-3-030-15712-8. doi: 10.1007/978-3-030-15712-8_59.

Liu, Ming-Yu and Tuzel, Oncel. Coupled Generative Adversarial Networks. *arXiv:1606.07536 [cs]*, September 2016. URL http://arxiv.org/abs/1606.07536. arXiv: 1606.07536.

Liu, Yi, Peng, Jialiang, Yu, James J. Q., and Wu, Yi. PPGAN: Privacy-preserving Generative Adversarial Network. *2019 IEEE 25th International Conference on Parallel and Distributed Systems (ICPADS)*, pages 985–989, December 2019. doi: 10.1109/ICPADS47876.2019.00150. URL http://arxiv.org/abs/1910.02007. arXiv: 1910.02007.

Lucas, Peter J., Gaag, Linda C., and Abu-Hanna, Ameen. Bayesian Networks in biomedicine and health-care. *Artificial Intelligence in Medicine*, 30:201–214, April 2004. doi: 10.1016/j.artmed.2003.11.001.

Mirza, Mehdi and Osindero, Simon. Conditional Generative Adversarial Nets. *arXiv:1411.1784 [cs, stat]*, November 2014. URL http://arxiv.org/abs/1411.1784. arXiv: 1411.1784.

Müller, Kirill and Axhausen, Kay W. Population synthesis for microsimulation: State of the art. *Arbeitsberichte Verkehrs- und Raumplanung*, 638, August 2010. doi: 10.3929/ethz-a-006127782. URL https://www.research-collection.ethz.ch/handle/20.500.11850/30298. Accepted: 2017-08-22T09:43:21Z Publisher: IVT, ETH Zurich.

Müller, Kirill and Axhausen, Kay W. Hierarchical IPF: Generating a synthetic population for Switzerland. Technical Report ersa11p305, European Regional Science Association, September 2011. URL https://ideas.repec.org/p/wiw/wiwrsa/ersa11p305.html. Publication Title: ERSA conference papers.

Noguchi, Atsuhiro and Harada, Tatsuya. Image Generation From Small Datasets via Batch Statistics Adaptation. *arXiv:1904.01774 [cs]*, October 2019. URL http://arxiv.org/abs/1904.01774. arXiv: 1904.01774.

Park, Noseong, Mohammadi, Mahmoud, Gorde, Kshitij, Jajodia, Sushil, Park, Hongkyu, and Kim, Youngmin. Data Synthesis based on Generative Adversarial Networks. *Proceedings of the VLDB Endowment*, 11(10):1071–1083, June 2018. ISSN 21508097. doi: 10.14778/3231751.3231757. URL http://arxiv.org/abs/1806.03384. arXiv: 1806.03384.

Philips, Ian, Clarke, Graham, and Watling, David. A Fine Grained Hybrid Spatial Microsimulation Technique for Generating Detailed Synthetic Individuals from Multiple Data Sources: An Application To Walking And Cycling. *International Journal of Microsimulation*, 10(1):167–200, 2017. URL https://ideas.repec.org/a/ijm/journl/v10y2017i1p167-200.html. Publisher: International Microsimulation Association.

Radford, Alec, Metz, Luke, and Chintala, Soumith. Unsupervised Representation Learning with Deep Convolutional Generative Adversarial Networks. *arXiv:1511.06434 [cs]*, January 2016. URL http://arxiv.org/abs/1511.06434. arXiv: 1511.06434.

Rich, Jeppe. Large-scale spatial population synthesis for Denmark. *European Transport Research Review*, 10(2):63, December 2018. ISSN 1866-8887. doi: 10.1186/s12544-018-0336-2. URL https://doi.org/10.1186/s12544-018-0336-2.

Rubin, Donald B. The Use of Matched Sampling and Regression Adjustment to Remove Bias in Observational Studies. *Biometrics*, 29(1):185–203, 1973. ISSN 0006-341X. doi: 10.2307/2529685. URL https://www.jstor.org/stable/2529685. Publisher: [Wiley, International Biometric Society].

Salimans, Tim, Goodfellow, Ian, Zaremba, Wojciech, Cheung, Vicki, Radford, Alec, and Chen, Xi. Improved Techniques for Training GANs. *arXiv:1606.03498 [cs]*, June 2016. URL http://arxiv.org/abs/1606.03498. arXiv: 1606.03498.

Shorten, Connor and Khoshgoftaar, Taghi M. A survey on Image Data Augmentation for Deep Learning. *Journal of Big Data*, 6(1):60, July 2019. ISSN 2196-1115. doi: 10.1186/s40537-019-0197-0. URL https://doi.org/10.1186/s40537-019-0197-0.

Sun, Lijun and Erath, Alexander. A Bayesian network approach for population synthesis. *Transportation Research Part C: Emerging Technologies*, 61:49–62, December 2015. ISSN 0968-090X. doi: 10.1016/j.trc.2015.10.010. URL http://www.sciencedirect.com/science/article/pii/S0968090X15003599.

Tieleman, Tijmen and Hinton, Geoffrey. Lecture 6.5-rmsprop: Divide the gradient by a running average of its recent magnitude. *COURSERA: Neural networks for machine learning*, 4(2):26–31, 2012. URL https://www.youtube.com/watch?v=SJ48OZ_qlrc.

Wang, Yaxing, Gonzalez-Garcia, Abel, Berga, David, Herranz, Luis, Khan, Fahad Shahbaz, and van de Weijer, Joost. MineGAN: effective knowledge transfer from GANs to target domains with few images. *arXiv:1912.05270 [cs]*, April 2020. URL http://arxiv.org/abs/1912.05270. arXiv: 1912.05270.

Wen, Bingyang, Colon, Luis Oliveros, Subbalakshmi, K. P., and Chandramouli, R. Causal-TGAN: Generating Tabular Data Using Causal Generative Adversarial Networks. *arXiv:2104.10680 [cs]*, April 2021. URL http://arxiv.org/abs/2104.10680. arXiv: 2104.10680.

Xu, Lei and Veeramachaneni, Kalyan. Synthesizing Tabular Data using Generative Adversarial Networks. *arXiv:1811.11264 [cs, stat]*, November 2018. URL http://arxiv.org/abs/1811.11264. arXiv: 1811.11264.

Xu, Lei, Skoularidou, Maria, Cuesta-Infante, Alfredo, and Veeramachaneni, Kalyan. Modeling Tabular data using Conditional GAN. In Wallach, H., Larochelle, H., Beygelzimer, A., Alché-Buc, F. d\textquotesingle, Fox, E., and Garnett, R., editors, *Advances in Neural Information Processing Systems 32*, pages 7335–7345. Curran Associates, Inc., 2019. URL http://papers.nips.cc/paper/8953-modeling-tabular-data-using-conditional-gan.pdf.

Yin, Dan and Yang, Qing. GANs Based Density Distribution Privacy-Preservation on Mobility Data. *Security and Communication Networks*, 2018:e9203076, December 2018. ISSN 1939-0114. doi: 10.1155/2018/9203076. URL https://www.hindawi.com/journals/scn/2018/9203076/. Publisher: Hindawi.

Yuxin, Wu. tensorpack, 2016. URL https://github.com/tensorpack/tensorpack.

Zhang, Danqing, Cao, Junyu, Feygin, Sid, Tang, Dounan, Shen, Zuo-Jun(Max), and Pozdnoukhov, Alexei. Connected population synthesis for transportation simulation. *Transportation Research Part C: Emerging Technologies*, 103: 1–16, June 2019. ISSN 0968-090X. doi: 10.1016/j.trc.2018.12.014. URL http://www.sciencedirect.com/science/article/pii/S0968090X18318515.

Zhao, Zilong, Kunar, Aditya, Van der Scheer, Hiek, Birke, Robert, and Chen, Lydia Y. CTAB-GAN: Effective Table Data Synthesizing. *arXiv:2102.08369 [cs]*, May 2021. URL http://arxiv.org/abs/2102.08369. arXiv: 2102.08369.

Zhu, Jun-Yan, Park, Taesung, Isola, Phillip, and Efros, Alexei A. Unpaired Image-to-Image Translation using Cycle-Consistent Adversarial Networks. *arXiv:1703.10593 [cs]*, November 2018. URL http://arxiv.org/abs/1703.10593. arXiv: 1703.10593.

7 Appendix

7.1 Case studies - dataset description

Table 8: CMAP dataset

Variables	Type	Details	Description
choice	Categorical	5 string categories	Chosen mode
travel_dow	Categorical	1-7 (Monday-Sunday)	Day of the week travel
trip_purpose	Categorical	7 string categories	Primary purpose for making trip
distance	Continuous	8'743 unique values between 0 and 69.71	Straight-line trip distance in miles
hh_vehicles	Categorical	0-8	Number of vehicles in household
hh_size	Categorical	1-8	Number of people in household
hh_bikes	Categorical	0-7	Number of bikes in household
hh_descr	Categorical	3 string categories	Household type
hh_income	Categorical	7 categories	Household income level
gender	Categorical	0 (female), 1 (male)	Gender of individual
age	Continuous	97 unique integers between 0 and 98	Age of individual
license	Categorical	0 (none), 1 (has driving license)	Driving license ownership
education_level	Categorical	6 categories	Highest level of education achieved
work_status	Categorical	8 string categories	Working status
departure_time	Continuous	949 unique values between 0 and 23.86	Departure time of trip (in decimal hours)

Table 9: LPMC dataset

Variables	Type	Details	Description
travel_mode	Categorical	4 string categories	Mode of travel chosen by LTDS trip
purpose	Categorical	5 string categories	Journey purpose for trip
fueltype	Categorical	6 string categories	Fuel type of passenger's vehicle
faretype	Categorical	5 string categories	Public transport fare type of passenger
bus_scale	Categorical	3 values (0, 0.5, 1)	Percentage of the full bus fare paid by the passenger
travel_year	Categorical	4 values between 2012 and 2015	Year of travel
travel_month	Categorical	12 values between 1 and 12	Month of year of travel
travel_date	Categorical	31 values between 1 and 31	Date of month of travel
day_of_week	Categorical	7 values between 1 and 7	Day of the week of travel
start_time_linear	Continuous	609 unique values between 0 and 23.92	Start time of trip (in decimal hours)
age	Continuous	90 unique values between 5 and 94	Age of passenger in years

Table 9 – continued from previous page

Variables	Type	Details	Description
female	Categorical	0 (male), 1 (female)	Gender of passenger
driving_license	Categorical	0 (none), 1 (has driving license)	Whether the traveller has a driving licence
car_ownership	Categorical	3 values between 0 and 2	Car ownership of household
distance	Continuous	8'972 unique values between 77 and 40'941	Straight line trip distance
dur_walking	Continuous	8'416 unique values between 0.028 and 9.28	Duration of walking route
dur_cycling	Continuous	4'350 unique values between 0.0075 and 3.05	Duration of cycling route
dur_pt_access	Continuous	1'656 unique values between 0 and 1.06	Duration walking to/from first/last stop on public transport route
dur_pt_rail	Continuous	76 unique values between 0 and 1.37	Duration spent on rail services on public transport route
dur_pt_bus	Continuous	2'469 unique values between 0 and 2.15	Duration spent on bus services on public transport route
dur_pt_int	Continuous	725 unique values between 0 and 0.57	Total duration of public transport interchanges
pt_n_interchanges	Categorical	5 values between 0 and 4	Total number of public transport interchanges
dur_driving	Continuous	3'544 unique values between 0.0042 and 1.79	Duration of driving route
cost_transit	Continuous	146 unique values between 0 and 11.7	Cost of public transport route
cost_driving_fuel	Continuous	507 unique values between 0.02 and 10.09	Vehicle operation costs of driving route
cost_driving_con_charge	Categorical	2 values (0 or 10.5)	Congestion charge for driving route
driving_traffic_percent	Continuous	15'787 unique values between 0 and 1.04	Traffic variability

Table 10: ADULT dataset

Variables	Type	Details	Description
age	Continuous	74 unique integers between 17 and 90	Age of individual
workclass	Categorical	9 string categories	Work status of the individual
education	Categorical	16 string categories	Education of the individual
education-num	Categorical	16 integer categories	Number of years of education
marital-status	Categorical	7 string categories	Marital status of the individual
occupation	Categorical	14 string categories	Occupation of the individual
relationship	Categorical	6 string categories	Relationship with a partner
race	Categorical	5 string categories	Race of the individual
gender	Categorical	2 string categories	Gender of the individual

Table 10 – continued from previous page

Variables	Type	Details	Description
capital-gain	Continuous	121 unique integers between 0 and 99'999	Capital gains
capital-loss	Continuous	97 unique integers between 0 and 4'356	Capital losses
hours-per-week	Categorical	96 unique integers between 1 and 99	Number of hours of work per week
native-country	Categorical	41 string categories	Native country of the individual
income	Categorical	2 string categories	Income greater or equal to 50k per year

7.2 Case studies - Directed Acyclic Graphs
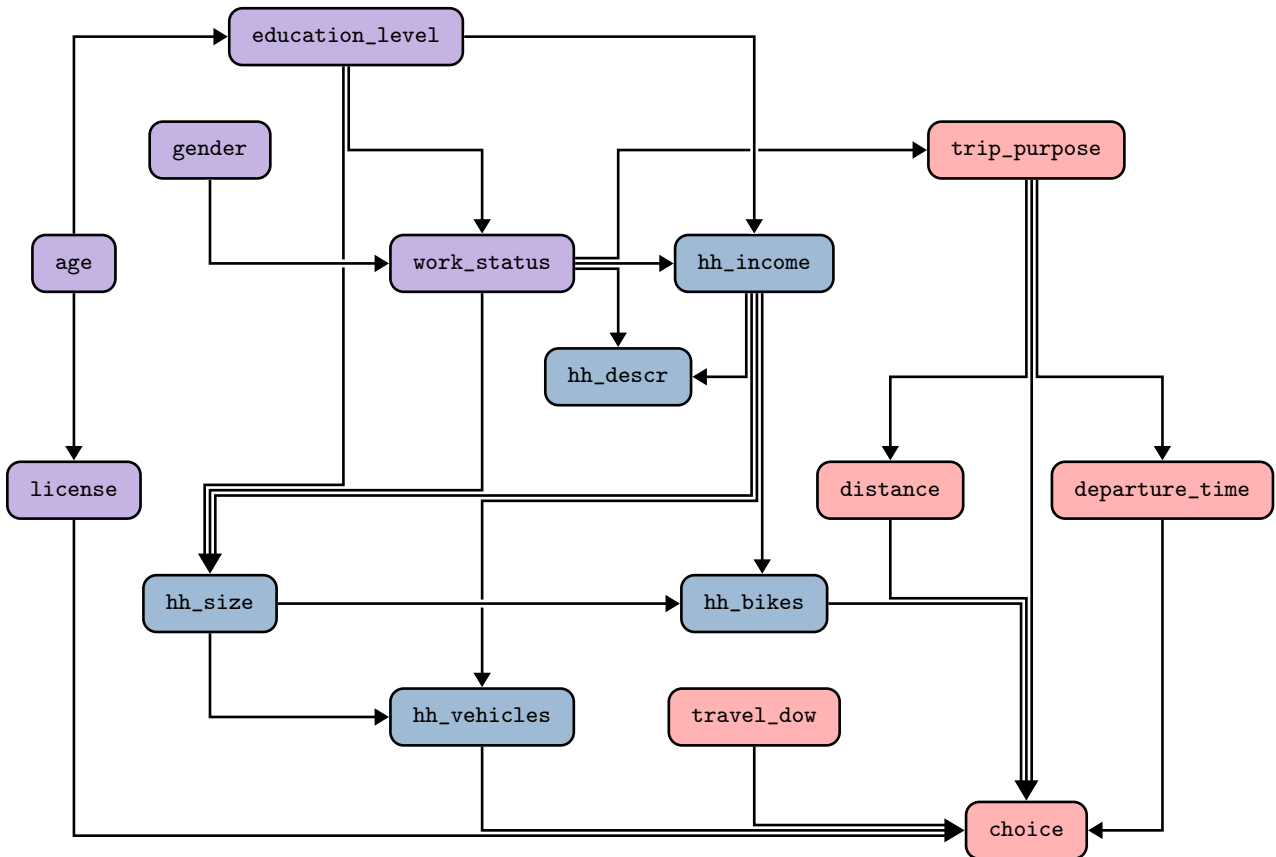
Figure 7: DAG used for the CMAP case study. We identified three categories of variables: purple corresponds to individuals, blue to households, and red to trips.
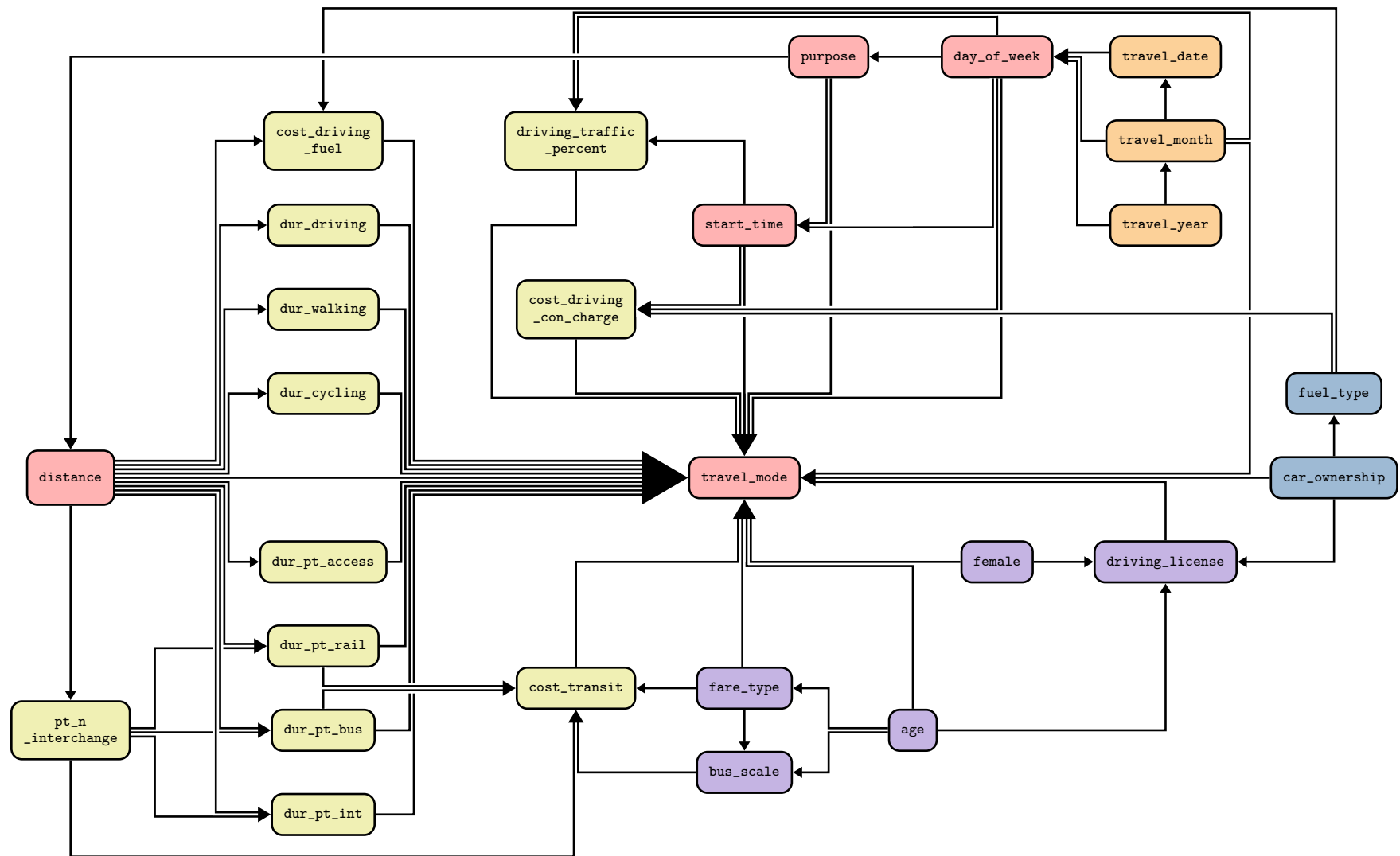
Figure 8: DAG used for the LPMC case study. We identified five categories of variables: purple corresponds to individuals, blue to households, red to trips, orange to survey, and yellow to alternatives.
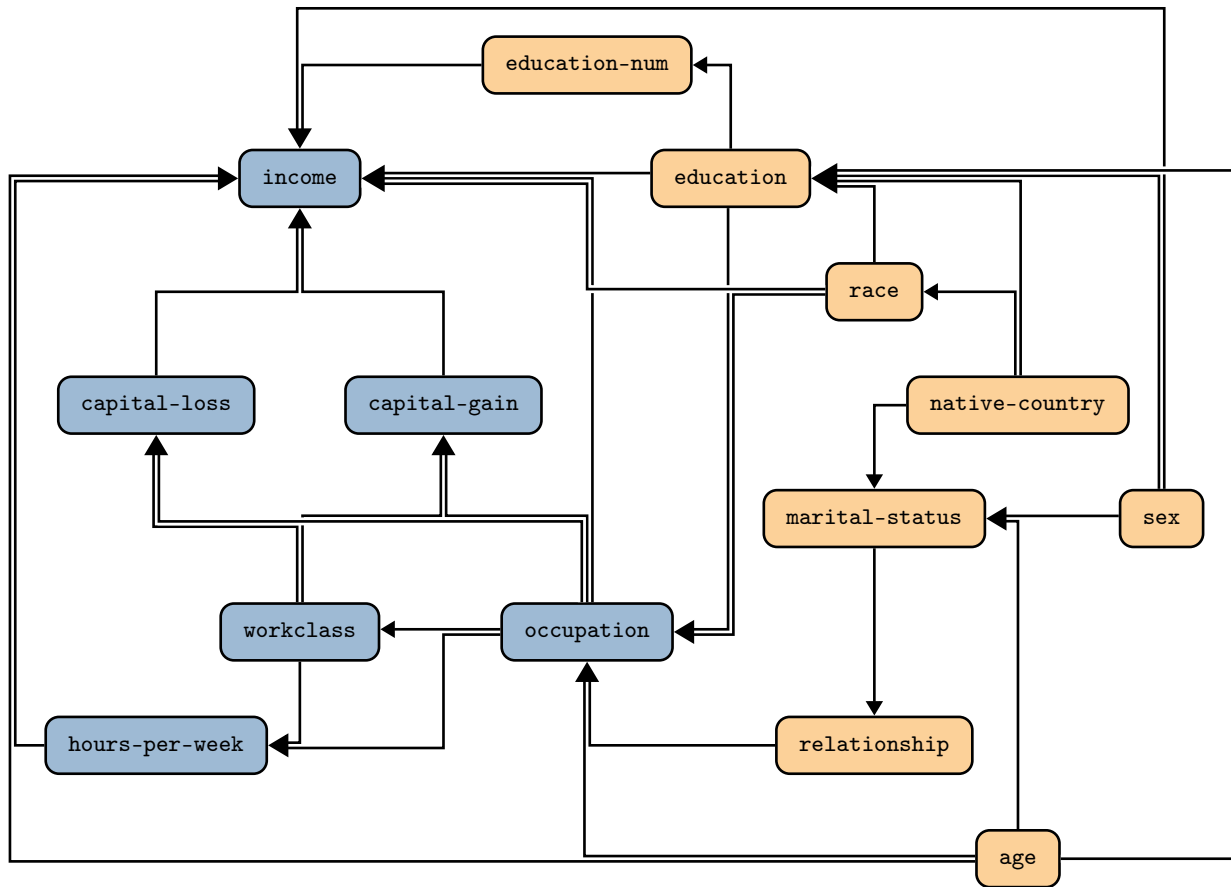
Figure 9: DAG used for the ADULT case study. We identified two categories of variables: orange corresponds to individuals, blue to occupation.

SUPPLEMENTARY MATERIALS
DATGAN: INTEGRATING EXPERT KNOWLEDGE INTO DEEP LEARNING FOR SYNTHETIC TABULAR DATA

1 Introduction

In this document, we present supplementary materials for the article names "*DATGAN: Integrating expert knowledge into deep learning for synthetic tabular data*". The original article provides the methodology to create multiple DATGAN versions. This document first summarizes these versions in Section 2. Then, in Section 3, we provide the comparison of the different DATGAN versions. This is used in the original article to choose the best-performing models depending on the case study. Next, Section 4 gives a notation table that can be helpful while following the methodology in the original article. Finally, Section 5 provide the complete results used for the rankings in the original article.

2 Summary of DATGAN versions

The methodology in the article provides a detailed overview of the different elements of the DATGAN model: the generator, the discriminator, the loss function, and the data encoding. The use of expert knowledge to build a DAG $\mathcal{G}$ and its usage to build the structure of the generator is the main contribution of this paper. Indeed, while this is respected, many things can change, such as the discriminator structure, keeping the DATGAN identity. Therefore, in our case, instead of sticking to a single model, we systematically test multiple aspects of the DATGAN:

- Three different loss functions:
    - standard loss (`SGAN`):
    $$\min_G \max_D \mathcal{L}^{\texttt{SGAN}}(D, G) = \mathop{\mathbb{E}}_{\left\{\widehat{\boldsymbol{v}}_{1:N_V}\right\} \sim \mathbb{P}(\widehat{\mathbf{T}})} \log D\left(\widehat{\boldsymbol{v}}_{1:N_V}\right) + \mathop{\mathbb{E}}_{\boldsymbol{z} \sim \mathcal{N}(0,1)} \log\left(1 - D(G(\boldsymbol{z}))\right) \tag{1}$$

    - wasserstein loss (`WGAN`):
    $$\min_G \max_D \mathcal{L}^{\texttt{WGAN}}(D, G) = \mathop{\mathbb{E}}_{\left\{\widehat{\boldsymbol{v}}_{1:N_V}\right\} \sim \mathbb{P}(\widehat{\mathbf{T}})} D\left(\widehat{\boldsymbol{v}}_{1:N_V}\right) - \mathop{\mathbb{E}}_{\boldsymbol{z} \sim \mathcal{N}(0,1)} D(G(\boldsymbol{z})) \tag{2}$$

    - wasserstein loss with gradient penalty (`WGGP`):
    $$\min_G \max_D \mathcal{L}^{\texttt{WGGP}}(D, G) = \mathop{\mathbb{E}}_{\left\{\widehat{\boldsymbol{v}}_{1:N_V}\right\} \sim \mathbb{P}(\widehat{\mathbf{T}})} D\left(\widehat{\boldsymbol{v}}_{1:N_V}\right) - \mathop{\mathbb{E}}_{\boldsymbol{z} \sim \mathcal{N}(0,1)} D(G(\boldsymbol{z})) + \lambda \mathop{\mathbb{E}}_{\widehat{\boldsymbol{v}} \sim \mathbb{P}(\widehat{\mathbf{T}}, G(\boldsymbol{z}))} \left(\|\nabla_{\widetilde{\boldsymbol{v}}} D(\widetilde{\boldsymbol{v}})\|_2 - 1\right)^2 \tag{3}$$

- Three different label smoothing strategies:
    - none (`NO`)
    - one-sided on the original data (`OS`)
    - two-sided (`TS`)
- Four different sampling strategies:
    - $\arg\max$ on continuous and categorical columns (`AA`)
    - `simulation` on continuous columns and $\arg\max$ on categorical columns (`SA`)
    - $\arg\max$ on continuous columns and `simulation` on categorical columns (`AS`)
    - `simulation` on continuous and categorical columns (`SS`)

By combining all of these different strategies, we obtain 36 different modeling approaches for the DATGAN. They are enumerated in Table 1. The next section systematically compares these different approaches on multiple case studies to identify the best-performing combination.

Table 1: Summary of all the possible models using the DATGAN concept.

Name	Loss function	Label smoothing	Sampling
SGAN_NO_AA			$\arg\max$ for C_t and D_t
SGAN_NO_SA		none	simulation for C_t, $\arg\max$ for D_t
SGAN_NO_AS			$\arg\max$ for C_t, simulation for D_t
SGAN_NO_SS			simulation for C_t and D_t
SGAN_OS_AA			$\arg\max$ for C_t and D_t
SGAN_OS_SA	SGAN	one-sided	simulation for C_t, $\arg\max$ for D_t
SGAN_OS_AS	(Eq. 1)		$\arg\max$ for C_t, simulation for D_t
SGAN_OS_SS			simulation for C_t and D_t
SGAN_TS_AA			$\arg\max$ for C_t and D_t
SGAN_TS_SA		two-sided	simulation for C_t, $\arg\max$ for D_t
SGAN_TS_AS			$\arg\max$ for C_t, simulation for D_t
SGAN_TS_SS			simulation for C_t and D_t
WGAN_NO_AA			$\arg\max$ for C_t and D_t
WGAN_NO_SA		none	simulation for C_t, $\arg\max$ for D_t
WGAN_NO_AS			$\arg\max$ for C_t, simulation for D_t
WGAN_NO_SS			simulation for C_t and D_t
WGAN_OS_AA			$\arg\max$ for C_t and D_t
WGAN_OS_SA	WGAN	one-sided	simulation for C_t, $\arg\max$ for D_t
WGAN_OS_AS	(Eq. 2)		$\arg\max$ for C_t, simulation for D_t
WGAN_OS_SS			simulation for C_t and D_t
WGAN_TS_AA			$\arg\max$ for C_t and D_t
WGAN_TS_SA		two-sided	simulation for C_t, $\arg\max$ for D_t
WGAN_TS_AS			$\arg\max$ for C_t, simulation for D_t
WGAN_TS_SS			simulation for C_t and D_t
WGGP_NO_AA			$\arg\max$ for C_t and D_t
WGGP_NO_SA		none	simulation for C_t, $\arg\max$ for D_t
WGGP_NO_AS			$\arg\max$ for C_t, simulation for D_t
WGGP_NO_SS			simulation for C_t and D_t
WGGP_OS_AA			$\arg\max$ for C_t and D_t
WGGP_OS_SA	WGGP	one-sided	simulation for C_t, $\arg\max$ for D_t
WGGP_OS_AS	(Eq. 3)		$\arg\max$ for C_t, simulation for D_t
WGGP_OS_SS			simulation for C_t and D_t
WGGP_TS_AA			$\arg\max$ for C_t and D_t
WGGP_TS_SA		two-sided	simulation for C_t, $\arg\max$ for D_t
WGGP_TS_AS			$\arg\max$ for C_t, simulation for D_t
WGGP_TS_SS			simulation for C_t and D_t

3 Comparison of DATGAN versions

This section compares the 36 DATGAN versions against each other using the result assessments methods presented in the original article on the first three case studies (CMAP, LPMC_half, and LPMC).

For the CMAP case study, we see that the DATGAN with the `WGGP` loss provides poorer results compared to the DATGAN with the `SGAN` or `WGAN` loss. It is the case with both assessment methods. This is quite unexpected since the `WGGP` loss is the most recent loss function available amongst the three. We do not clearly explain why the model fails with this loss on this particular dataset. Secondly, we see that all the models using the one-sided label smoothing (`OS`) tend to perform worse than their counterparts. This result was expected, especially when using simulation while sampling the synthetic variables. Indeed, if the model only uses one-sided label smoothing, the Generator will learn the noisy version of the categorical variables. If we use $\arg\max$ for selecting the categorical variable, it does not have a large effect since the noise is quite small. However, the final synthetic probability distribution does not correspond to the original one when using simulation. Therefore, the model will sample the values wrongly and thus lead to poor results. When we compare two-sided label smoothing (`TS`) against no label smoothing (`NO`), we see that the results are different for the `SGAN` and the `WGAN` loss functions. Indeed, it seems that it is better to use the two-sided label smoothing with the `WGAN` loss, and it is better to avoid label smoothing with the `SGAN` loss. Table 2 shows the ten best models in terms of average ranking on the two assessment methods. We see that both loss functions are viable. However, the `WGAN` loss seems to be slightly better on average. The sampling method seems to have less influence than the label smoothing and the loss function on the final results.

Table 2: Average rankings for the ten best DATGAN models on the CMAP dataset.

Name	Avg. rank stats	Avg. rank ML	rank
WGAN_TS_AS	**2.88**	8.0	**5.44**
WGAN_TS_AA	8.24	4.0	6.12
WGAN_TS_SS	4.04	9.5	6.77
SGAN_NO_SA	10.08	3.5	6.79
SGAN_NO_SS	8.56	6.0	7.28
WGAN_TS_SA	6.84	8.0	7.42
SGAN_NO_AS	12.68	4.0	8.34
SGAN_NO_AA	15.96	**2.0**	8.98
SGAN_TS_AS	8.68	9.5	9.09
SGAN_TS_SA	7.88	10.5	9.19

For the LPMC dataset, we have quite unexpected results compared to the CMAP case study. The conclusions on the label smoothing remain the same. However, the best loss function to use in this case is the `WGGP` loss. This is especially visible when using the Machine Learning efficacy method to assess the results. All the models with the `WGGP` loss consistently outperforms the models with the other losses. The `WGAN` loss performs slightly worse than the `SGAN` loss. Table 3 shows the ten best models in terms of average on both assessment methods. We see that both models using simulation for the categorical variables and two-sided label smoothing outperform the other models. It is interesting to note that, in this case, the sampling method for continuous variables does not affect much the final results. This result can be explained thanks to the encoding we use for the continuous variables. Indeed, all the encoded values $w_{t,j}$ are computed such that they all correspond to the continuous value $c_{t,j}$ once drawn from their respective Gaussian mixture. Therefore, if the algorithm fails to choose the right mixture, the sampling will return the same continuous synthetic value.

If we compare the two previous case studies, there are two hypotheses as to why the `WGAN` loss works better with the CMAP dataset and the `WGGP` loss with the LPMC dataset:(i) the number of data points in the dataset influences the optimization process with a given loss function; (ii) the ratio of continuous/categorical variables influences the choice of the loss function. The first hypothesis is easier to test since we can use the LPMC_half case study to compare with the LPMC case study. The results in the appendix show the same behavior with the smaller LPMC dataset than with the complete one. Indeed, the `WGGP` loss leads to significantly better results across both assessments methods compared to the other loss functions. Table 4 shows the ten best models in terms of average on both assessment methods. Once again, the version with the `WGGP` loss, two-sided label smoothing, and sampling using simulation for both continuous and categorical variables appears to be the best model. However, it is interesting to note that the versions with the `WGAN` loss function shows the best statistics when only looking at the first aggregation level on categorical variables. This hints at the fact that the `WGAN` loss is the most appropriate loss to use when a dataset contains a majority of categorical variables.

For further analyses, we settle on one particular version of the DATGAN. As seen across all the case studies, two-sided label smoothing is the best method for the discriminator. In addition, using simulation on both types of variables for the

Table 3: Average rankings for the ten best DATGAN models on the LPMC dataset.

Name	Avg. rank stats	Avg. rank ML	rank
WGGP_TS_SS	**2.96**	4.0	**3.48**
WGGP_TS_AS	5.16	3.0	4.08
WGGP_NO_AS	9.52	8.0	8.76
WGGP_NO_SS	9.76	8.5	9.13
WGGP_OS_SA	15.60	4.0	9.80
WGGP_OS_AA	18.36	**2.5**	10.43
WGGP_TS_SA	12.36	9.5	10.93
WGGP_NO_AA	12.72	9.5	11.11
WGGP_TS_AA	14.80	7.5	11.15
WGGP_NO_SA	13.04	10.0	11.52

Table 4: Average rankings for the ten best DATGAN models on the LPMC_half dataset.

Name	Avg. rank stats	Avg. rank ML	rank
WGGP_TS_SS	**3.12**	4.5	**3.81**
WGGP_TS_AS	4.84	4.0	4.42
WGGP_NO_SS	8.20	8.5	8.35
WGGP_OS_SA	14.36	4.0	9.18
WGGP_NO_AS	11.88	7.0	9.44
WGGP_OS_AA	16.00	**3.5**	9.75
WGGP_OS_SS	18.04	5.5	11.77
WGGP_OS_AS	20.24	5.0	12.62
SGAN_TS_SS	9.52	16.0	12.76
SGAN_NO_AS	10.96	16.0	13.48

sampling leads to better results for the two LPMC case studies. For the CMAP case study, it is amongst the best models. We, thus, choose to use this sampling method to stay consistent across both variable types. Finally, we cannot use the same one for all the datasets for the loss function. As stated earlier, the WGAN loss performs best when there are more categorical variables than continuous in the dataset. Therefore, the DATGANs presented in the original article are using the WGAN loss function for the CMAP case study and the WGGP loss function for the LPMC case studies.

4 Notations table

In this section, we present a notation table that can be used while following the methodology in the original article.

Table 5: Notations used in the methodology grouped by categories

Notation	Name	Description
Main elements		
D	Discriminator	Neural network model used to discriminate/critic the original and synthetic data. (see Section 3.2)
G	Generator	Neural network model used to generate synthetic data from random noise. (see Section 3.1)

Continues on next page...

Table 5 – continued from previous page

Notation	Name	Description
$\mathbf{T}$	original dataset	Original dataset provided by the modeler. (size: $N_V \times N_{\text{rows}}$)
$\mathbb{P}(\mathbf{T})$	distributions	Unknown joint distribution that the random variables V_t follow.
$\mathbf{T_{synth}}$	synthetic dataset	Final synthetic dataset after the sampling procedure; it corresponds to the final output of the generator (size: $N_V \times N_{\text{rows}}$).
$\widehat{\mathbf{T}}$	encoded original dataset	Original dataset that has been encoded. (size: $\left(\sum_{t=1}^{N_C} 2N_{m,t} + \sum_{t=1}^{N_D} |D_t| \right) \times N_{\text{rows}}$)
$\widehat{\mathbf{T}}_{\mathbf{synth}}$	encoded synthetic dataset	Synthetic dataset that is directly returned by the generator before the sampling step. (see Section 3.4.4; size: $\left(\sum_{t=1}^{N_C} 2N_{m,t} + \sum_{t=1}^{N_D} |D_t| \right) \times N_{\text{rows}}$)
Main variables		
V_t	random variable	t-th random variable.
$\boldsymbol{v}_t$	column data in $\mathbf{T}$	Column-vectors of data that define the table $\mathbf{T}$. (size: N_{rows})
$v_{t,j}$	single value in $\mathbf{T}$	Scalar value in a column-vector.
$\boldsymbol{z}$	noise	Random noise tensor used as an input for the Generator G. (size: $N_V \times N_{\text{rows}} \times N_{\text{sources}}$)
$\boldsymbol{v}_t^{\mathbf{synth}}$	column data in $\mathbf{T_{synth}}$	Column-vectors of data that define the table $\mathbf{T_{synth}}$. (size: N_{rows})
$v_{t,j}^{\mathbf{synth}}$	single value in $\mathbf{T_{synth}}$	Scalar value in a column-vector.
$\widehat{\boldsymbol{v}}_t$	encoded column data in $\mathbf{T}$	Encoded version of $\boldsymbol{v}_t$.
$\widehat{v}_{t,j}$	encoded single value in $\mathbf{T}$	Encoded version of $v_{t,j}$.
$\widehat{\boldsymbol{v}}_t^{\mathbf{synth}}$	encoded column data in $\mathbf{T_{synth}}$	Encoded version of $\boldsymbol{v}_t^{\mathbf{synth}}$.
$\widehat{v}_{t,j}^{\mathbf{synth}}$	encoded single value in $\mathbf{T_{synth}}$	Encoded version of $v_{t,j}^{\mathbf{synth}}$.
Directed Acyclic Graph (Section 3.1.1)		
$\mathcal{G}$	DAG	Directed Acyclic Graph (DAG) used to represent the interdependencies between the variables.
$\mathcal{A}(V_t)$	ancestors	Set of all the ancestors of the variable V_t in the DAG $\mathcal{G}$.
$\mathcal{D}(V_t)$	direct ancestors	Set of all the direct ancestors of the variable V_t in the DAG $\mathcal{G}$.
$\mathcal{S}(V_t)$	source nodes	Set of all the source nodes leading to variable V_t in the DAG $\mathcal{G}$.
$\mathcal{E}(V_t)$	in-edges	Set of all in-edges of the variable V_t in the DAG $\mathcal{G}$.
LSTM cells (Section 3.1.2)		
$\mathbf{LSTM_t}$	LSTM cell	LSTM cell used to generate synthetic values for the variable V_t.
C_t	cell state	Output cell state of the LSTM cell $\mathbf{LSTM_t}$. (size: $N_h \times N_b$)
$\boldsymbol{h}_t$	output	Output tensor of the LSTM cell $\mathbf{LSTM_t}$. (size: $N_h \times N_b$)
$\boldsymbol{x}_t$	generic input	Generic input tensor for a LSTM cell. (size: $N_x \times N_b$)
$\boldsymbol{i}_t$	input	Input tensor of the LSTM cell $\mathbf{LSTM_t}$. (generic size: $(N_h + N_x) \times N_b$; DATGAN size: $(2N_h + N_z) \times N_b$)
$\boldsymbol{z}_t$	noise	Random noise tensor used as an input for the LSTM cell $\mathbf{LSTM_t}$. (size: $N_z \times N_b$)
$\boldsymbol{f}_t$	transformed output	Transformed output of the variable $\widehat{\boldsymbol{v}}_t^{\mathbf{synth}}$ to resize it according to the LSTM cell. (size: $N_h \times N_b$)
$\boldsymbol{a}_t$	attention	Attention tensor used in the input of the LSTM cell $\mathbf{LSTM_t}$. (size: $N_h \times N_b$)

Table 5 – continued from previous page

Notation	Name	Description
$\boldsymbol{\alpha}_t$	attention weights	Attention weight vector used to compute a_t. (size: $|\mathcal{A}(V(t))|$)
$\boldsymbol{h}'_t$	reduced output	Reduced output tensor of the LSTM cell $\mathbf{LSTM_t}$ after using a convolutional layer. (size: $N_{\text{conv}} \times N_b$)
Discriminator (Section 3.2)		
$\boldsymbol{l}_i$	internal layer	Internal layer used in the discriminator. (undefined size)
$\widehat{\boldsymbol{l}}_i$	standardized internal layer	Internal layer after passing it through a fully connected layer to resize it (size: $N_L \times N_b$)
l_D	discriminator output	Final unbounded scalar result used as an output of the discriminator.
$\boldsymbol{l}_0$	discriminator input	Input layer used for the discriminator.
Loss function (Section 3.3)		
$\mathcal{L}(D, G)$	loss function	Generic loss function. The generator is trying to minimize it while the discriminator is trying to maximize it at the same time.
$\mathcal{L}_G$	generator loss function	Loss function applying only to the generator, which is trying to minimize it.
$\mathcal{L}_D$	discriminator loss function	Loss function applying only to the discriminator, which is trying to minimize it.
Data processing (Section 3.4)		
$\boldsymbol{c}_t$	continuous column data in $\mathbf{T}$	Column-vectors of continuous data that define the table $\mathbf{T}$. (size: N_{rows})
$\boldsymbol{d}_t$	categorical column data in $\mathbf{T}$	Column-vectors of continuous data that define the table $\mathbf{T}$. (size: N_{rows})
$\boldsymbol{c}_t^{\mathbf{synth}}$	continuous column data in $\mathbf{T_{synth}}$	Column-vectors of continuous data that define the table $\mathbf{T_{synth}}$. (size: N_{rows})
$\boldsymbol{d}_t^{\mathbf{synth}}$	categorical column data in $\mathbf{T_{synth}}$	Column-vectors of continuous data that define the table $\mathbf{T_{synth}}$. (size: N_{rows})
$\boldsymbol{\eta}_t$	means of VGM	Vector containing the mean of each component in the Gaussian mixture for the continuous variable C_t. (size: $N_{m,t}$)
$\boldsymbol{\sigma}_t$	variances of VGM	Vector containing the variance of each component in the Gaussian mixture for the continuous variable C_t. (size: $N_{m,t}$)
$\boldsymbol{w}_t$	values of encoded continuous variable	Matrix containing the values of the encoded variable $\boldsymbol{c}_t$. (size: $N_{m,t} \times N_{\text{rows}}$)
$\boldsymbol{p}_t$	probabilities of encoded continuous variable	Matrix containing the probabilities of the encoded variable $\boldsymbol{c}_t$. (size: $N_{m,t} \times N_{\text{rows}}$)
$\boldsymbol{o}_t$	one-hot encoding of categorical variable	Matrix containing the one-hot encoding of the categorical variable $\boldsymbol{d}_t$. (size: $|D_t| \times N_{\text{rows}}$)
$\boldsymbol{w}_t^{\mathbf{synth}}$	generated matrix similar to $\boldsymbol{w}_t$	Output of the generator for the values of the encoded continuous variables. (size: $N_{m,t} \times N_{\text{rows}}$)
$\boldsymbol{p}_t^{\mathbf{synth}}$	generated matrix similar to $\boldsymbol{p}_t$	Output of the generator for the probabilities of the encoded continuous variables. (size: $N_{m,t} \times N_{\text{rows}}$)
$\boldsymbol{o}_t^{\mathbf{synth}}$	generated matrix similar to $\boldsymbol{o}_t$	Output of the generator for the one-hot encoded categorical variables. (size: $|D_t| \times N_{\text{rows}}$)
$\widetilde{\boldsymbol{o}}_t$	Noisy version of $\boldsymbol{o}_t$	Corresponds to $\boldsymbol{o}_t$ after adding uniform noise for the label smoothing (size: $|D_t| \times N_{\text{rows}}$)

Table 5 – continued from previous page

Notation	Name	Description
$\widetilde{o}_t^{\mathbf{synth}}$	Noisy version of $o_t^{\mathbf{synth}}$	Corresponds to $o_t^{\mathbf{synth}}$ after adding uniform noise for the label smoothing (size: $|D_t| \times N_{\mathrm{rows}}$)
Results assessments (Section 3.5)		
$\boldsymbol{\pi}$	Frequencies of original data	Frequency list computed on the original dataset $\mathbf{T}$.
$\boldsymbol{\pi}^{\mathbf{synth}}$	Frequencies of synthetic data	Frequency list computed on the synthetic dataset $\mathbf{T}^{\mathbf{synth}}$.
MAE	Mean Absolute Error	Mean Absolute Error computed between frequencies lists on original and synthetic datasets.
RMSE	Root Mean Square Error	Root Mean Square Error computed between frequencies lists on original and synthetic datasets.
SRMSE	Standardized Root Mean Square Error	Standardized Root Mean Square Error computed between frequencies lists on original and synthetic datasets.
R^2	Coefficient of determination	Coefficient of determination computed between frequencies lists on original and synthetic datasets.
ρ_{Pearson}	Pearson's correlation	Pearson's correlation computed between frequencies lists on original and synthetic datasets.
$\mathcal{L}_{\mathrm{MSE}}$	Mean Square Error	Mean Square error loss used in the supervised learning validation on continuous variables.
$\mathcal{L}_{\text{log-loss}}$	Log loss error	Log loss error used in the supervised learning validation on categorical variables.
m_t	LightGBM model	LightGBM model trained on variable v_t. It corresponds to a classification model ($m_{\mathrm{class},t}$) for categorical variables, and to a regression model ($m_{\mathrm{reg},t}$) for continuous variables.
g_t^{reg}	Score for the continuous variables	Final score of the supervised learning-based validation for continuous variables based on a regression model.
g_t^{class}	Score for the categorical variables	Final score of the supervised learning-based validation for categorical variables based on a classification model.
DATGAN versions		
SGAN	SGAN loss function	Standard two-player minimax loss function is used while optimising the DATGAN, see Equation 9.
WGAN	WGAN loss function	Wasserstein loss function is used while optimising the DATGAN, see Equation 12.
WGGP	WGGP loss function	Wasserstein loss function with a gradient penalty is used while optimising the DATGAN, see Equation 15.
NO	no label smoothing	No label smoothing applied for the discriminator input, see Equation 28.
OS	one-sided label smoothing	One-sided smoothing applied on the original data for the discriminator input, see Equation 29.
TS	two-sided label smoothing	Two-sided smoothing applied on the original and synthetic data for the discriminator input, see Equation 30.
AA	$\arg\max$ sampling for continuous and categorical	Maxmimum probability assignment used to sample both final continuous and categorical synthetic column data.

Continues on next page...

Table 5 – continued from previous page

Notation	Name	Description
SA	simulation sampling for continuous and $\arg\max$ sampling for categorical	Probability assignment for continuous synthetic column data and maximum probability assignment for categorical synthetic column data.
AS	$\arg\max$ sampling for continuous and simulation sampling for categorical	Maximum probability assignment for continuous synthetic column data and probability assignment for categorical synthetic column data.
SS	simulation sampling for continuous and categorical	Probability assignement used to sample both continuous and categorical final synthetic column data.
Sizes		
N_V	#variables	Number of random variables in the original dataset $\mathbf{T}$.
N_{rows}	#rows	Number of rows in the original dataset $\mathbf{T}$.
N_{sources}	#sources	Number of source nodes in the DAG $\mathcal{G}$.
N_h	size of hidden layer	Size of the hidden layers used in the LSTM cells. ($N_h = 100$)
N_x	size of input	Size of the generic input of the LSTM cell.
N_z	size of noise tensor	Number of elements in the noise vector. ($N_z = 200$)
N_b	batch size	Batch size. ($N_b = 500$)
N_L	#layers in discriminator	Number of layers used in the discriminator. ($N_L = 1$)
N_l	size of discriminator	Size of the hidden layers inside the discriminator. ($N_l = 100$)
N_C	#continuous variables	Number of continuous variables in the original dataset $\mathbf{T}$.
N_D	#categorical variables	Number of categorical variables in the original dataset $\mathbf{T}$.
$N_{m,t}$	#modes	Number of modes used to encode the continuous variable C_t with a VGM.
$|D_t|$	#categories	Number of unique categories in the categorical variable D_t.
N_{conv}	size of convolutional layer	Size of the layer used in the output transformer to act as a convolution. Ideally, we want to have $N_{\text{conv}} < N_h$. ($N_{\text{conv}} = 50$)
Layers in Neural Networks		
FC	Fully Connected	Fully connected layer without any activation function.
LeakyReLU	LeakyReLU	Layer with a leaky reflect linear activation function.
BN	Batch Normalization	Batch Normalization.
LN	Layer Normalization	Layer Normalization as described by Ba et al. (2016).
div	mini-batch discrimination	Mini-batch discriminator vector as described by Salimans et al. (2016).
tanh	$\tanh$ FC	Fully connected layer FC with a $\tanh$ activation function.
softmax	softmax FC	Fully connected layer FC with a softmax activation function.

5 Tables of results

In this section, we provide the complete tables of results used in the original article and in the previous section. Each section is named after the corresponding sections in the original article.

5.1 Comparison of DATGAN versions

5.1.1 CMAP case study

Table 6: Results of the statistics on the first aggregation level (all columns) for the CMAP dataset. Lighter grey tone corresponds to better results compared to darker ones.

Name	MAE		RMSE		R^2		SRMSE		ρ_{Pearson}		rank
SGAN_NO_AA	12	$7.52e-3$	12	$9.31e-3$	17	$9.80e-1$	15	$6.63e-2$	24	$9.92e-1$	16.0
SGAN_NO_AS	06	$6.50e-3$	06	$8.19e-3$	15	$9.82e-1$	09	$6.19e-2$	23	$9.92e-1$	11.8
SGAN_NO_SA	07	$6.70e-3$	07	$8.55e-3$	09	$9.85e-1$	07	$6.15e-2$	17	$9.94e-1$	9.4
SGAN_NO_SS	04	$6.13e-3$	05	$7.80e-3$	11	$9.85e-1$	05	$5.76e-2$	13	$9.94e-1$	7.6
SGAN_OS_AA	24	$9.80e-3$	24	$1.22e-2$	20	$9.73e-1$	24	$8.31e-2$	21	$9.93e-1$	22.6
SGAN_OS_AS	34	$3.36e-2$	33	$4.06e-2$	27	$8.75e-1$	34	$2.70e-1$	22	$9.93e-1$	30.0
SGAN_OS_SA	23	$9.70e-3$	23	$1.21e-2$	19	$9.74e-1$	23	$8.28e-2$	16	$9.94e-1$	20.8
SGAN_OS_SS	32	$3.32e-2$	31	$4.04e-2$	25	$8.78e-1$	33	$2.68e-1$	10	$9.94e-1$	26.2
SGAN_TS_AA	11	$7.19e-3$	11	$8.92e-3$	06	$9.86e-1$	12	$6.32e-2$	08	$9.95e-1$	9.6
SGAN_TS_AS	09	$6.94e-3$	08	$8.59e-3$	03	$9.87e-1$	06	$6.08e-2$	07	$9.95e-1$	6.6
SGAN_TS_SA	08	$6.94e-3$	09	$8.72e-3$	04	$9.87e-1$	10	$6.22e-2$	06	$9.95e-1$	7.4
SGAN_TS_SS	10	$7.02e-3$	10	$8.79e-3$	05	$9.87e-1$	08	$6.17e-2$	05	$9.95e-1$	7.6
WGAN_NO_AA	22	$9.56e-3$	22	$1.18e-2$	18	$9.80e-1$	18	$7.90e-2$	20	$9.93e-1$	20.0
WGAN_NO_AS	01	$5.53e-3$	01	$7.07e-3$	12	$9.85e-1$	04	$5.36e-2$	19	$9.93e-1$	7.4
WGAN_NO_SA	21	$9.55e-3$	21	$1.17e-2$	16	$9.81e-1$	17	$7.87e-2$	15	$9.94e-1$	18.0
WGAN_NO_SS	02	$5.65e-3$	02	$7.09e-3$	07	$9.85e-1$	02	$5.29e-2$	14	$9.94e-1$	5.4
WGAN_OS_AA	13	$7.58e-3$	14	$9.48e-3$	14	$9.83e-1$	14	$6.58e-2$	12	$9.94e-1$	13.4
WGAN_OS_AS	31	$3.32e-2$	32	$4.04e-2$	26	$8.75e-1$	31	$2.66e-1$	18	$9.93e-1$	27.6
WGAN_OS_SA	15	$7.64e-3$	15	$9.51e-3$	13	$9.83e-1$	16	$6.67e-2$	09	$9.94e-1$	13.6
WGAN_OS_SS	33	$3.35e-2$	34	$4.07e-2$	28	$8.75e-1$	32	$2.67e-1$	11	$9.94e-1$	27.6
WGAN_TS_AA	16	$7.75e-3$	16	$9.58e-3$	10	$9.85e-1$	13	$6.41e-2$	04	$9.96e-1$	11.8
WGAN_TS_AS	03	$6.11e-3$	03	$7.58e-3$	02	$9.87e-1$	01	$5.23e-2$	02	$9.96e-1$	2.2
WGAN_TS_SA	14	$7.63e-3$	13	$9.34e-3$	08	$9.85e-1$	11	$6.23e-2$	01	$9.96e-1$	9.4
WGAN_TS_SS	05	$6.33e-3$	04	$7.76e-3$	01	$9.88e-1$	03	$5.32e-2$	03	$9.96e-1$	3.2
WGGP_NO_AA	20	$8.76e-3$	20	$1.10e-2$	23	$9.65e-1$	22	$8.26e-2$	28	$9.86e-1$	22.6
WGGP_NO_AS	18	$8.28e-3$	18	$1.06e-2$	21	$9.66e-1$	20	$8.06e-2$	25	$9.87e-1$	20.4
WGGP_NO_SA	19	$8.65e-3$	19	$1.08e-2$	22	$9.66e-1$	21	$8.14e-2$	27	$9.86e-1$	21.6
WGGP_NO_SS	17	$8.26e-3$	17	$1.05e-2$	24	$9.65e-1$	19	$7.96e-2$	26	$9.87e-1$	20.6
WGGP_OS_AA	30	$2.65e-2$	30	$3.45e-2$	34	$6.03e-1$	30	$2.52e-1$	36	$9.61e-1$	32.0
WGGP_OS_AS	36	$3.85e-2$	36	$4.84e-2$	36	$5.85e-1$	36	$3.49e-1$	35	$9.63e-1$	35.8
WGGP_OS_SA	29	$2.49e-2$	29	$3.17e-2$	29	$7.79e-1$	29	$2.25e-1$	34	$9.68e-1$	30.0
WGGP_OS_SS	35	$3.72e-2$	35	$4.59e-2$	30	$7.58e-1$	35	$3.24e-1$	33	$9.71e-1$	33.6
WGGP_TS_AA	28	$1.71e-2$	28	$2.05e-2$	35	$5.97e-1$	28	$1.35e-1$	31	$9.79e-1$	30.0
WGGP_TS_AS	26	$1.54e-2$	26	$1.89e-2$	33	$6.16e-1$	27	$1.26e-1$	32	$9.79e-1$	28.8
WGGP_TS_SA	27	$1.62e-2$	27	$1.95e-2$	32	$6.20e-1$	26	$1.25e-1$	29	$9.81e-1$	28.2
WGGP_TS_SS	25	$1.47e-2$	25	$1.78e-2$	31	$6.34e-1$	25	$1.15e-1$	30	$9.80e-1$	27.2

Table 7: Results of the statistics on the first aggregation level (continuous columns) for the CMAP dataset. Lighter grey tone corresponds to better results compared to darker ones.

Name	MAE		RMSE		R^2		SRMSE		ρ_{Pearson}		rank
SGAN_NO_AA	24	$1.23e-2$	24	$1.61e-2$	24	$9.31e-1$	24	$1.61e-1$	24	$9.67e-1$	24.0
SGAN_NO_AS	23	$1.21e-2$	23	$1.61e-2$	23	$9.31e-1$	23	$1.61e-1$	23	$9.67e-1$	23.0
SGAN_NO_SA	17	$1.02e-2$	17	$1.43e-2$	14	$9.47e-1$	17	$1.43e-1$	18	$9.75e-1$	16.6
SGAN_NO_SS	18	$1.03e-2$	18	$1.43e-2$	15	$9.47e-1$	18	$1.43e-1$	16	$9.76e-1$	17.0
SGAN_OS_AA	21	$1.16e-2$	21	$1.51e-2$	21	$9.37e-1$	21	$1.51e-1$	15	$9.76e-1$	19.8
SGAN_OS_AS	22	$1.18e-2$	22	$1.55e-2$	22	$9.36e-1$	22	$1.55e-1$	19	$9.75e-1$	21.4
SGAN_OS_SA	20	$1.09e-2$	20	$1.47e-2$	18	$9.45e-1$	20	$1.47e-1$	08	$9.83e-1$	17.2
SGAN_OS_SS	19	$1.07e-2$	19	$1.45e-2$	16	$9.47e-1$	19	$1.45e-1$	07	$9.83e-1$	16.0
SGAN_TS_AA	12	$9.59e-3$	07	$1.25e-2$	08	$9.60e-1$	07	$1.25e-1$	10	$9.82e-1$	8.8
SGAN_TS_AS	09	$9.44e-3$	05	$1.24e-2$	07	$9.61e-1$	05	$1.24e-1$	09	$9.82e-1$	7.0
SGAN_TS_SA	08	$9.42e-3$	08	$1.27e-2$	06	$9.61e-1$	08	$1.27e-1$	06	$9.83e-1$	7.2
SGAN_TS_SS	07	$9.24e-3$	06	$1.24e-2$	05	$9.62e-1$	06	$1.24e-1$	05	$9.84e-1$	5.8
WGAN_NO_AA	13	$9.86e-3$	16	$1.37e-2$	20	$9.39e-1$	16	$1.37e-1$	22	$9.70e-1$	17.4
WGAN_NO_AS	14	$9.91e-3$	15	$1.37e-2$	19	$9.40e-1$	15	$1.37e-1$	21	$9.70e-1$	16.8
WGAN_NO_SA	15	$9.93e-3$	13	$1.34e-2$	13	$9.47e-1$	13	$1.34e-1$	17	$9.75e-1$	14.2
WGAN_NO_SS	16	$1.00e-2$	14	$1.36e-2$	17	$9.46e-1$	14	$1.36e-1$	20	$9.75e-1$	16.2
WGAN_OS_AA	06	$8.91e-3$	09	$1.27e-2$	11	$9.56e-1$	09	$1.27e-1$	13	$9.79e-1$	9.6
WGAN_OS_AS	05	$8.89e-3$	10	$1.28e-2$	12	$9.55e-1$	10	$1.28e-1$	14	$9.79e-1$	10.2
WGAN_OS_SA	11	$9.46e-3$	12	$1.30e-2$	10	$9.58e-1$	12	$1.30e-1$	12	$9.82e-1$	11.4
WGAN_OS_SS	10	$9.44e-3$	11	$1.29e-2$	09	$9.59e-1$	11	$1.29e-1$	11	$9.82e-1$	10.4
WGAN_TS_AA	02	$7.58e-3$	03	$1.05e-2$	04	$9.69e-1$	03	$1.05e-1$	04	$9.85e-1$	3.2
WGAN_TS_AS	01	$7.48e-3$	01	$1.04e-2$	01	$9.71e-1$	01	$1.04e-1$	02	$9.86e-1$	1.2
WGAN_TS_SA	03	$7.85e-3$	02	$1.04e-2$	02	$9.71e-1$	02	$1.04e-1$	01	$9.86e-1$	2.0
WGAN_TS_SS	04	$7.98e-3$	04	$1.05e-2$	03	$9.70e-1$	04	$1.05e-1$	03	$9.86e-1$	3.6
WGGP_NO_AA	28	$1.64e-2$	28	$2.21e-2$	28	$8.58e-1$	28	$2.21e-1$	28	$9.39e-1$	28.0
WGGP_NO_AS	27	$1.63e-2$	27	$2.21e-2$	25	$8.61e-1$	27	$2.21e-1$	26	$9.40e-1$	26.4
WGGP_NO_SA	26	$1.61e-2$	26	$2.14e-2$	26	$8.59e-1$	26	$2.14e-1$	25	$9.40e-1$	25.8
WGGP_NO_SS	25	$1.61e-2$	25	$2.13e-2$	27	$8.58e-1$	25	$2.13e-1$	27	$9.40e-1$	25.8
WGGP_OS_AA	36	$3.67e-2$	36	$5.46e-2$	36	$-5.05e-1$	36	$5.46e-1$	36	$8.31e-1$	36.0
WGGP_OS_AS	35	$3.67e-2$	35	$5.45e-2$	35	$-5.01e-1$	35	$5.45e-1$	35	$8.32e-1$	35.0
WGGP_OS_SA	34	$3.01e-2$	34	$4.18e-2$	34	$3.68e-1$	34	$4.18e-1$	34	$8.70e-1$	34.0
WGGP_OS_SS	33	$2.99e-2$	33	$4.15e-2$	33	$3.74e-1$	33	$4.15e-1$	33	$8.72e-1$	33.0
WGGP_TS_AA	32	$2.40e-2$	32	$3.32e-2$	31	$7.38e-1$	32	$3.32e-1$	31	$9.12e-1$	31.6
WGGP_TS_AS	31	$2.39e-2$	31	$3.31e-2$	32	$7.37e-1$	31	$3.31e-1$	32	$9.12e-1$	31.4
WGGP_TS_SA	30	$2.02e-2$	30	$2.81e-2$	30	$8.12e-1$	30	$2.81e-1$	29	$9.22e-1$	29.8
WGGP_TS_SS	29	$2.02e-2$	29	$2.80e-2$	29	$8.12e-1$	29	$2.80e-1$	30	$9.22e-1$	29.2

Table 8: Results of the statistics on the first aggregation level (categorical columns) for the CMAP dataset. Lighter grey tone corresponds to better results compared to darker ones.

Name	MAE		RMSE		R^2		SRMSE		ρ_{Pearson}		rank
SGAN_NO_AA	12	$6.33e-3$	08	$7.60e-3$	11	$9.92e-1$	08	$4.25e-2$	11	$9.98e-1$	10.0
SGAN_NO_AS	03	$5.09e-3$	04	$6.23e-3$	04	$9.95e-1$	04	$3.73e-2$	05	$9.99e-1$	4.0

Table 8 – continued from previous page

Name		MAE		RMSE		R^2		SRMSE		ρ_{Pearson}		rank
SGAN_NO_SA	**06**	$5.83\mathrm{e}-3$	**07**	$7.12\mathrm{e}-3$	**03**	$9.95\mathrm{e}-1$	**07**	$4.12\mathrm{e}-2$	**07**	$9.99\mathrm{e}-1$		**6.0**
SGAN_NO_SS	**04**	$5.10\mathrm{e}-3$	**03**	$6.17\mathrm{e}-3$	**05**	$9.94\mathrm{e}-1$	**03**	$3.62\mathrm{e}-2$	**04**	$9.99\mathrm{e}-1$		**3.8**
SGAN_OS_AA	21	$9.36\mathrm{e}-3$	23	$1.15\mathrm{e}-2$	23	$9.82\mathrm{e}-1$	23	$6.63\mathrm{e}-2$	26	$9.97\mathrm{e}-1$		23.2
SGAN_OS_AS	33	$3.90\mathrm{e}-2$	33	$4.69\mathrm{e}-2$	28	$8.60\mathrm{e}-1$	32	$2.99\mathrm{e}-1$	24	$9.97\mathrm{e}-1$		30.0
SGAN_OS_SA	22	$9.40\mathrm{e}-3$	24	$1.15\mathrm{e}-2$	24	$9.82\mathrm{e}-1$	24	$6.68\mathrm{e}-2$	28	$9.97\mathrm{e}-1$		24.4
SGAN_OS_SS	31	$3.89\mathrm{e}-2$	31	$4.69\mathrm{e}-2$	27	$8.61\mathrm{e}-1$	31	$2.98\mathrm{e}-1$	25	$9.97\mathrm{e}-1$		29.0
SGAN_TS_AA	14	$6.59\mathrm{e}-3$	14	$8.03\mathrm{e}-3$	**09**	$9.93\mathrm{e}-1$	14	$4.78\mathrm{e}-2$	20	$9.98\mathrm{e}-1$		14.2
SGAN_TS_AS	**10**	$6.32\mathrm{e}-3$	**09**	$7.65\mathrm{e}-3$	**06**	$9.94\mathrm{e}-1$	**09**	$4.50\mathrm{e}-2$	14	$9.98\mathrm{e}-1$		**9.6**
SGAN_TS_SA	11	$6.32\mathrm{e}-3$	**10**	$7.73\mathrm{e}-3$	**07**	$9.93\mathrm{e}-1$	11	$4.60\mathrm{e}-2$	18	$9.98\mathrm{e}-1$		11.4
SGAN_TS_SS	13	$6.47\mathrm{e}-3$	13	$7.88\mathrm{e}-3$	**08**	$9.93\mathrm{e}-1$	12	$4.60\mathrm{e}-2$	17	$9.98\mathrm{e}-1$		12.6
WGAN_NO_AA	24	$9.48\mathrm{e}-3$	21	$1.13\mathrm{e}-2$	18	$9.90\mathrm{e}-1$	21	$6.46\mathrm{e}-2$	**03**	$9.99\mathrm{e}-1$		17.4
WGAN_NO_AS	**01**	$4.43\mathrm{e}-3$	**01**	$5.42\mathrm{e}-3$	**01**	$9.96\mathrm{e}-1$	**02**	$3.28\mathrm{e}-2$	**02**	$9.99\mathrm{e}-1$		**1.4**
WGAN_NO_SA	23	$9.45\mathrm{e}-3$	22	$1.13\mathrm{e}-2$	20	$9.89\mathrm{e}-1$	22	$6.49\mathrm{e}-2$	**06**	$9.99\mathrm{e}-1$		18.6
WGAN_NO_SS	**02**	$4.56\mathrm{e}-3$	**02**	$5.46\mathrm{e}-3$	**02**	$9.95\mathrm{e}-1$	**01**	$3.22\mathrm{e}-2$	**01**	$9.99\mathrm{e}-1$		**1.6**
WGAN_OS_AA	18	$7.25\mathrm{e}-3$	18	$8.67\mathrm{e}-3$	17	$9.90\mathrm{e}-1$	17	$5.04\mathrm{e}-2$	21	$9.98\mathrm{e}-1$		18.2
WGAN_OS_AS	35	$3.93\mathrm{e}-2$	35	$4.74\mathrm{e}-2$	30	$8.56\mathrm{e}-1$	33	$3.00\mathrm{e}-1$	27	$9.97\mathrm{e}-1$		32.0
WGAN_OS_SA	17	$7.19\mathrm{e}-3$	17	$8.64\mathrm{e}-3$	19	$9.90\mathrm{e}-1$	18	$5.08\mathrm{e}-2$	22	$9.98\mathrm{e}-1$		18.6
WGAN_OS_SS	36	$3.95\mathrm{e}-2$	36	$4.76\mathrm{e}-2$	32	$8.54\mathrm{e}-1$	36	$3.02\mathrm{e}-1$	23	$9.97\mathrm{e}-1$		32.6
WGAN_TS_AA	20	$7.79\mathrm{e}-3$	20	$9.34\mathrm{e}-3$	21	$9.89\mathrm{e}-1$	20	$5.37\mathrm{e}-2$	12	$9.98\mathrm{e}-1$		18.6
WGAN_TS_AS	**05**	$5.77\mathrm{e}-3$	**05**	$6.89\mathrm{e}-3$	16	$9.91\mathrm{e}-1$	**05**	$3.95\mathrm{e}-2$	**09**	$9.98\mathrm{e}-1$		**8.0**
WGAN_TS_SA	19	$7.57\mathrm{e}-3$	19	$9.08\mathrm{e}-3$	22	$9.89\mathrm{e}-1$	19	$5.19\mathrm{e}-2$	**10**	$9.98\mathrm{e}-1$		17.8
WGAN_TS_SS	**07**	$5.92\mathrm{e}-3$	**06**	$7.06\mathrm{e}-3$	13	$9.92\mathrm{e}-1$	**06**	$4.01\mathrm{e}-2$	**08**	$9.98\mathrm{e}-1$		**8.0**
WGGP_NO_AA	16	$6.84\mathrm{e}-3$	15	$8.19\mathrm{e}-3$	14	$9.92\mathrm{e}-1$	15	$4.80\mathrm{e}-2$	16	$9.98\mathrm{e}-1$		15.2
WGGP_NO_AS	**08**	$6.27\mathrm{e}-3$	11	$7.74\mathrm{e}-3$	**10**	$9.92\mathrm{e}-1$	**10**	$4.55\mathrm{e}-2$	13	$9.98\mathrm{e}-1$		10.4
WGGP_NO_SA	15	$6.78\mathrm{e}-3$	16	$8.19\mathrm{e}-3$	12	$9.92\mathrm{e}-1$	16	$4.84\mathrm{e}-2$	19	$9.98\mathrm{e}-1$		15.6
WGGP_NO_SS	**09**	$6.31\mathrm{e}-3$	12	$7.81\mathrm{e}-3$	15	$9.91\mathrm{e}-1$	13	$4.61\mathrm{e}-2$	15	$9.98\mathrm{e}-1$		12.8
WGGP_OS_AA	30	$2.39\mathrm{e}-2$	30	$2.95\mathrm{e}-2$	26	$8.81\mathrm{e}-1$	30	$1.79\mathrm{e}-1$	36	$9.93\mathrm{e}-1$		30.4
WGGP_OS_AS	32	$3.89\mathrm{e}-2$	32	$4.69\mathrm{e}-2$	29	$8.57\mathrm{e}-1$	34	$3.00\mathrm{e}-1$	29	$9.96\mathrm{e}-1$		31.2
WGGP_OS_SA	29	$2.37\mathrm{e}-2$	29	$2.91\mathrm{e}-2$	25	$8.81\mathrm{e}-1$	29	$1.77\mathrm{e}-1$	35	$9.93\mathrm{e}-1$		29.4
WGGP_OS_SS	34	$3.90\mathrm{e}-2$	34	$4.70\mathrm{e}-2$	31	$8.54\mathrm{e}-1$	35	$3.01\mathrm{e}-1$	30	$9.96\mathrm{e}-1$		32.8
WGGP_TS_AA	28	$1.53\mathrm{e}-2$	28	$1.74\mathrm{e}-2$	36	$5.62\mathrm{e}-1$	27	$8.60\mathrm{e}-2$	31	$9.95\mathrm{e}-1$		30.0
WGGP_TS_AS	25	$1.33\mathrm{e}-2$	26	$1.53\mathrm{e}-2$	34	$5.85\mathrm{e}-1$	26	$7.45\mathrm{e}-2$	34	$9.95\mathrm{e}-1$		29.0
WGGP_TS_SA	27	$1.52\mathrm{e}-2$	27	$1.73\mathrm{e}-2$	35	$5.72\mathrm{e}-1$	28	$8.61\mathrm{e}-2$	32	$9.95\mathrm{e}-1$		29.8
WGGP_TS_SS	26	$1.33\mathrm{e}-2$	25	$1.52\mathrm{e}-2$	33	$5.89\mathrm{e}-1$	25	$7.34\mathrm{e}-2$	33	$9.95\mathrm{e}-1$		28.4

Table 9: Results of the statistics on the second aggregation level for the CMAP dataset. Lighter grey tone corresponds to better results compared to darker ones.

Name		MAE		RMSE		R^2		SRMSE		ρ_{Pearson}		rank
SGAN_NO_AA	14	$3.19\mathrm{e}-3$	14	$4.95\mathrm{e}-3$	16	$9.72\mathrm{e}-1$	15	$1.86\mathrm{e}-1$	19	$9.87\mathrm{e}-1$		15.6
SGAN_NO_AS	**07**	$3.09\mathrm{e}-3$	**08**	$4.77\mathrm{e}-3$	15	$9.73\mathrm{e}-1$	13	$1.82\mathrm{e}-1$	17	$9.87\mathrm{e}-1$		12.0
SGAN_NO_SA	**05**	$3.00\mathrm{e}-3$	**06**	$4.66\mathrm{e}-3$	12	$9.76\mathrm{e}-1$	**09**	$1.75\mathrm{e}-1$	12	$9.89\mathrm{e}-1$		**8.8**
SGAN_NO_SS	**03**	$2.96\mathrm{e}-3$	**03**	$4.54\mathrm{e}-3$	11	$9.77\mathrm{e}-1$	**05**	$1.71\mathrm{e}-1$	11	$9.89\mathrm{e}-1$		**6.6**
SGAN_OS_AA	24	$3.87\mathrm{e}-3$	24	$6.08\mathrm{e}-3$	20	$9.66\mathrm{e}-1$	24	$2.17\mathrm{e}-1$	20	$9.86\mathrm{e}-1$		22.4
SGAN_OS_AS	34	$1.18\mathrm{e}-2$	34	$1.80\mathrm{e}-2$	32	$8.16\mathrm{e}-1$	33	$6.25\mathrm{e}-1$	30	$9.63\mathrm{e}-1$		32.6

Table 9 – continued from previous page

Name	MAE		RMSE		R^2		SRMSE		ρ_{Pearson}		rank
SGAN_OS_SA	23	$3.83e-3$	23	$6.01e-3$	19	$9.68e-1$	23	$2.13e-1$	14	$9.88e-1$	20.4
SGAN_OS_SS	33	$1.18e-2$	33	$1.79e-2$	31	$8.19e-1$	32	$6.21e-1$	28	$9.65e-1$	31.4
SGAN_TS_AA	12	$3.17e-3$	13	$4.83e-3$	**10**	$9.77e-1$	11	$1.77e-1$	**10**	$9.89e-1$	11.2
SGAN_TS_AS	**10**	$3.15e-3$	11	$4.81e-3$	**07**	$9.78e-1$	12	$1.78e-1$	**08**	$9.90e-1$	**9.6**
SGAN_TS_SA	**08**	$3.09e-3$	**07**	$4.73e-3$	**05**	$9.78e-1$	**06**	$1.74e-1$	**05**	$9.90e-1$	**6.2**
SGAN_TS_SS	11	$3.16e-3$	12	$4.82e-3$	**06**	$9.78e-1$	**10**	$1.77e-1$	**06**	$9.90e-1$	**9.0**
WGAN_NO_AA	22	$3.68e-3$	22	$5.69e-3$	18	$9.70e-1$	19	$2.03e-1$	16	$9.87e-1$	19.4
WGAN_NO_AS	15	$3.28e-3$	16	$5.02e-3$	14	$9.73e-1$	16	$1.86e-1$	18	$9.87e-1$	15.8
WGAN_NO_SA	21	$3.66e-3$	21	$5.65e-3$	17	$9.72e-1$	18	$2.02e-1$	13	$9.88e-1$	18.0
WGAN_NO_SS	16	$3.31e-3$	15	$5.02e-3$	13	$9.74e-1$	14	$1.85e-1$	15	$9.88e-1$	14.6
WGAN_OS_AA	**09**	$3.12e-3$	**09**	$4.77e-3$	**09**	$9.78e-1$	**07**	$1.74e-1$	**09**	$9.89e-1$	**8.6**
WGAN_OS_AS	31	$1.16e-2$	31	$1.77e-2$	29	$8.23e-1$	30	$6.15e-1$	25	$9.69e-1$	29.2
WGAN_OS_SA	13	$3.18e-3$	**10**	$4.80e-3$	**08**	$9.78e-1$	**08**	$1.75e-1$	**07**	$9.90e-1$	**9.2**
WGAN_OS_SS	32	$1.16e-2$	32	$1.78e-2$	30	$8.22e-1$	31	$6.17e-1$	26	$9.69e-1$	30.2
WGAN_TS_AA	**06**	$3.01e-3$	**05**	$4.63e-3$	**04**	$9.81e-1$	**04**	$1.64e-1$	**03**	$9.92e-1$	**4.4**
WGAN_TS_AS	**01**	$2.78e-3$	**01**	$4.21e-3$	**01**	$9.83e-1$	**01**	$1.53e-1$	**02**	$9.92e-1$	**1.2**
WGAN_TS_SA	**04**	$2.98e-3$	**04**	$4.54e-3$	**03**	$9.82e-1$	**03**	$1.61e-1$	**01**	$9.92e-1$	**3.0**
WGAN_TS_SS	**02**	$2.83e-3$	**02**	$4.27e-3$	**02**	$9.83e-1$	**02**	$1.56e-1$	**04**	$9.92e-1$	**2.4**
WGGP_NO_AA	20	$3.52e-3$	20	$5.33e-3$	24	$9.57e-1$	21	$2.03e-1$	24	$9.81e-1$	21.8
WGGP_NO_AS	17	$3.42e-3$	18	$5.30e-3$	21	$9.58e-1$	20	$2.03e-1$	21	$9.81e-1$	19.4
WGGP_NO_SA	19	$3.48e-3$	17	$5.27e-3$	22	$9.57e-1$	17	$2.02e-1$	22	$9.81e-1$	19.4
WGGP_NO_SS	18	$3.42e-3$	19	$5.31e-3$	23	$9.57e-1$	22	$2.04e-1$	23	$9.81e-1$	21.0
WGGP_OS_AA	30	$9.46e-3$	30	$1.69e-2$	36	$4.37e-1$	34	$6.40e-1$	34	$9.31e-1$	32.8
WGGP_OS_AS	36	$1.35e-2$	36	$2.13e-2$	35	$5.23e-1$	36	$7.78e-1$	36	$9.18e-1$	35.8
WGGP_OS_SA	29	$8.87e-3$	29	$1.53e-2$	33	$7.06e-1$	29	$5.61e-1$	33	$9.44e-1$	30.6
WGGP_OS_SS	35	$1.29e-2$	35	$2.00e-2$	34	$7.05e-1$	35	$7.20e-1$	35	$9.31e-1$	34.8
WGGP_TS_AA	28	$6.30e-3$	28	$9.80e-3$	28	$8.91e-1$	28	$3.31e-1$	31	$9.62e-1$	28.6
WGGP_TS_AS	27	$6.08e-3$	27	$9.39e-3$	27	$8.97e-1$	27	$3.19e-1$	32	$9.61e-1$	28.0
WGGP_TS_SA	26	$6.04e-3$	26	$9.29e-3$	26	$9.07e-1$	26	$3.10e-1$	27	$9.65e-1$	26.2
WGGP_TS_SS	25	$5.80e-3$	25	$8.88e-3$	25	$9.12e-1$	25	$2.99e-1$	29	$9.64e-1$	25.8

Table 10: Results of the statistics on the third aggregation level for the CMAP dataset. Lighter grey tone corresponds to better results compared to darker ones.

Name	MAE		RMSE		R^2		SRMSE		ρ_{Pearson}		rank
SGAN_NO_AA	13	$1.19e-3$	14	$2.19e-3$	14	$9.51e-1$	14	$3.75e-1$	16	$9.77e-1$	14.2
SGAN_NO_AS	**10**	$1.19e-3$	12	$2.14e-3$	13	$9.53e-1$	13	$3.70e-1$	15	$9.77e-1$	12.6
SGAN_NO_SA	**06**	$1.15e-3$	**08**	$2.09e-3$	12	$9.57e-1$	**10**	$3.58e-1$	12	$9.80e-1$	**9.6**
SGAN_NO_SS	**05**	$1.15e-3$	**05**	$2.06e-3$	**10**	$9.58e-1$	**08**	$3.53e-1$	11	$9.80e-1$	**7.8**
SGAN_OS_AA	24	$1.37e-3$	24	$2.58e-3$	20	$9.42e-1$	24	$4.16e-1$	18	$9.76e-1$	22.0
SGAN_OS_AS	34	$3.30e-3$	33	$6.42e-3$	32	$7.42e-1$	33	1.14	32	$9.27e-1$	32.8
SGAN_OS_SA	23	$1.36e-3$	23	$2.53e-3$	19	$9.46e-1$	23	$4.06e-1$	14	$9.78e-1$	20.4
SGAN_OS_SS	33	$3.30e-3$	32	$6.39e-3$	31	$7.45e-1$	32	1.14	31	$9.28e-1$	31.8
SGAN_TS_AA	14	$1.20e-3$	13	$2.15e-3$	11	$9.57e-1$	**09**	$3.58e-1$	**10**	$9.80e-1$	11.4
SGAN_TS_AS	12	$1.19e-3$	11	$2.13e-3$	**09**	$9.58e-1$	12	$3.66e-1$	**09**	$9.80e-1$	10.6
SGAN_TS_SA	**08**	$1.18e-3$	**09**	$2.10e-3$	**07**	$9.59e-1$	**07**	$3.50e-1$	**05**	$9.81e-1$	**7.2**

Table 10 – continued from previous page

Name		MAE		RMSE		R^2		SRMSE		ρ_{Pearson}		rank
SGAN_TS_SS	**09**	$1.18e-3$	**10**	$2.11e-3$	**08**	$9.59e-1$	11	$3.62e-1$	**07**	$9.81e-1$	**9.0**
WGAN_NO_AA	21	$1.32e-3$	22	$2.39e-3$	17	$9.50e-1$	18	$3.90e-1$	17	$9.77e-1$	19.0
WGAN_NO_AS	20	$1.31e-3$	20	$2.36e-3$	18	$9.49e-1$	22	$4.03e-1$	20	$9.75e-1$	20.0
WGAN_NO_SA	19	$1.31e-3$	21	$2.38e-3$	15	$9.51e-1$	17	$3.89e-1$	13	$9.78e-1$	17.0
WGAN_NO_SS	22	$1.32e-3$	19	$2.35e-3$	16	$9.50e-1$	21	$4.01e-1$	19	$9.76e-1$	19.4
WGAN_OS_AA	**07**	$1.17e-3$	**06**	$2.07e-3$	**06**	$9.60e-1$	**05**	$3.48e-1$	**08**	$9.80e-1$	**6.4**
WGAN_OS_AS	31	$3.21e-3$	30	$6.26e-3$	29	$7.52e-1$	30	1.13	29	$9.37e-1$	29.8
WGAN_OS_SA	11	$1.19e-3$	**07**	$2.08e-3$	**05**	$9.60e-1$	**06**	$3.48e-1$	**06**	$9.81e-1$	**7.0**
WGAN_OS_SS	32	$3.23e-3$	31	$6.28e-3$	30	$7.51e-1$	31	1.13	30	$9.36e-1$	30.8
WGAN_TS_AA	**04**	$1.11e-3$	**04**	$1.97e-3$	**04**	$9.65e-1$	**02**	$3.26e-1$	**02**	$9.84e-1$	**3.2**
WGAN_TS_AS	**01**	$1.08e-3$	**01**	$1.90e-3$	**01**	$9.66e-1$	**03**	$3.27e-1$	**03**	$9.83e-1$	**1.8**
WGAN_TS_SA	**03**	$1.10e-3$	**03**	$1.95e-3$	**02**	$9.66e-1$	**01**	$3.22e-1$	**01**	$9.84e-1$	**2.0**
WGAN_TS_SS	**02**	$1.09e-3$	**02**	$1.92e-3$	**03**	$9.65e-1$	**04**	$3.31e-1$	**04**	$9.83e-1$	**3.0**
WGGP_NO_AA	18	$1.30e-3$	18	$2.29e-3$	24	$9.37e-1$	16	$3.84e-1$	24	$9.70e-1$	20.0
WGGP_NO_AS	16	$1.26e-3$	17	$2.27e-3$	21	$9.39e-1$	19	$3.92e-1$	21	$9.71e-1$	18.8
WGGP_NO_SA	17	$1.28e-3$	15	$2.26e-3$	23	$9.38e-1$	15	$3.83e-1$	22	$9.71e-1$	18.4
WGGP_NO_SS	15	$1.25e-3$	16	$2.27e-3$	22	$9.38e-1$	20	$3.96e-1$	23	$9.70e-1$	19.2
WGGP_OS_AA	30	$2.92e-3$	34	$7.01e-3$	36	$9.66e-2$	34	1.19	34	$8.97e-1$	33.6
WGGP_OS_AS	36	$3.79e-3$	36	$7.52e-3$	35	$4.50e-1$	36	1.36	36	$8.67e-1$	35.8
WGGP_OS_SA	29	$2.71e-3$	29	$6.18e-3$	34	$5.38e-1$	29	1.03	33	$9.15e-1$	30.8
WGGP_OS_SS	35	$3.60e-3$	35	$7.04e-3$	33	$6.35e-1$	35	1.27	35	$8.84e-1$	34.6
WGGP_TS_AA	28	$2.06e-3$	28	$3.93e-3$	28	$8.57e-1$	28	$5.92e-1$	27	$9.44e-1$	27.8
WGGP_TS_AS	27	$1.97e-3$	27	$3.71e-3$	27	$8.70e-1$	27	$5.85e-1$	28	$9.43e-1$	27.2
WGGP_TS_SA	26	$1.97e-3$	26	$3.70e-3$	26	$8.77e-1$	26	$5.66e-1$	25	$9.48e-1$	25.8
WGGP_TS_SS	25	$1.88e-3$	25	$3.51e-3$	25	$8.85e-1$	25	$5.65e-1$	26	$9.46e-1$	25.2

Table 11: Results of the Machine Learning efficacy for the CMAP dataset. Lighter grey tone corresponds to better results compared to darker ones.

Name		Continuous		Categorical		rank
SGAN_NO_AA	**02**	3.04	**02**	$6.23e-1$		**2.0**
SGAN_NO_AS	**04**	3.05	**04**	$6.51e-1$		4.0
SGAN_NO_SA	**06**	3.06	**01**	$6.15e-1$		**3.5**
SGAN_NO_SS	**09**	3.06	**03**	$6.38e-1$		6.0
SGAN_OS_AA	13	3.07	27	$1.61e2$		20.0
SGAN_OS_AS	27	3.38	23	2.95		25.0
SGAN_OS_SA	17	3.13	28	$4.01e2$		22.5
SGAN_OS_SS	28	3.43	24	2.97		26.0
SGAN_TS_AA	**10**	3.06	11	$7.25e-1$		10.5
SGAN_TS_AS	**07**	3.06	12	$7.34e-1$		**9.5**
SGAN_TS_SA	12	3.07	**09**	$7.02e-1$		10.5
SGAN_TS_SS	14	3.08	**10**	$7.22e-1$		12.0
WGAN_NO_AA	21	3.16	32	$7.04e3$		26.5
WGAN_NO_AS	19	3.14	17	1.18		18.0
WGAN_NO_SA	23	3.17	31	$6.64e3$		27.0
WGAN_NO_SS	22	3.17	18	1.19		20.0

Table 11 – continued from previous page

Name	Continuous		Categorical		rank
WGAN_OS_AA	11	3.07	15	$8.78e-1$	13.0
WGAN_OS_AS	25	3.32	21	2.80	23.0
WGAN_OS_SA	15	3.08	16	$8.92e-1$	15.5
WGAN_OS_SS	26	3.34	22	2.82	24.0
WGAN_TS_AA	**01**	3.04	**07**	$6.78e-1$	**4.0**
WGAN_TS_AS	**03**	3.04	13	$7.47e-1$	**8.0**
WGAN_TS_SA	**08**	3.06	**08**	$6.87e-1$	**8.0**
WGAN_TS_SS	**05**	3.05	14	$7.56e-1$	**9.5**
WGGP_NO_AA	20	3.15	35	1.13e4	27.5
WGGP_NO_AS	16	3.12	**06**	$6.72e-1$	11.0
WGGP_NO_SA	24	3.18	36	1.23e4	30.0
WGGP_NO_SS	18	3.13	**05**	$6.71e-1$	11.5
WGGP_OS_AA	30	3.89	30	4.48e3	30.0
WGGP_OS_AS	36	4.50	25	3.10	30.5
WGGP_OS_SA	29	3.87	29	4.08e3	29.0
WGGP_OS_SS	35	4.25	26	3.30	30.5
WGGP_TS_AA	33	4.10	33	8.00e3	33.0
WGGP_TS_AS	34	4.15	20	1.28	27.0
WGGP_TS_SA	32	3.94	34	8.80e3	33.0
WGGP_TS_SS	31	3.91	19	1.20	25.0

5.1.2 LPMC case study

Table 12: Results of the statistics on the first aggregation level (all columns) for the LPMC dataset. Lighter grey tone corresponds to better results compared to darker ones.

Name	MAE		RMSE		R^2		SRMSE		ρ_{Pearson}		rank
SGAN_NO_AA	22	$1.26e-2$	22	$1.74e-2$	24	$8.72e-1$	22	$1.36e-1$	24	$9.69e-1$	22.8
SGAN_NO_AS	16	$9.78e-3$	16	$1.40e-2$	16	$9.06e-1$	18	$1.22e-1$	22	$9.73e-1$	17.6
SGAN_NO_SA	20	$1.22e-2$	20	$1.65e-2$	21	$8.86e-1$	19	$1.27e-1$	20	$9.74e-1$	20.0
SGAN_NO_SS	13	$9.40e-3$	14	$1.32e-2$	14	$9.17e-1$	14	$1.13e-1$	21	$9.73e-1$	15.2
SGAN_OS_AA	24	$1.41e-2$	24	$1.84e-2$	30	$3.91e-1$	23	$1.43e-1$	36	$9.36e-1$	27.4
SGAN_OS_AS	34	$2.34e-2$	33	$2.89e-2$	22	$8.85e-1$	33	$1.81e-1$	32	$9.62e-1$	30.8
SGAN_OS_SA	23	$1.31e-2$	21	$1.68e-2$	29	$4.07e-1$	20	$1.27e-1$	35	$9.40e-1$	25.6
SGAN_OS_SS	31	$2.24e-2$	31	$2.74e-2$	17	$8.95e-1$	29	$1.66e-1$	29	$9.65e-1$	27.4
SGAN_TS_AA	15	$9.71e-3$	13	$1.28e-2$	15	$9.13e-1$	**09**	$1.00e-1$	18	$9.74e-1$	14.0
SGAN_TS_AS	**05**	$8.22e-3$	**05**	$1.10e-2$	**09**	$9.27e-1$	**04**	$9.24e-2$	14	$9.76e-1$	**7.4**
SGAN_TS_SA	14	$9.41e-3$	11	$1.25e-2$	13	$9.17e-1$	**06**	$9.75e-2$	13	$9.76e-1$	11.4
SGAN_TS_SS	**02**	$7.94e-3$	**02**	$1.07e-2$	**08**	$9.29e-1$	**03**	$8.99e-2$	12	$9.77e-1$	**5.4**
WGAN_NO_AA	36	$2.42e-2$	36	$3.25e-2$	26	$8.01e-1$	36	$2.30e-1$	17	$9.75e-1$	30.2
WGAN_NO_AS	18	$1.17e-2$	23	$1.77e-2$	12	$9.20e-1$	28	$1.65e-1$	15	$9.76e-1$	19.2
WGAN_NO_SA	32	$2.25e-2$	34	$2.93e-2$	25	$8.22e-1$	35	$1.98e-1$	**06**	$9.80e-1$	26.4
WGAN_NO_SS	17	$9.98e-3$	17	$1.45e-2$	**05**	$9.41e-1$	21	$1.33e-1$	**05**	$9.81e-1$	13.0
WGAN_OS_AA	26	$1.61e-2$	26	$2.12e-2$	32	$2.09e-1$	27	$1.63e-1$	26	$9.67e-1$	27.4
WGAN_OS_AS	35	$2.40e-2$	35	$2.98e-2$	23	$8.76e-1$	34	$1.89e-1$	33	$9.60e-1$	32.0
WGAN_OS_SA	25	$1.52e-2$	25	$1.97e-2$	31	$2.21e-1$	24	$1.48e-1$	31	$9.63e-1$	27.2

Continues on next page...

Table 12 – continued from previous page

Name		MAE		RMSE		R^2		SRMSE		ρ_{Pearson}		rank
WGAN_OS_SS	33	$2.29e-2$	32	$2.81e-2$	18	$8.92e-1$	30	$1.72e-1$	25	$9.68e-1$	27.6
WGAN_TS_AA	28	$1.71e-2$	28	$2.26e-2$	36	$-7.22e-1$	32	$1.79e-1$	16	$9.75e-1$	28.0
WGAN_TS_AS	11	$9.03e-3$	15	$1.32e-2$	**04**	$9.49e-1$	16	$1.18e-1$	**03**	$9.85e-1$	**9.8**
WGAN_TS_SA	27	$1.70e-2$	27	$2.21e-2$	35	$-7.16e-1$	31	$1.74e-1$	**10**	$9.79e-1$	26.0
WGAN_TS_SS	**10**	$8.98e-3$	12	$1.27e-2$	**02**	$9.59e-1$	13	$1.12e-1$	**01**	$9.88e-1$	**7.6**
WGGP_NO_AA	**09**	$8.80e-3$	**09**	$1.18e-2$	10	$9.22e-1$	10	$1.00e-1$	08	$9.79e-1$	**9.2**
WGGP_NO_AS	**04**	$8.09e-3$	**06**	$1.11e-2$	06	$9.37e-1$	05	$9.53e-2$	11	$9.78e-1$	**6.4**
WGGP_NO_SA	12	$9.11e-3$	**10**	$1.23e-2$	11	$9.22e-1$	12	$1.05e-1$	07	$9.80e-1$	10.4
WGGP_NO_SS	**07**	$8.48e-3$	**08**	$1.17e-2$	07	$9.36e-1$	08	$1.00e-1$	09	$9.79e-1$	**7.8**
WGGP_OS_AA	21	$1.25e-2$	19	$1.59e-2$	28	$5.81e-1$	17	$1.20e-1$	34	$9.56e-1$	23.8
WGGP_OS_AS	30	$2.20e-2$	30	$2.68e-2$	20	$8.87e-1$	26	$1.62e-1$	28	$9.65e-1$	26.8
WGGP_OS_SA	19	$1.21e-2$	18	$1.55e-2$	27	$5.89e-1$	15	$1.15e-1$	27	$9.65e-1$	21.2
WGGP_OS_SS	29	$2.17e-2$	29	$2.64e-2$	19	$8.90e-1$	25	$1.58e-1$	30	$9.63e-1$	26.4
WGGP_TS_AA	**08**	$8.59e-3$	**07**	$1.14e-2$	33	$2.03e-1$	11	$1.04e-1$	23	$9.72e-1$	16.4
WGGP_TS_AS	**06**	$8.26e-3$	**04**	$1.09e-2$	**03**	$9.56e-1$	**02**	$8.77e-2$	**04**	$9.82e-1$	**3.8**
WGGP_TS_SA	**03**	$8.04e-3$	**03**	$1.07e-2$	34	$2.01e-1$	07	$9.77e-2$	19	$9.74e-1$	13.2
WGGP_TS_SS	**01**	$7.64e-3$	**01**	$1.02e-2$	**01**	$9.63e-1$	**01**	$8.13e-2$	**02**	$9.85e-1$	**1.2**

Table 13: Results of the statistics on the first aggregation level (continuous columns) for the LPMC dataset. Lighter grey tone corresponds to better results compared to darker ones.

Name		MAE		RMSE		R^2		SRMSE		ρ_{Pearson}		rank
SGAN_NO_AA	30	$1.39e-2$	30	$2.16e-2$	33	$8.87e-1$	30	$2.16e-1$	33	$9.67e-1$	31.2
SGAN_NO_AS	31	$1.39e-2$	29	$2.16e-2$	34	$8.86e-1$	29	$2.16e-1$	34	$9.67e-1$	31.4
SGAN_NO_SA	23	$1.28e-2$	23	$1.96e-2$	31	$9.18e-1$	23	$1.96e-1$	27	$9.75e-1$	25.4
SGAN_NO_SS	24	$1.29e-2$	24	$1.97e-2$	32	$9.17e-1$	24	$1.97e-1$	28	$9.75e-1$	26.4
SGAN_OS_AA	22	$1.28e-2$	22	$1.91e-2$	21	$9.36e-1$	22	$1.91e-1$	23	$9.76e-1$	22.0
SGAN_OS_AS	21	$1.28e-2$	21	$1.90e-2$	23	$9.36e-1$	21	$1.90e-1$	24	$9.76e-1$	22.0
SGAN_OS_SA	14	$1.07e-2$	14	$1.58e-2$	11	$9.56e-1$	14	$1.58e-1$	**08**	$9.84e-1$	12.2
SGAN_OS_SS	13	$1.07e-2$	13	$1.58e-2$	12	$9.56e-1$	13	$1.58e-1$	**07**	$9.84e-1$	11.6
SGAN_TS_AA	12	$1.05e-2$	11	$1.51e-2$	18	$9.47e-1$	11	$1.51e-1$	16	$9.80e-1$	13.6
SGAN_TS_AS	11	$1.05e-2$	12	$1.52e-2$	17	$9.47e-1$	12	$1.52e-1$	15	$9.80e-1$	13.4
SGAN_TS_SA	**07**	$9.97e-3$	**07**	$1.46e-2$	13	$9.54e-1$	**07**	$1.46e-1$	**10**	$9.83e-1$	**8.8**
SGAN_TS_SS	**08**	$9.97e-3$	**08**	$1.47e-2$	14	$9.54e-1$	**08**	$1.47e-1$	09	$9.83e-1$	**9.4**
WGAN_NO_AA	36	$1.99e-2$	36	$3.18e-2$	35	$8.75e-1$	36	$3.18e-1$	35	$9.64e-1$	35.6
WGAN_NO_AS	35	$1.99e-2$	35	$3.17e-2$	36	$8.75e-1$	35	$3.17e-1$	36	$9.64e-1$	35.4
WGAN_NO_SA	34	$1.65e-2$	34	$2.51e-2$	30	$9.25e-1$	34	$2.51e-1$	25	$9.76e-1$	31.4
WGAN_NO_SS	33	$1.64e-2$	33	$2.50e-2$	29	$9.25e-1$	33	$2.50e-1$	26	$9.76e-1$	30.8
WGAN_OS_AA	26	$1.35e-2$	26	$2.04e-2$	24	$9.36e-1$	26	$2.04e-1$	20	$9.79e-1$	24.4
WGAN_OS_AS	25	$1.35e-2$	25	$2.03e-2$	22	$9.36e-1$	25	$2.03e-1$	19	$9.79e-1$	23.2
WGAN_OS_SA	18	$1.15e-2$	18	$1.72e-2$	**04**	$9.63e-1$	18	$1.72e-1$	**04**	$9.87e-1$	12.4
WGAN_OS_SS	15	$1.13e-2$	17	$1.69e-2$	**03**	$9.63e-1$	17	$1.69e-1$	**03**	$9.88e-1$	11.0
WGAN_TS_AA	29	$1.38e-2$	31	$2.17e-2$	19	$9.39e-1$	31	$2.17e-1$	11	$9.82e-1$	24.2
WGAN_TS_AS	32	$1.40e-2$	32	$2.18e-2$	20	$9.38e-1$	32	$2.18e-1$	14	$9.82e-1$	26.0
WGAN_TS_SA	28	$1.37e-2$	28	$2.06e-2$	**08**	$9.59e-1$	28	$2.06e-1$	**01**	$9.89e-1$	18.6

Table 13 – continued from previous page

Name		MAE		RMSE		R^2		SRMSE		ρ_{Pearson}		rank
WGAN_TS_SS	27	$1.37\mathrm{e}-2$	27	$2.06\mathrm{e}-2$	**07**	$9.59\mathrm{e}-1$	27	$2.06\mathrm{e}-1$	**02**	$9.89\mathrm{e}-1$		18.0
WGGP_NO_AA	17	$1.14\mathrm{e}-2$	15	$1.67\mathrm{e}-2$	27	$9.29\mathrm{e}-1$	15	$1.67\mathrm{e}-1$	31	$9.72\mathrm{e}-1$		21.0
WGGP_NO_AS	16	$1.14\mathrm{e}-2$	16	$1.67\mathrm{e}-2$	28	$9.28\mathrm{e}-1$	16	$1.67\mathrm{e}-1$	32	$9.72\mathrm{e}-1$		21.6
WGGP_NO_SA	19	$1.19\mathrm{e}-2$	19	$1.76\mathrm{e}-2$	25	$9.30\mathrm{e}-1$	19	$1.76\mathrm{e}-1$	29	$9.73\mathrm{e}-1$		22.2
WGGP_NO_SS	20	$1.19\mathrm{e}-2$	20	$1.77\mathrm{e}-2$	26	$9.30\mathrm{e}-1$	20	$1.77\mathrm{e}-1$	30	$9.73\mathrm{e}-1$		23.2
WGGP_OS_AA	**10**	$1.03\mathrm{e}-2$	**10**	$1.50\mathrm{e}-2$	16	$9.52\mathrm{e}-1$	**10**	$1.50\mathrm{e}-1$	22	$9.77\mathrm{e}-1$		13.6
WGGP_OS_AS	**09**	$1.03\mathrm{e}-2$	**09**	$1.50\mathrm{e}-2$	15	$9.53\mathrm{e}-1$	**09**	$1.50\mathrm{e}-1$	21	$9.77\mathrm{e}-1$		12.6
WGGP_OS_SA	**03**	$9.49\mathrm{e}-3$	**03**	$1.40\mathrm{e}-2$	10	$9.56\mathrm{e}-1$	**03**	$1.40\mathrm{e}-1$	17	$9.79\mathrm{e}-1$		**7.2**
WGGP_OS_SS	**04**	$9.49\mathrm{e}-3$	**04**	$1.40\mathrm{e}-2$	09	$9.56\mathrm{e}-1$	**04**	$1.40\mathrm{e}-1$	18	$9.79\mathrm{e}-1$		7.8
WGGP_TS_AA	**06**	$9.84\mathrm{e}-3$	**06**	$1.43\mathrm{e}-2$	**06**	$9.61\mathrm{e}-1$	**06**	$1.43\mathrm{e}-1$	12	$9.82\mathrm{e}-1$		**7.2**
WGGP_TS_AS	**05**	$9.82\mathrm{e}-3$	**05**	$1.42\mathrm{e}-2$	**05**	$9.61\mathrm{e}-1$	**05**	$1.42\mathrm{e}-1$	13	$9.82\mathrm{e}-1$		6.6
WGGP_TS_SA	**01**	$8.91\mathrm{e}-3$	**01**	$1.31\mathrm{e}-2$	**02**	$9.69\mathrm{e}-1$	**01**	$1.31\mathrm{e}-1$	**06**	$9.86\mathrm{e}-1$		**2.2**
WGGP_TS_SS	**02**	$8.93\mathrm{e}-3$	**02**	$1.31\mathrm{e}-2$	**01**	$9.69\mathrm{e}-1$	**02**	$1.31\mathrm{e}-1$	**05**	$9.86\mathrm{e}-1$		2.4

Table 14: Results of the statistics on the first aggregation level (categorical columns) for the LPMC dataset. Lighter grey tone corresponds to better results compared to darker ones.

Name		MAE		RMSE		R^2		SRMSE		ρ_{Pearson}		rank
SGAN_NO_AA	19	$1.13\mathrm{e}-2$	19	$1.34\mathrm{e}-2$	17	$8.58\mathrm{e}-1$	17	$6.17\mathrm{e}-2$	19	$9.70\mathrm{e}-1$		18.2
SGAN_NO_AS	**07**	$5.93\mathrm{e}-3$	**07**	$6.93\mathrm{e}-3$	**09**	$9.23\mathrm{e}-1$	**07**	$3.43\mathrm{e}-2$	13	$9.79\mathrm{e}-1$		**8.6**
SGAN_NO_SA	20	$1.15\mathrm{e}-2$	20	$1.37\mathrm{e}-2$	18	$8.56\mathrm{e}-1$	18	$6.24\mathrm{e}-2$	16	$9.72\mathrm{e}-1$		18.4
SGAN_NO_SS	**10**	$6.18\mathrm{e}-3$	**10**	$7.17\mathrm{e}-3$	11	$9.16\mathrm{e}-1$	**09**	$3.54\mathrm{e}-2$	17	$9.72\mathrm{e}-1$		11.4
SGAN_OS_AA	24	$1.53\mathrm{e}-2$	24	$1.78\mathrm{e}-2$	30	$-1.14\mathrm{e}{-1}$	24	$9.85\mathrm{e}-2$	36	$8.99\mathrm{e}-1$		27.6
SGAN_OS_AS	34	$3.33\mathrm{e}-2$	34	$3.82\mathrm{e}-2$	20	$8.38\mathrm{e}-1$	33	$1.73\mathrm{e}-1$	29	$9.49\mathrm{e}-1$		30.0
SGAN_OS_SA	23	$1.52\mathrm{e}-2$	23	$1.77\mathrm{e}-2$	29	$-1.03\mathrm{e}{-1}$	23	$9.79\mathrm{e}-2$	35	$9.00\mathrm{e}-1$		26.6
SGAN_OS_SS	33	$3.33\mathrm{e}-2$	33	$3.81\mathrm{e}-2$	19	$8.39\mathrm{e}-1$	34	$1.74\mathrm{e}-1$	31	$9.47\mathrm{e}-1$		30.0
SGAN_TS_AA	18	$8.98\mathrm{e}-3$	18	$1.06\mathrm{e}-2$	16	$8.81\mathrm{e}-1$	16	$5.26\mathrm{e}-2$	22	$9.69\mathrm{e}-1$		18.0
SGAN_TS_AS	**09**	$6.13\mathrm{e}-3$	**09**	$7.08\mathrm{e}-3$	13	$9.08\mathrm{e}-1$	12	$3.75\mathrm{e}-2$	14	$9.72\mathrm{e}-1$		11.4
SGAN_TS_SA	17	$8.90\mathrm{e}-3$	17	$1.05\mathrm{e}-2$	15	$8.83\mathrm{e}-1$	15	$5.20\mathrm{e}-2$	18	$9.70\mathrm{e}-1$		16.4
SGAN_TS_SS	**08**	$6.06\mathrm{e}-3$	**08**	$6.99\mathrm{e}-3$	14	$9.05\mathrm{e}-1$	11	$3.71\mathrm{e}-2$	15	$9.72\mathrm{e}-1$		11.2
WGAN_NO_AA	29	$2.81\mathrm{e}-2$	29	$3.32\mathrm{e}-2$	25	$7.32\mathrm{e}-1$	29	$1.49\mathrm{e}-1$	**07**	$9.85\mathrm{e}-1$		23.8
WGAN_NO_AS	**02**	$4.04\mathrm{e}-3$	**02**	$4.75\mathrm{e}-3$	**01**	$9.62\mathrm{e}-1$	**02**	$2.45\mathrm{e}-2$	**03**	$9.87\mathrm{e}-1$		**2.0**
WGAN_NO_SA	30	$2.81\mathrm{e}-2$	30	$3.32\mathrm{e}-2$	26	$7.27\mathrm{e}-1$	30	$1.50\mathrm{e}-1$	10	$9.84\mathrm{e}-1$		25.2
WGAN_NO_SS	**01**	$3.98\mathrm{e}-3$	**01**	$4.67\mathrm{e}-3$	**05**	$9.56\mathrm{e}-1$	**01**	$2.42\mathrm{e}-2$	**04**	$9.86\mathrm{e}-1$		**2.4**
WGAN_OS_AA	25	$1.86\mathrm{e}-2$	25	$2.20\mathrm{e}-2$	31	$-4.65\mathrm{e}{-1}$	25	$1.26\mathrm{e}-1$	25	$9.56\mathrm{e}-1$		26.2
WGAN_OS_AS	36	$3.39\mathrm{e}-2$	36	$3.87\mathrm{e}-2$	24	$8.20\mathrm{e}-1$	36	$1.75\mathrm{e}-1$	32	$9.42\mathrm{e}-1$		32.8
WGAN_OS_SA	26	$1.87\mathrm{e}-2$	26	$2.21\mathrm{e}-2$	32	$-4.68\mathrm{e}{-1}$	26	$1.26\mathrm{e}-1$	33	$9.40\mathrm{e}-1$		28.6
WGAN_OS_SS	35	$3.37\mathrm{e}-2$	35	$3.85\mathrm{e}-2$	23	$8.25\mathrm{e}-1$	35	$1.74\mathrm{e}-1$	28	$9.50\mathrm{e}-1$		31.2
WGAN_TS_AA	28	$2.00\mathrm{e}-2$	28	$2.35\mathrm{e}-2$	35	-2.26	27	$1.44\mathrm{e}-1$	20	$9.69\mathrm{e}-1$		27.6
WGAN_TS_AS	**03**	$4.45\mathrm{e}-3$	**03**	$5.21\mathrm{e}-3$	**02**	$9.59\mathrm{e}-1$	**03**	$2.48\mathrm{e}-2$	**02**	$9.87\mathrm{e}-1$		**2.6**
WGAN_TS_SA	27	$2.00\mathrm{e}-2$	27	$2.35\mathrm{e}-2$	36	-2.27	28	$1.44\mathrm{e}-1$	21	$9.69\mathrm{e}-1$		27.8
WGAN_TS_SS	**04**	$4.61\mathrm{e}-3$	**04**	$5.38\mathrm{e}-3$	**03**	$9.59\mathrm{e}-1$	**04**	$2.50\mathrm{e}-2$	**01**	$9.88\mathrm{e}-1$		**3.2**
WGGP_NO_AA	11	$6.36\mathrm{e}-3$	11	$7.25\mathrm{e}-3$	**10**	$9.16\mathrm{e}-1$	13	$3.77\mathrm{e}-2$	**05**	$9.86\mathrm{e}-1$		**10.0**
WGGP_NO_AS	**05**	$5.01\mathrm{e}-3$	**05**	$5.79\mathrm{e}-3$	**07**	$9.45\mathrm{e}-1$	**05**	$2.83\mathrm{e}-2$	11	$9.83\mathrm{e}-1$		6.6
WGGP_NO_SA	13	$6.48\mathrm{e}-3$	12	$7.39\mathrm{e}-3$	12	$9.14\mathrm{e}-1$	14	$3.77\mathrm{e}-2$	**06**	$9.85\mathrm{e}-1$		11.4

Continues on next page...

Table 14 – continued from previous page

Name	MAE		RMSE		R^2		SRMSE		ρ_{Pearson}		rank
WGGP_NO_SS	**06**	5.26e − 3	**06**	6.05e − 3	08	9.42e − 1	**06**	2.86e − 2	08	9.84e − 1	**6.8**
WGGP_OS_AA	21	1.45e − 2	21	1.68e − 2	28	2.37e − 1	21	9.11e − 2	34	9.36e − 1	25.0
WGGP_OS_AS	31	3.30e − 2	31	3.77e − 2	22	8.26e − 1	31	1.72e − 1	26	9.53e − 1	28.2
WGGP_OS_SA	22	1.45e − 2	22	1.68e − 2	27	2.49e − 1	22	9.13e − 2	27	9.52e − 1	24.0
WGGP_OS_SS	32	3.30e − 2	32	3.79e − 2	21	8.29e − 1	32	1.73e − 1	30	9.48e − 1	29.4
WGGP_TS_AA	16	7.43e − 3	16	8.74e − 3	33	−5.01e−1	20	6.80e − 2	23	9.63e − 1	21.6
WGGP_TS_AS	14	6.82e − 3	14	7.88e − 3	**06**	9.51e − 1	**10**	3.70e − 2	12	9.82e − 1	11.2
WGGP_TS_SA	15	7.23e − 3	15	8.49e − 3	34	−5.12e−1	19	6.70e − 2	24	9.62e − 1	21.4
WGGP_TS_SS	12	6.44e − 3	13	7.47e − 3	**04**	9.56e − 1	**08**	3.52e − 2	**09**	9.84e − 1	**9.2**

Table 15: Results of the statistics on the second aggregation level for the LPMC dataset. Lighter grey tone corresponds to better results compared to darker ones.

Name	MAE		RMSE		R^2		SRMSE		ρ_{Pearson}		rank
SGAN_NO_AA	21	5.21e − 3	21	9.27e − 3	21	8.90e − 1	21	3.50e − 1	26	9.62e − 1	22.0
SGAN_NO_AS	17	4.89e − 3	16	8.70e − 3	18	9.02e − 1	18	3.37e − 1	22	9.64e − 1	18.2
SGAN_NO_SA	18	5.07e − 3	19	8.96e − 3	17	9.08e − 1	19	3.38e − 1	14	9.67e − 1	17.4
SGAN_NO_SS	15	4.79e − 3	15	8.47e − 3	11	9.18e − 1	15	3.27e − 1	13	9.69e − 1	13.8
SGAN_OS_AA	22	5.50e − 3	22	9.34e − 3	30	8.15e − 1	22	3.69e − 1	36	9.49e − 1	26.4
SGAN_OS_AS	34	8.75e − 3	32	1.38e − 2	22	8.90e − 1	32	4.51e − 1	30	9.60e − 1	30.0
SGAN_OS_SA	20	5.21e − 3	18	8.80e − 3	28	8.32e − 1	20	3.48e − 1	35	9.55e − 1	24.2
SGAN_OS_SS	32	8.50e − 3	31	1.34e − 2	19	9.01e − 1	28	4.35e − 1	20	9.65e − 1	26.0
SGAN_TS_AA	12	4.34e − 3	12	7.38e − 3	**10**	9.23e − 1	11	2.85e − 1	12	9.70e − 1	11.4
SGAN_TS_AS	**08**	4.19e − 3	**08**	7.15e − 3	**06**	9.30e − 1	**08**	2.79e − 1	11	9.71e − 1	**8.2**
SGAN_TS_SA	**09**	4.24e − 3	**09**	7.30e − 3	08	9.28e − 1	**09**	2.82e − 1	**09**	9.72e − 1	**8.8**
SGAN_TS_SS	**07**	4.13e − 3	**07**	7.10e − 3	**04**	9.34e − 1	**07**	2.78e − 1	**06**	9.73e − 1	**6.2**
WGAN_NO_AA	33	8.53e − 3	36	1.58e − 2	29	8.28e − 1	36	5.49e − 1	33	9.59e − 1	33.4
WGAN_NO_AS	26	6.19e − 3	27	1.14e − 2	24	8.88e − 1	29	4.41e − 1	29	9.60e − 1	27.0
WGAN_NO_SA	31	8.26e − 3	35	1.46e − 2	27	8.59e − 1	35	4.99e − 1	21	9.65e − 1	29.8
WGAN_NO_SS	23	5.92e − 3	23	1.04e − 2	13	9.16e − 1	25	3.98e − 1	17	9.66e − 1	20.2
WGAN_OS_AA	25	6.14e − 3	25	1.09e − 2	32	7.97e − 1	27	4.11e − 1	27	9.62e − 1	27.2
WGAN_OS_AS	36	8.99e − 3	34	1.42e − 2	23	8.88e − 1	34	4.61e − 1	32	9.60e − 1	31.8
WGAN_OS_SA	24	6.14e − 3	24	1.06e − 2	31	8.12e − 1	26	4.03e − 1	18	9.66e − 1	24.6
WGAN_OS_SS	35	8.94e − 3	33	1.41e − 2	20	9.01e − 1	33	4.59e − 1	23	9.64e − 1	28.8
WGAN_TS_AA	27	6.27e − 3	26	1.14e − 2	36	6.26e − 1	30	4.46e − 1	34	9.57e − 1	30.6
WGAN_TS_AS	16	4.89e − 3	17	8.80e − 3	**05**	9.34e − 1	16	3.28e − 1	**04**	9.75e − 1	11.6
WGAN_TS_SA	28	6.49e − 3	28	1.14e − 2	35	6.38e − 1	31	4.47e − 1	31	9.60e − 1	30.6
WGAN_TS_SS	19	5.14e − 3	20	8.97e − 3	**03**	9.44e − 1	17	3.33e − 1	**02**	9.77e − 1	12.2
WGGP_NO_AA	11	4.29e − 3	**10**	7.32e − 3	14	9.15e − 1	**10**	2.85e − 1	10	9.71e − 1	11.0
WGGP_NO_AS	**06**	4.04e − 3	**05**	7.00e − 3	**09**	9.28e − 1	**04**	2.75e − 1	08	9.72e − 1	**6.4**
WGGP_NO_SA	**10**	4.27e − 3	11	7.32e − 3	12	9.17e − 1	12	2.86e − 1	07	9.72e − 1	10.4
WGGP_NO_SS	**05**	4.02e − 3	**06**	7.01e − 3	**07**	9.29e − 1	**05**	2.77e − 1	**05**	9.73e − 1	**5.6**
WGGP_OS_AA	14	4.70e − 3	14	7.79e − 3	26	8.70e − 1	14	2.97e − 1	24	9.64e − 1	18.4
WGGP_OS_AS	30	7.81e − 3	30	1.22e − 2	16	9.08e − 1	24	3.91e − 1	16	9.66e − 1	23.2
WGGP_OS_SA	13	4.64e − 3	13	7.67e − 3	25	8.77e − 1	13	2.88e − 1	19	9.65e − 1	16.6
WGGP_OS_SS	29	7.78e − 3	29	1.22e − 2	15	9.10e − 1	23	3.90e − 1	15	9.67e − 1	22.2

Table 15 – continued from previous page

Name		MAE		RMSE		R^2		SRMSE		ρ_{Pearson}	rank
WGGP_TS_AA	04	$3.85\mathrm{e}-3$	04	$6.39\mathrm{e}-3$	34	$7.89\mathrm{e}-1$	06	$2.77\mathrm{e}-1$	28	$9.62\mathrm{e}-1$	15.2
WGGP_TS_AS	02	$3.70\mathrm{e}-3$	02	$6.16\mathrm{e}-3$	02	$9.47\mathrm{e}-1$	02	$2.35\mathrm{e}-1$	03	$9.75\mathrm{e}-1$	**2.2**
WGGP_TS_SA	03	$3.71\mathrm{e}-3$	03	$6.23\mathrm{e}-3$	33	$7.91\mathrm{e}-1$	03	$2.71\mathrm{e}-1$	25	$9.64\mathrm{e}-1$	13.4
WGGP_TS_SS	01	$3.52\mathrm{e}-3$	01	$5.91\mathrm{e}-3$	01	$9.51\mathrm{e}-1$	01	$2.26\mathrm{e}-1$	01	$9.78\mathrm{e}-1$	**1.0**

Table 16: Results of the statistics on the third aggregation level for the LPMC dataset. Lighter grey tone corresponds to better results compared to darker ones.

Name		MAE		RMSE		R^2		SRMSE		ρ_{Pearson}	rank
SGAN_NO_AA	20	$1.87\mathrm{e}-3$	21	$4.21\mathrm{e}-3$	23	$8.64\mathrm{e}-1$	20	$6.48\mathrm{e}-1$	24	$9.49\mathrm{e}-1$	21.6
SGAN_NO_AS	18	$1.84\mathrm{e}-3$	18	$4.09\mathrm{e}-3$	20	$8.75\mathrm{e}-1$	18	$6.37\mathrm{e}-1$	20	$9.51\mathrm{e}-1$	18.8
SGAN_NO_SA	16	$1.81\mathrm{e}-3$	17	$4.02\mathrm{e}-3$	18	$8.86\mathrm{e}-1$	17	$6.33\mathrm{e}-1$	18	$9.55\mathrm{e}-1$	17.2
SGAN_NO_SS	15	$1.80\mathrm{e}-3$	16	$3.98\mathrm{e}-3$	15	$8.94\mathrm{e}-1$	16	$6.32\mathrm{e}-1$	15	$9.56\mathrm{e}-1$	15.4
SGAN_OS_AA	21	$1.97\mathrm{e}-3$	20	$4.20\mathrm{e}-3$	33	$8.25\mathrm{e}-1$	22	$6.96\mathrm{e}-1$	36	$9.35\mathrm{e}-1$	26.4
SGAN_OS_AS	34	$2.79\mathrm{e}-3$	32	$5.75\mathrm{e}-3$	24	$8.57\mathrm{e}-1$	32	$8.38\mathrm{e}-1$	29	$9.44\mathrm{e}-1$	30.2
SGAN_OS_SA	19	$1.86\mathrm{e}-3$	15	$3.94\mathrm{e}-3$	27	$8.54\mathrm{e}-1$	21	$6.64\mathrm{e}-1$	30	$9.44\mathrm{e}-1$	22.4
SGAN_OS_SS	32	$2.71\mathrm{e}-3$	31	$5.60\mathrm{e}-3$	21	$8.72\mathrm{e}-1$	31	$8.34\mathrm{e}-1$	23	$9.50\mathrm{e}-1$	27.6
SGAN_TS_AA	13	$1.62\mathrm{e}-3$	13	$3.49\mathrm{e}-3$	10	$8.99\mathrm{e}-1$	14	$5.62\mathrm{e}-1$	12	$9.58\mathrm{e}-1$	12.4
SGAN_TS_AS	10	$1.59\mathrm{e}-3$	11	$3.44\mathrm{e}-3$	09	$9.06\mathrm{e}-1$	12	$5.60\mathrm{e}-1$	10	$9.59\mathrm{e}-1$	10.4
SGAN_TS_SA	09	$1.58\mathrm{e}-3$	10	$3.40\mathrm{e}-3$	06	$9.08\mathrm{e}-1$	11	$5.55\mathrm{e}-1$	07	$9.61\mathrm{e}-1$	**8.6**
SGAN_TS_SS	07	$1.56\mathrm{e}-3$	09	$3.39\mathrm{e}-3$	04	$9.13\mathrm{e}-1$	13	$5.60\mathrm{e}-1$	05	$9.62\mathrm{e}-1$	**7.6**
WGAN_NO_AA	33	$2.73\mathrm{e}-3$	36	$6.71\mathrm{e}-3$	34	$7.81\mathrm{e}-1$	36	$9.66\mathrm{e}-1$	32	$9.43\mathrm{e}-1$	34.2
WGAN_NO_AS	27	$2.27\mathrm{e}-3$	30	$5.22\mathrm{e}-3$	30	$8.48\mathrm{e}-1$	29	$8.08\mathrm{e}-1$	31	$9.44\mathrm{e}-1$	29.4
WGAN_NO_SA	31	$2.71\mathrm{e}-3$	35	$6.20\mathrm{e}-3$	32	$8.25\mathrm{e}-1$	34	$8.89\mathrm{e}-1$	27	$9.47\mathrm{e}-1$	31.8
WGAN_NO_SS	28	$2.28\mathrm{e}-3$	29	$5.00\mathrm{e}-3$	19	$8.79\mathrm{e}-1$	27	$7.73\mathrm{e}-1$	26	$9.48\mathrm{e}-1$	25.8
WGAN_OS_AA	23	$2.05\mathrm{e}-3$	24	$4.75\mathrm{e}-3$	31	$8.34\mathrm{e}-1$	26	$7.47\mathrm{e}-1$	22	$9.50\mathrm{e}-1$	25.2
WGAN_OS_AS	35	$2.86\mathrm{e}-3$	33	$5.86\mathrm{e}-3$	25	$8.57\mathrm{e}-1$	33	$8.59\mathrm{e}-1$	34	$9.43\mathrm{e}-1$	32.0
WGAN_OS_SA	25	$2.11\mathrm{e}-3$	23	$4.65\mathrm{e}-3$	26	$8.55\mathrm{e}-1$	25	$7.42\mathrm{e}-1$	19	$9.53\mathrm{e}-1$	23.6
WGAN_OS_SS	36	$2.92\mathrm{e}-3$	34	$6.00\mathrm{e}-3$	22	$8.65\mathrm{e}-1$	35	$9.06\mathrm{e}-1$	28	$9.46\mathrm{e}-1$	31.0
WGAN_TS_AA	24	$2.08\mathrm{e}-3$	28	$4.98\mathrm{e}-3$	36	$7.47\mathrm{e}-1$	30	$8.09\mathrm{e}-1$	35	$9.41\mathrm{e}-1$	30.6
WGAN_TS_AS	17	$1.83\mathrm{e}-3$	19	$4.14\mathrm{e}-3$	08	$9.06\mathrm{e}-1$	15	$6.22\mathrm{e}-1$	04	$9.62\mathrm{e}-1$	12.6
WGAN_TS_SA	26	$2.21\mathrm{e}-3$	26	$4.95\mathrm{e}-3$	35	$7.66\mathrm{e}-1$	28	$8.02\mathrm{e}-1$	33	$9.43\mathrm{e}-1$	29.6
WGAN_TS_SS	22	$1.99\mathrm{e}-3$	22	$4.30\mathrm{e}-3$	03	$9.14\mathrm{e}-1$	19	$6.47\mathrm{e}-1$	03	$9.63\mathrm{e}-1$	13.8
WGGP_NO_AA	14	$1.64\mathrm{e}-3$	14	$3.51\mathrm{e}-3$	14	$8.96\mathrm{e}-1$	09	$5.49\mathrm{e}-1$	11	$9.58\mathrm{e}-1$	12.4
WGGP_NO_AS	06	$1.54\mathrm{e}-3$	08	$3.35\mathrm{e}-3$	07	$9.08\mathrm{e}-1$	04	$5.36\mathrm{e}-1$	08	$9.60\mathrm{e}-1$	**6.6**
WGGP_NO_SA	12	$1.61\mathrm{e}-3$	12	$3.48\mathrm{e}-3$	11	$8.99\mathrm{e}-1$	10	$5.50\mathrm{e}-1$	09	$9.59\mathrm{e}-1$	10.8
WGGP_NO_SS	05	$1.52\mathrm{e}-3$	06	$3.33\mathrm{e}-3$	05	$9.10\mathrm{e}-1$	05	$5.37\mathrm{e}-1$	06	$9.61\mathrm{e}-1$	**5.4**
WGGP_OS_AA	11	$1.60\mathrm{e}-3$	07	$3.33\mathrm{e}-3$	13	$8.97\mathrm{e}-1$	08	$5.44\mathrm{e}-1$	16	$9.56\mathrm{e}-1$	11.0
WGGP_OS_AS	30	$2.43\mathrm{e}-3$	27	$4.95\mathrm{e}-3$	17	$8.89\mathrm{e}-1$	24	$7.31\mathrm{e}-1$	17	$9.56\mathrm{e}-1$	23.0
WGGP_OS_SA	08	$1.57\mathrm{e}-3$	05	$3.29\mathrm{e}-3$	12	$8.98\mathrm{e}-1$	07	$5.42\mathrm{e}-1$	13	$9.57\mathrm{e}-1$	**9.0**
WGGP_OS_SS	29	$2.40\mathrm{e}-3$	25	$4.91\mathrm{e}-3$	16	$8.90\mathrm{e}-1$	23	$7.31\mathrm{e}-1$	14	$9.56\mathrm{e}-1$	21.4
WGGP_TS_AA	04	$1.45\mathrm{e}-3$	04	$3.03\mathrm{e}-3$	29	$8.48\mathrm{e}-1$	06	$5.39\mathrm{e}-1$	25	$9.48\mathrm{e}-1$	13.6
WGGP_TS_AS	02	$1.39\mathrm{e}-3$	02	$2.90\mathrm{e}-3$	02	$9.31\mathrm{e}-1$	02	$4.61\mathrm{e}-1$	02	$9.66\mathrm{e}-1$	**2.0**
WGGP_TS_SA	03	$1.40\mathrm{e}-3$	03	$2.96\mathrm{e}-3$	28	$8.51\mathrm{e}-1$	03	$5.33\mathrm{e}-1$	21	$9.50\mathrm{e}-1$	11.6
WGGP_TS_SS	01	$1.32\mathrm{e}-3$	01	$2.79\mathrm{e}-3$	01	$9.35\mathrm{e}-1$	01	$4.50\mathrm{e}-1$	01	$9.69\mathrm{e}-1$	**1.0**

Table 17: Results of the Machine Learning efficacy for the LPMC dataset. Lighter grey tone corresponds to better results compared to darker ones.

Name	Continuous		Categorical		rank
SGAN_NO_AA	15	2.81e1	32	5.98	23.5
SGAN_NO_AS	16	2.94e1	19	3.89	17.5
SGAN_NO_SA	29	4.59e1	23	4.55	26.0
SGAN_NO_SS	30	4.74e1	18	3.77	24.0
SGAN_OS_AA	17	3.08e1	25	4.61	21.0
SGAN_OS_AS	20	3.37e1	27	4.73	23.5
SGAN_OS_SA	27	4.16e1	21	4.18	24.0
SGAN_OS_SS	28	4.44e1	24	4.55	26.0
SGAN_TS_AA	13	2.78e1	26	4.67	19.5
SGAN_TS_AS	14	2.80e1	16	3.71	15.0
SGAN_TS_SA	18	3.21e1	17	3.73	17.5
SGAN_TS_SS	19	3.31e1	14	3.48	16.5
WGAN_NO_AA	24	3.93e1	35	1.49e4	29.5
WGAN_NO_AS	26	4.14e1	29	5.00	27.5
WGAN_NO_SA	35	6.60e1	36	1.62e4	35.5
WGAN_NO_SS	36	6.87e1	28	4.94	32.0
WGAN_OS_AA	21	3.55e1	13	3.45	17.0
WGAN_OS_AS	22	3.90e1	30	5.30	26.0
WGAN_OS_SA	31	5.87e1	15	3.49	23.0
WGAN_OS_SS	33	6.15e1	31	5.40	32.0
WGAN_TS_AA	23	3.91e1	33	7.28e3	28.0
WGAN_TS_AS	25	4.05e1	20	4.14	22.5
WGAN_TS_SA	32	6.15e1	34	7.68e3	33.0
WGAN_TS_SS	34	6.34e1	22	4.31	28.0
WGGP_NO_AA	**09**	2.31e1	**10**	3.09	**9.5**
WGGP_NO_AS	**10**	2.32e1	**06**	2.65	**8.0**
WGGP_NO_SA	11	2.57e1	**09**	3.04	**10.0**
WGGP_NO_SS	12	2.60e1	**05**	2.61	**8.5**
WGGP_OS_AA	**01**	1.96e1	**04**	2.56	**2.5**
WGGP_OS_AS	**02**	2.03e1	**07**	2.94	**4.5**
WGGP_OS_SA	**05**	2.09e1	**03**	2.50	**4.0**
WGGP_OS_SS	**06**	2.16e1	**08**	2.94	**7.0**
WGGP_TS_AA	**03**	2.03e1	12	3.19	**7.5**
WGGP_TS_AS	**04**	2.03e1	**02**	2.21	**3.0**
WGGP_TS_SA	**08**	2.21e1	11	3.14	**9.5**
WGGP_TS_SS	**07**	2.20e1	**01**	2.19	**4.0**

5.1.3 LPMC_half case study

Table 18: Results of the statistics on the first aggregation level (all columns) for the LPMC_half dataset. Lighter grey tone corresponds to better results compared to darker ones.

Name	MAE		RMSE		R^2		SRMSE		ρ_{Pearson}		rank
SGAN_NO_AA	22	$1.59e-2$	23	$2.18e-2$	19	$8.15e-1$	21	$1.62e-1$	**10**	$9.63e-1$	19.0

Continues on next page...

Table 18 – continued from previous page

Name	MAE		RMSE		R^2		SRMSE		ρ_{Pearson}		rank
SGAN_NO_AS	**10**	$1.12\mathrm{e}-2$	11	$1.60\mathrm{e}-2$	**05**	$9.04\mathrm{e}-1$	12	$1.38\mathrm{e}-1$	04	$9.71\mathrm{e}-1$	**8.4**
SGAN_NO_SA	19	$1.55\mathrm{e}-2$	21	$2.09\mathrm{e}-2$	17	$8.28\mathrm{e}-1$	17	$1.55\mathrm{e}-1$	05	$9.67\mathrm{e}-1$	15.8
SGAN_NO_SS	**07**	$1.09\mathrm{e}-2$	**08**	$1.53\mathrm{e}-2$	**02**	$9.17\mathrm{e}-1$	**06**	$1.31\mathrm{e}-1$	02	$9.74\mathrm{e}-1$	**5.0**
SGAN_OS_AA	21	$1.57\mathrm{e}-2$	22	$2.12\mathrm{e}-2$	26	$1.56\mathrm{e}-1$	22	$1.72\mathrm{e}-1$	36	$9.20\mathrm{e}-1$	25.4
SGAN_OS_AS	32	$2.56\mathrm{e}-2$	31	$3.23\mathrm{e}-2$	20	$8.08\mathrm{e}-1$	28	$2.10\mathrm{e}-1$	32	$9.37\mathrm{e}-1$	28.6
SGAN_OS_SA	18	$1.48\mathrm{e}-2$	18	$1.97\mathrm{e}-2$	25	$1.94\mathrm{e}-1$	19	$1.57\mathrm{e}-1$	34	$9.27\mathrm{e}-1$	22.8
SGAN_OS_SS	30	$2.45\mathrm{e}-2$	29	$3.06\mathrm{e}-2$	14	$8.43\mathrm{e}-1$	26	$1.94\mathrm{e}-1$	26	$9.50\mathrm{e}-1$	25.0
SGAN_TS_AA	16	$1.34\mathrm{e}-2$	16	$1.85\mathrm{e}-2$	18	$8.18\mathrm{e}-1$	16	$1.50\mathrm{e}-1$	19	$9.55\mathrm{e}-1$	17.0
SGAN_TS_AS	11	$1.12\mathrm{e}-2$	**10**	$1.58\mathrm{e}-2$	15	$8.39\mathrm{e}-1$	11	$1.38\mathrm{e}-1$	18	$9.55\mathrm{e}-1$	13.0
SGAN_TS_SA	14	$1.26\mathrm{e}-2$	14	$1.70\mathrm{e}-2$	16	$8.37\mathrm{e}-1$	**09**	$1.34\mathrm{e}-1$	16	$9.57\mathrm{e}-1$	13.8
SGAN_TS_SS	**03**	$1.01\mathrm{e}-2$	**03**	$1.41\mathrm{e}-2$	11	$8.67\mathrm{e}-1$	**03**	$1.21\mathrm{e}-1$	11	$9.62\mathrm{e}-1$	**6.2**
WGAN_NO_AA	36	$4.92\mathrm{e}-2$	36	$6.44\mathrm{e}-2$	32	$-3.48\mathrm{e}-1$	36	$4.37\mathrm{e}-1$	35	$9.21\mathrm{e}-1$	35.0
WGAN_NO_AS	24	$2.01\mathrm{e}-2$	30	$3.09\mathrm{e}-2$	22	$6.11\mathrm{e}-1$	34	$2.94\mathrm{e}-1$	33	$9.30\mathrm{e}-1$	28.6
WGAN_NO_SA	35	$4.28\mathrm{e}-2$	35	$5.33\mathrm{e}-2$	29	$-8.45\mathrm{e}-2$	35	$3.26\mathrm{e}-1$	21	$9.52\mathrm{e}-1$	31.0
WGAN_NO_SS	17	$1.37\mathrm{e}-2$	19	$1.99\mathrm{e}-2$	**08**	$8.78\mathrm{e}-1$	25	$1.84\mathrm{e}-1$	12	$9.62\mathrm{e}-1$	16.2
WGAN_OS_AA	31	$2.51\mathrm{e}-2$	33	$3.37\mathrm{e}-2$	28	$2.59\mathrm{e}-2$	32	$2.53\mathrm{e}-1$	30	$9.46\mathrm{e}-1$	30.8
WGAN_OS_AS	34	$2.79\mathrm{e}-2$	34	$3.63\mathrm{e}-2$	21	$7.77\mathrm{e}-1$	33	$2.55\mathrm{e}-1$	31	$9.39\mathrm{e}-1$	30.6
WGAN_OS_SA	27	$2.27\mathrm{e}-2$	27	$2.94\mathrm{e}-2$	27	$1.13\mathrm{e}-1$	29	$2.11\mathrm{e}-1$	13	$9.59\mathrm{e}-1$	24.6
WGAN_OS_SS	33	$2.57\mathrm{e}-2$	32	$3.24\mathrm{e}-2$	13	$8.60\mathrm{e}-1$	30	$2.14\mathrm{e}-1$	22	$9.52\mathrm{e}-1$	26.0
WGAN_TS_AA	26	$2.23\mathrm{e}-2$	26	$2.93\mathrm{e}-2$	36	-1.09	31	$2.23\mathrm{e}-1$	15	$9.57\mathrm{e}-1$	26.8
WGAN_TS_AS	12	$1.13\mathrm{e}-2$	12	$1.65\mathrm{e}-2$	**06**	$8.92\mathrm{e}-1$	14	$1.47\mathrm{e}-1$	**06**	$9.67\mathrm{e}-1$	**10.0**
WGAN_TS_SA	25	$2.14\mathrm{e}-2$	24	$2.73\mathrm{e}-2$	35	-1.04	27	$2.05\mathrm{e}-1$	**07**	$9.66\mathrm{e}-1$	23.6
WGAN_TS_SS	**04**	$1.07\mathrm{e}-2$	**06**	$1.48\mathrm{e}-2$	**01**	$9.26\mathrm{e}-1$	**05**	$1.30\mathrm{e}-1$	**01**	$9.75\mathrm{e}-1$	**3.4**
WGGP_NO_AA	15	$1.29\mathrm{e}-2$	15	$1.74\mathrm{e}-2$	34	$-5.08\mathrm{e}-1$	20	$1.60\mathrm{e}-1$	28	$9.47\mathrm{e}-1$	22.4
WGGP_NO_AS	**09**	$1.12\mathrm{e}-2$	**09**	$1.54\mathrm{e}-2$	**10**	$8.68\mathrm{e}-1$	**08**	$1.33\mathrm{e}-1$	14	$9.57\mathrm{e}-1$	**10.0**
WGGP_NO_SA	13	$1.25\mathrm{e}-2$	13	$1.69\mathrm{e}-2$	33	$-4.74\mathrm{e}-1$	18	$1.55\mathrm{e}-1$	20	$9.54\mathrm{e}-1$	19.4
WGGP_NO_SS	**05**	$1.08\mathrm{e}-2$	**07**	$1.49\mathrm{e}-2$	**07**	$8.86\mathrm{e}-1$	**04**	$1.27\mathrm{e}-1$	**09**	$9.63\mathrm{e}-1$	**6.4**
WGGP_OS_AA	23	$1.63\mathrm{e}-2$	20	$2.04\mathrm{e}-2$	24	$4.53\mathrm{e}-1$	15	$1.49\mathrm{e}-1$	24	$9.50\mathrm{e}-1$	21.2
WGGP_OS_AS	29	$2.45\mathrm{e}-2$	28	$2.97\mathrm{e}-2$	12	$8.65\mathrm{e}-1$	24	$1.82\mathrm{e}-1$	27	$9.48\mathrm{e}-1$	24.0
WGGP_OS_SA	20	$1.57\mathrm{e}-2$	17	$1.96\mathrm{e}-2$	23	$4.59\mathrm{e}-1$	13	$1.42\mathrm{e}-1$	29	$9.47\mathrm{e}-1$	20.4
WGGP_OS_SS	28	$2.39\mathrm{e}-2$	25	$2.89\mathrm{e}-2$	**09**	$8.72\mathrm{e}-1$	23	$1.75\mathrm{e}-1$	23	$9.50\mathrm{e}-1$	21.6
WGGP_TS_AA	**08**	$1.11\mathrm{e}-2$	**05**	$1.44\mathrm{e}-2$	30	$-2.19\mathrm{e}-1$	**10**	$1.35\mathrm{e}-1$	25	$9.50\mathrm{e}-1$	15.6
WGGP_TS_AS	**02**	$9.61\mathrm{e}-3$	**02**	$1.28\mathrm{e}-2$	**04**	$9.09\mathrm{e}-1$	**02**	$1.05\mathrm{e}-1$	**08**	$9.64\mathrm{e}-1$	**3.6**
WGGP_TS_SA	**06**	$1.08\mathrm{e}-2$	**04**	$1.41\mathrm{e}-2$	31	$-2.20\mathrm{e}-1$	**07**	$1.33\mathrm{e}-1$	17	$9.57\mathrm{e}-1$	13.0
WGGP_TS_SS	**01**	$9.32\mathrm{e}-3$	**01**	$1.25\mathrm{e}-2$	**03**	$9.11\mathrm{e}-1$	**01**	$1.03\mathrm{e}-1$	**03**	$9.73\mathrm{e}-1$	**1.8**

Table 19: Results of the statistics on the first aggregation level (continuous columns) for the LPMC_half dataset. Lighter grey tone corresponds to better results compared to darker ones.

Name	MAE		RMSE		R^2		SRMSE		ρ_{Pearson}		rank
SGAN_NO_AA	20	$1.57\mathrm{e}-2$	25	$2.43\mathrm{e}-2$	15	$8.97\mathrm{e}-1$	25	$2.43\mathrm{e}-1$	15	$9.69\mathrm{e}-1$	20.0
SGAN_NO_AS	21	$1.57\mathrm{e}-2$	26	$2.45\mathrm{e}-2$	16	$8.96\mathrm{e}-1$	26	$2.45\mathrm{e}-1$	16	$9.69\mathrm{e}-1$	21.0
SGAN_NO_SA	15	$1.51\mathrm{e}-2$	15	$2.29\mathrm{e}-2$	**09**	$9.31\mathrm{e}-1$	15	$2.29\mathrm{e}-1$	**01**	$9.78\mathrm{e}-1$	11.0
SGAN_NO_SS	16	$1.51\mathrm{e}-2$	16	$2.30\mathrm{e}-2$	**10**	$9.31\mathrm{e}-1$	16	$2.30\mathrm{e}-1$	**02**	$9.78\mathrm{e}-1$	12.0
SGAN_OS_AA	22	$1.58\mathrm{e}-2$	24	$2.43\mathrm{e}-2$	30	$8.30\mathrm{e}-1$	24	$2.43\mathrm{e}-1$	20	$9.66\mathrm{e}-1$	24.0

Table 19 – continued from previous page

Name		MAE		RMSE		R^2		SRMSE		ρ_{Pearson}		rank
SGAN_OS_AS	19	$1.56e-2$	23	$2.41e-2$	29	$8.33e-1$	23	$2.41e-1$	19	$9.67e-1$		22.6
SGAN_OS_SA	12	$1.38e-2$	12	$2.11e-2$	17	$8.95e-1$	12	$2.11e-1$	08	$9.73e-1$		12.2
SGAN_OS_SS	11	$1.37e-2$	11	$2.09e-2$	18	$8.94e-1$	11	$2.09e-1$	09	$9.73e-1$		12.0
SGAN_TS_AA	17	$1.55e-2$	21	$2.40e-2$	31	$8.27e-1$	21	$2.40e-1$	21	$9.65e-1$		22.2
SGAN_TS_AS	18	$1.56e-2$	22	$2.40e-2$	32	$8.26e-1$	22	$2.40e-1$	22	$9.65e-1$		23.2
SGAN_TS_SA	10	$1.37e-2$	10	$2.06e-2$	22	$8.69e-1$	10	$2.06e-1$	14	$9.71e-1$		13.2
SGAN_TS_SS	09	$1.36e-2$	09	$2.05e-2$	21	$8.70e-1$	09	$2.05e-1$	12	$9.72e-1$		12.0
WGAN_NO_AA	36	$3.61e-2$	36	$5.76e-2$	35	$2.86e-1$	36	$5.76e-1$	36	$8.80e-1$		35.8
WGAN_NO_AS	35	$3.60e-2$	35	$5.75e-2$	36	$2.85e-1$	35	$5.75e-1$	35	$8.80e-1$		35.2
WGAN_NO_SA	34	$2.27e-2$	34	$3.47e-2$	28	$8.34e-1$	34	$3.47e-1$	30	$9.47e-1$		32.0
WGAN_NO_SS	33	$2.27e-2$	33	$3.47e-2$	27	$8.35e-1$	33	$3.47e-1$	29	$9.47e-1$		31.0
WGAN_OS_AA	32	$2.17e-2$	31	$3.41e-2$	33	$7.35e-1$	31	$3.41e-1$	32	$9.46e-1$		31.8
WGAN_OS_AS	31	$2.17e-2$	32	$3.41e-2$	34	$7.33e-1$	32	$3.41e-1$	31	$9.46e-1$		32.0
WGAN_OS_SA	27	$1.68e-2$	27	$2.53e-2$	13	$9.16e-1$	27	$2.53e-1$	11	$9.72e-1$		21.0
WGAN_OS_SS	28	$1.69e-2$	28	$2.54e-2$	14	$9.15e-1$	28	$2.54e-1$	13	$9.71e-1$		22.2
WGAN_TS_AA	30	$1.74e-2$	30	$2.71e-2$	26	$8.47e-1$	30	$2.71e-1$	26	$9.54e-1$		28.4
WGAN_TS_AS	29	$1.73e-2$	29	$2.71e-2$	25	$8.49e-1$	29	$2.71e-1$	25	$9.54e-1$		27.4
WGAN_TS_SA	23	$1.58e-2$	17	$2.33e-2$	11	$9.30e-1$	17	$2.33e-1$	05	$9.74e-1$		14.6
WGAN_TS_SS	26	$1.59e-2$	18	$2.35e-2$	12	$9.30e-1$	18	$2.35e-1$	07	$9.73e-1$		16.2
WGGP_NO_AA	25	$1.59e-2$	19	$2.36e-2$	24	$8.53e-1$	19	$2.36e-1$	34	$9.40e-1$		24.2
WGGP_NO_AS	24	$1.59e-2$	20	$2.36e-2$	23	$8.53e-1$	20	$2.36e-1$	33	$9.40e-1$		24.0
WGGP_NO_SA	14	$1.48e-2$	14	$2.23e-2$	20	$8.83e-1$	14	$2.23e-1$	28	$9.51e-1$		18.0
WGGP_NO_SS	13	$1.47e-2$	13	$2.21e-2$	19	$8.84e-1$	13	$2.21e-1$	27	$9.51e-1$		17.0
WGGP_OS_AA	08	$1.30e-2$	08	$1.85e-2$	08	$9.31e-1$	08	$1.85e-1$	24	$9.64e-1$		11.2
WGGP_OS_AS	07	$1.29e-2$	07	$1.83e-2$	07	$9.32e-1$	07	$1.83e-1$	23	$9.64e-1$		10.2
WGGP_OS_SA	06	$1.20e-2$	06	$1.71e-2$	05	$9.37e-1$	06	$1.71e-1$	17	$9.67e-1$		8.0
WGGP_OS_SS	05	$1.20e-2$	03	$1.69e-2$	06	$9.36e-1$	03	$1.69e-1$	18	$9.67e-1$		7.0
WGGP_TS_AA	04	$1.18e-2$	05	$1.71e-2$	04	$9.43e-1$	05	$1.71e-1$	10	$9.73e-1$		5.6
WGGP_TS_AS	03	$1.17e-2$	04	$1.70e-2$	03	$9.45e-1$	04	$1.70e-1$	06	$9.74e-1$		4.0
WGGP_TS_SA	02	$1.13e-2$	02	$1.66e-2$	01	$9.48e-1$	02	$1.66e-1$	03	$9.75e-1$		2.0
WGGP_TS_SS	01	$1.12e-2$	01	$1.65e-2$	02	$9.47e-1$	01	$1.65e-1$	04	$9.75e-1$		1.8

Table 20: Results of the statistics on the first aggregation level (categorical columns) for the LPMC_half dataset. Lighter grey tone corresponds to better results compared to darker ones.

Name		MAE		RMSE		R^2		SRMSE		ρ_{Pearson}		rank
SGAN_NO_AA	22	$1.62e-2$	22	$1.94e-2$	21	$7.40e-1$	16	$8.70e-2$	14	$9.57e-1$		19.0
SGAN_NO_AS	06	$6.97e-3$	07	$8.10e-3$	05	$9.11e-1$	07	$3.93e-2$	07	$9.73e-1$		6.4
SGAN_NO_SA	21	$1.59e-2$	21	$1.91e-2$	22	$7.32e-1$	15	$8.63e-2$	15	$9.56e-1$		18.8
SGAN_NO_SS	08	$7.02e-3$	08	$8.14e-3$	06	$9.04e-1$	08	$3.97e-2$	09	$9.71e-1$		7.8
SGAN_OS_AA	20	$1.57e-2$	20	$1.84e-2$	26	$-4.69e-1$	22	$1.07e-1$	36	$8.77e-1$		24.8
SGAN_OS_AS	32	$3.48e-2$	32	$3.99e-2$	20	$7.86e-1$	32	$1.80e-1$	34	$9.10e-1$		30.0
SGAN_OS_SA	19	$1.57e-2$	19	$1.83e-2$	25	$-4.56e-1$	21	$1.07e-1$	35	$8.84e-1$		23.8
SGAN_OS_SS	31	$3.46e-2$	31	$3.96e-2$	19	$7.96e-1$	30	$1.79e-1$	32	$9.28e-1$		28.6
SGAN_TS_AA	17	$1.13e-2$	17	$1.33e-2$	15	$8.10e-1$	13	$6.68e-2$	23	$9.45e-1$		17.0

Table 20 – continued from previous page

Name		MAE		RMSE		R^2		SRMSE		ρ_{Pearson}	rank
SGAN_TS_AS	**10**	$7.15e-3$	**10**	$8.20e-3$	12	$8.51e-1$	**10**	$4.29e-2$	21	$9.47e-1$	12.6
SGAN_TS_SA	18	$1.17e-2$	18	$1.37e-2$	17	$8.08e-1$	14	$6.77e-2$	24	$9.44e-1$	18.2
SGAN_TS_SS	**07**	$6.97e-3$	**06**	$8.05e-3$	11	$8.63e-1$	**09**	$4.23e-2$	18	$9.54e-1$	10.2
WGAN_NO_AA	36	$6.15e-2$	36	$7.07e-2$	29	$-9.35e{-}1$	36	$3.07e-1$	12	$9.59e-1$	29.8
WGAN_NO_AS	**01**	$5.26e-3$	**02**	$6.17e-3$	**04**	$9.14e-1$	**03**	$3.23e-2$	**03**	$9.76e-1$	**2.6**
WGAN_NO_SA	35	$6.14e-2$	35	$7.05e-2$	30	$-9.37e{-}1$	35	$3.07e-1$	13	$9.58e-1$	29.6
WGAN_NO_SS	**02**	$5.29e-3$	**01**	$6.15e-3$	**03**	$9.19e-1$	**01**	$3.20e-2$	**04**	$9.76e-1$	**2.2**
WGAN_OS_AA	28	$2.82e-2$	28	$3.33e-2$	27	$-6.32e{-}1$	26	$1.72e-1$	22	$9.46e-1$	26.2
WGAN_OS_AS	29	$3.36e-2$	29	$3.84e-2$	13	$8.18e-1$	27	$1.74e-1$	29	$9.32e-1$	25.4
WGAN_OS_SA	27	$2.81e-2$	27	$3.33e-2$	28	$-6.34e{-}1$	25	$1.72e-1$	20	$9.47e-1$	25.4
WGAN_OS_SS	30	$3.39e-2$	30	$3.88e-2$	16	$8.09e-1$	28	$1.76e-1$	27	$9.35e-1$	26.2
WGAN_TS_AA	26	$2.69e-2$	26	$3.13e-2$	36	-2.89	31	$1.79e-1$	**10**	$9.61e-1$	25.8
WGAN_TS_AS	**03**	$5.71e-3$	**03**	$6.60e-3$	**01**	$9.31e-1$	**02**	$3.20e-2$	**01**	$9.79e-1$	**2.0**
WGAN_TS_SA	25	$2.67e-2$	25	$3.10e-2$	35	-2.87	29	$1.78e-1$	11	$9.60e-1$	25.0
WGAN_TS_SS	**04**	$5.79e-3$	**04**	$6.72e-3$	**02**	$9.23e-1$	**04**	$3.23e-2$	**02**	$9.77e-1$	**3.2**
WGGP_NO_AA	13	$1.02e-2$	13	$1.16e-2$	34	-1.77	17	$9.02e-2$	19	$9.53e-1$	19.2
WGGP_NO_AS	**05**	$6.78e-3$	**05**	$7.74e-3$	**08**	$8.82e-1$	**05**	$3.80e-2$	**06**	$9.73e-1$	**5.8**
WGGP_NO_SA	15	$1.04e-2$	14	$1.19e-2$	33	-1.73	18	$9.15e-2$	16	$9.56e-1$	19.2
WGGP_NO_SS	**09**	$7.12e-3$	**09**	$8.14e-3$	**07**	$8.88e-1$	**06**	$3.90e-2$	**05**	$9.75e-1$	**7.2**
WGGP_OS_AA	24	$1.95e-2$	24	$2.23e-2$	24	$9.64e-3$	24	$1.16e-1$	26	$9.37e-1$	24.4
WGGP_OS_AS	34	$3.53e-2$	34	$4.03e-2$	18	$8.03e-1$	34	$1.81e-1$	30	$9.32e-1$	30.0
WGGP_OS_SA	23	$1.92e-2$	23	$2.19e-2$	23	$1.54e-2$	23	$1.15e-1$	33	$9.28e-1$	25.0
WGGP_OS_SS	33	$3.49e-2$	33	$4.00e-2$	14	$8.12e-1$	33	$1.81e-1$	28	$9.34e-1$	28.2
WGGP_TS_AA	16	$1.04e-2$	16	$1.19e-2$	31	-1.30	19	$1.02e-1$	31	$9.29e-1$	22.6
WGGP_TS_AS	12	$7.64e-3$	12	$8.90e-3$	**10**	$8.75e-1$	12	$4.59e-2$	17	$9.55e-1$	12.6
WGGP_TS_SA	14	$1.03e-2$	15	$1.19e-2$	32	-1.31	20	$1.02e-1$	25	$9.40e-1$	21.2
WGGP_TS_SS	11	$7.56e-3$	11	$8.80e-3$	**09**	$8.78e-1$	11	$4.57e-2$	**08**	$9.71e-1$	**10.0**

Table 21: Results of the statistics on the second aggregation level for the LPMC_half dataset. Lighter grey tone corresponds to better results compared to darker ones.

Name		MAE		RMSE		R^2		SRMSE		ρ_{Pearson}	rank
SGAN_NO_AA	21	$6.14e-3$	21	$1.09e-2$	13	$8.69e-1$	17	$4.03e-1$	**09**	$9.58e-1$	16.2
SGAN_NO_AS	**09**	$5.40e-3$	11	$9.56e-3$	**06**	$8.94e-1$	11	$3.72e-1$	**06**	$9.62e-1$	**8.6**
SGAN_NO_SA	19	$5.99e-3$	18	$1.05e-2$	**07**	$8.92e-1$	14	$3.85e-1$	**05**	$9.64e-1$	12.6
SGAN_NO_SS	**08**	$5.33e-3$	**09**	$9.32e-3$	**04**	$9.15e-1$	**05**	$3.59e-1$	**03**	$9.68e-1$	**5.8**
SGAN_OS_AA	22	$6.37e-3$	22	$1.13e-2$	26	$7.08e-1$	24	$4.58e-1$	30	$9.35e-1$	24.8
SGAN_OS_AS	31	$9.39e-3$	30	$1.51e-2$	20	$8.30e-1$	26	$5.14e-1$	25	$9.45e-1$	26.4
SGAN_OS_SA	20	$6.03e-3$	20	$1.05e-2$	24	$7.50e-1$	20	$4.21e-1$	26	$9.42e-1$	22.0
SGAN_OS_SS	30	$9.09e-3$	29	$1.45e-2$	15	$8.62e-1$	25	$4.83e-1$	15	$9.52e-1$	22.8
SGAN_TS_AA	17	$5.82e-3$	19	$1.05e-2$	22	$8.27e-1$	19	$4.18e-1$	20	$9.50e-1$	19.4
SGAN_TS_AS	11	$5.45e-3$	15	$9.75e-3$	18	$8.44e-1$	16	$4.00e-1$	16	$9.52e-1$	15.2
SGAN_TS_SA	12	$5.51e-3$	13	$9.67e-3$	16	$8.54e-1$	13	$3.81e-1$	11	$9.55e-1$	13.0
SGAN_TS_SS	**06**	$5.11e-3$	**07**	$8.94e-3$	12	$8.72e-1$	**07**	$3.63e-1$	**07**	$9.58e-1$	**7.8**
WGAN_NO_AA	36	$1.63e-2$	36	$3.13e-2$	36	$1.27e-1$	36	1.09	36	$8.76e-1$	36.0

Continues on next page...

Table 21 – continued from previous page

Name		MAE		RMSE		R^2		SRMSE		ρ_{Pearson}		rank
WGAN_NO_AS	32	9.52e − 3	34	1.86e − 2	34	5.18e − 1	34	7.77e − 1	35	8.95e − 1		33.8
WGAN_NO_SA	35	1.43e − 2	35	2.52e − 2	33	5.22e − 1	35	8.02e − 1	34	9.20e − 1		34.4
WGAN_NO_SS	23	7.42e − 3	24	1.33e − 2	17	8.51e − 1	29	5.19e − 1	27	9.42e − 1		24.0
WGAN_OS_AA	29	8.92e − 3	32	1.65e − 2	29	6.29e − 1	33	6.13e − 1	32	9.33e − 1		31.0
WGAN_OS_AS	34	1.03e − 2	33	1.70e − 2	23	7.77e − 1	32	5.94e − 1	33	9.31e − 1		31.0
WGAN_OS_SA	26	8.29e − 3	28	1.44e − 2	25	7.41e − 1	28	5.18e − 1	19	9.50e − 1		25.2
WGAN_OS_SS	33	9.82e − 3	31	1.56e − 2	14	8.67e − 1	30	5.26e − 1	21	9.49e − 1		25.8
WGAN_TS_AA	25	7.99e − 3	27	1.42e − 2	35	4.90e − 1	31	5.49e − 1	29	9.37e − 1		29.4
WGAN_TS_AS	15	5.70e − 3	17	1.02e − 2	11	8.80e − 1	15	3.94e − 1	12	9.55e − 1		14.0
WGAN_TS_SA	24	7.92e − 3	26	1.35e − 2	32	5.43e − 1	27	5.17e − 1	23	9.47e − 1		26.4
WGAN_TS_SS	16	5.70e − 3	16	9.88e − 3	**03**	9.20e − 1	12	3.75e − 1	**04**	9.66e − 1		10.2
WGGP_NO_AA	13	5.65e − 3	14	9.71e − 3	31	5.90e − 1	22	4.29e − 1	31	9.35e − 1		22.2
WGGP_NO_AS	**07**	5.12e − 3	**06**	8.93e − 3	**10**	8.82e − 1	**09**	3.63e − 1	17	9.51e − 1		**9.8**
WGGP_NO_SA	**10**	5.42e − 3	**10**	9.39e − 3	30	6.07e − 1	18	4.15e − 1	28	9.41e − 1		19.2
WGGP_NO_SS	**04**	4.87e − 3	**05**	8.54e − 3	**05**	8.98e − 1	**03**	3.45e − 1	**08**	9.58e − 1		**5.0**
WGGP_OS_AA	18	5.86e − 3	12	9.58e − 3	21	8.30e − 1	**06**	3.61e − 1	18	9.51e − 1		15.0
WGGP_OS_AS	28	8.58e − 3	25	1.34e − 2	**09**	8.88e − 1	23	4.37e − 1	13	9.55e − 1		19.6
WGGP_OS_SA	14	5.69e − 3	**08**	9.30e − 3	19	8.34e − 1	**04**	3.52e − 1	14	9.53e − 1		11.8
WGGP_OS_SS	27	8.41e − 3	23	1.31e − 2	**08**	8.91e − 1	21	4.28e − 1	**10**	9.57e − 1		17.8
WGGP_TS_AA	**05**	4.91e − 3	**04**	8.18e − 3	28	6.55e − 1	**10**	3.67e − 1	24	9.46e − 1		14.2
WGGP_TS_AS	**02**	4.31e − 3	**02**	7.24e − 3	**02**	9.29e − 1	**02**	2.82e − 1	**02**	9.69e − 1		**2.0**
WGGP_TS_SA	**03**	4.76e − 3	**03**	8.02e − 3	27	6.55e − 1	**08**	3.63e − 1	22	9.48e − 1		12.6
WGGP_TS_SS	**01**	4.19e − 3	**01**	7.12e − 3	**01**	9.30e − 1	**01**	2.79e − 1	**01**	9.70e − 1		**1.0**

Table 22: Results of the statistics on the third aggregation level for the LPMC_half dataset. Lighter grey tone corresponds to better results compared to darker ones.

Name		MAE		RMSE		R^2		SRMSE		ρ_{Pearson}		rank
SGAN_NO_AA	18	2.16e − 3	20	4.84e − 3	15	8.30e − 1	16	7.36e − 1	11	9.41e − 1		16.0
SGAN_NO_AS	13	2.06e − 3	12	4.46e − 3	11	8.55e − 1	**08**	6.92e − 1	**08**	9.45e − 1		10.4
SGAN_NO_SA	16	2.11e − 3	15	4.57e − 3	**07**	8.66e − 1	**10**	6.94e − 1	**04**	9.50e − 1		10.4
SGAN_NO_SS	11	2.04e − 3	11	4.36e − 3	**04**	8.84e − 1	**06**	6.72e − 1	**03**	9.53e − 1		**7.0**
SGAN_OS_AA	22	2.31e − 3	22	5.22e − 3	29	7.10e − 1	24	8.67e − 1	31	9.14e − 1		25.6
SGAN_OS_AS	31	3.03e − 3	30	6.29e − 3	21	7.93e − 1	28	9.40e − 1	26	9.24e − 1		27.2
SGAN_OS_SA	19	2.18e − 3	19	4.77e − 3	23	7.71e − 1	19	7.91e − 1	24	9.26e − 1		20.8
SGAN_OS_SS	30	2.93e − 3	26	6.00e − 3	16	8.29e − 1	25	9.00e − 1	17	9.33e − 1		22.8
SGAN_TS_AA	20	2.19e − 3	21	4.99e − 3	24	7.70e − 1	22	8.04e − 1	23	9.27e − 1		22.0
SGAN_TS_AS	14	2.09e − 3	16	4.67e − 3	20	7.95e − 1	17	7.75e − 1	19	9.30e − 1		17.2
SGAN_TS_SA	12	2.05e − 3	14	4.53e − 3	18	8.13e − 1	15	7.33e − 1	16	9.36e − 1		15.0
SGAN_TS_SS	**09**	1.96e − 3	**09**	4.28e − 3	14	8.35e − 1	12	7.10e − 1	13	9.40e − 1		11.4
WGAN_NO_AA	36	5.00e − 3	36	1.38e − 2	36	−1.01e−1	36	1.98	36	8.33e − 1		36.0
WGAN_NO_AS	34	3.41e − 3	34	8.55e − 3	35	3.75e − 1	34	1.41	35	8.58e − 1		34.4
WGAN_NO_SA	35	4.42e − 3	35	1.06e − 2	34	5.02e − 1	35	1.42	34	8.85e − 1		34.6
WGAN_NO_SS	28	2.82e − 3	29	6.29e − 3	19	7.97e − 1	30	9.81e − 1	30	9.14e − 1		27.2
WGAN_OS_AA	29	2.89e − 3	33	7.10e − 3	32	6.27e − 1	33	1.08	32	9.10e − 1		31.8
WGAN_OS_AS	33	3.31e − 3	32	6.97e − 3	27	7.36e − 1	32	1.05	33	9.04e − 1		31.4

Continues on next page...

Table 22 – continued from previous page

Name		MAE		RMSE		R^2		SRMSE		ρ_{Pearson}	rank
WGAN_OS_SA	27	$2.76e-3$	27	$6.10e-3$	22	$7.75e-1$	26	$9.10e-1$	18	$9.32e-1$	24.0
WGAN_OS_SS	32	$3.22e-3$	31	$6.58e-3$	17	$8.25e-1$	31	$9.88e-1$	22	$9.27e-1$	26.6
WGAN_TS_AA	24	$2.62e-3$	28	$6.14e-3$	33	$6.18e-1$	29	$9.80e-1$	28	$9.16e-1$	28.4
WGAN_TS_AS	17	$2.13e-3$	18	$4.73e-3$	13	$8.45e-1$	14	$7.29e-1$	14	$9.40e-1$	15.2
WGAN_TS_SA	26	$2.66e-3$	25	$5.78e-3$	31	$6.91e-1$	27	$9.14e-1$	25	$9.25e-1$	26.8
WGAN_TS_SS	21	$2.21e-3$	17	$4.72e-3$	**03**	$8.86e-1$	13	$7.19e-1$	**05**	$9.49e-1$	11.8
WGGP_NO_AA	15	$2.09e-3$	13	$4.51e-3$	30	$7.03e-1$	23	$8.05e-1$	29	$9.16e-1$	22.0
WGGP_NO_AS	**07**	$1.91e-3$	**08**	$4.15e-3$	12	$8.55e-1$	**07**	$6.89e-1$	15	$9.38e-1$	**9.8**
WGGP_NO_SA	**10**	$1.99e-3$	**10**	$4.33e-3$	28	$7.21e-1$	18	$7.80e-1$	27	$9.23e-1$	18.6
WGGP_NO_SS	**04**	$1.81e-3$	**06**	$3.94e-3$	**05**	$8.72e-1$	**05**	$6.56e-1$	**07**	$9.46e-1$	**5.4**
WGGP_OS_AA	**08**	$1.95e-3$	**07**	$4.02e-3$	**10**	$8.62e-1$	**04**	$6.55e-1$	12	$9.40e-1$	**8.2**
WGGP_OS_AS	25	$2.65e-3$	24	$5.38e-3$	**08**	$8.66e-1$	21	$8.03e-1$	**09**	$9.44e-1$	17.4
WGGP_OS_SA	**06**	$1.90e-3$	**05**	$3.93e-3$	**09**	$8.65e-1$	**03**	$6.47e-1$	**10**	$9.42e-1$	**6.6**
WGGP_OS_SS	23	$2.60e-3$	23	$5.27e-3$	**06**	$8.69e-1$	20	$7.92e-1$	**06**	$9.46e-1$	15.6
WGGP_TS_AA	**05**	$1.83e-3$	**04**	$3.84e-3$	26	$7.44e-1$	11	$7.00e-1$	21	$9.28e-1$	13.4
WGGP_TS_AS	**02**	$1.62e-3$	**02**	$3.37e-3$	**02**	$9.09e-1$	**02**	$5.37e-1$	**02**	$9.59e-1$	**2.0**
WGGP_TS_SA	**03**	$1.77e-3$	**03**	$3.76e-3$	25	$7.46e-1$	**09**	$6.94e-1$	20	$9.30e-1$	12.0
WGGP_TS_SS	**01**	$1.57e-3$	**01**	$3.32e-3$	**01**	$9.11e-1$	**01**	$5.34e-1$	**01**	$9.60e-1$	**1.0**

Table 23: Results of the Machine Learning efficacy for the LPMC_half dataset. Lighter grey tone corresponds to better results compared to darker ones.

Name		Continuous		Categorical	rank
SGAN_NO_AA	18	4.04e1	24	5.66	21.0
SGAN_NO_AS	20	4.27e1	12	4.34	16.0
SGAN_NO_SA	29	6.41e1	17	4.94	23.0
SGAN_NO_SS	30	6.55e1	**10**	4.07	20.0
SGAN_OS_AA	11	3.41e1	19	5.10	15.0
SGAN_OS_AS	16	3.78e1	20	5.11	18.0
SGAN_OS_SA	24	4.66e1	21	5.12	22.5
SGAN_OS_SS	26	4.85e1	18	4.96	22.0
SGAN_TS_AA	12	3.60e1	16	4.70	14.0
SGAN_TS_AS	15	3.73e1	11	4.16	13.0
SGAN_TS_SA	22	4.50e1	15	4.64	18.5
SGAN_TS_SS	23	4.57e1	**09**	4.01	16.0
WGAN_NO_AA	27	5.88e1	36	4.79e4	31.5
WGAN_NO_AS	28	6.08e1	22	5.59	25.0
WGAN_NO_SA	35	1.01e2	35	4.74e4	35.0
WGAN_NO_SS	36	1.03e2	23	5.62	29.5
WGAN_OS_AA	21	4.42e1	32	6.48e3	26.5
WGAN_OS_AS	25	4.80e1	26	5.79	25.5
WGAN_OS_SA	33	8.27e1	31	6.40e3	32.0
WGAN_OS_SS	34	8.64e1	25	5.77	29.5
WGAN_TS_AA	17	3.84e1	33	1.93e4	25.0
WGAN_TS_AS	19	4.13e1	13	4.59	16.0
WGAN_TS_SA	31	6.74e1	34	1.95e4	32.5

Table 23 – continued from previous page

Name	Continuous		Categorical		rank
WGAN_TS_SS	32	6.76e1	14	4.59	23.0
WGGP_NO_AA	**09**	3.39e1	30	5.60e3	19.5
WGGP_NO_AS	**10**	3.39e1	**04**	2.60	**7.0**
WGGP_NO_SA	13	3.61e1	29	3.20e3	21.0
WGGP_NO_SS	14	3.63e1	**03**	2.57	**8.5**
WGGP_OS_AA	**01**	2.36e1	**06**	2.70	**3.5**
WGGP_OS_AS	**02**	2.43e1	**08**	3.10	**5.0**
WGGP_OS_SA	**03**	2.52e1	**05**	2.68	**4.0**
WGGP_OS_SS	**04**	2.59e1	**07**	3.10	**5.5**
WGGP_TS_AA	**05**	2.59e1	27	1.36e3	16.0
WGGP_TS_AS	**06**	2.62e1	**02**	2.54	**4.0**
WGGP_TS_SA	**07**	2.88e1	28	3.04e3	17.5
WGGP_TS_SS	**08**	2.90e1	**01**	2.54	**4.5**

5.2 Comparison with state-of-the-art models

5.2.1 CMAP case study

Table 24: Results of the statistical assessments between the best DATGAN version and the state-of-the-art models for the CMAP dataset. Lighter grey tone corresponds to better results compared to darker ones.

Name	MAE		RMSE		R^2		SRMSE		ρ_{Pearson}		rank
First aggregation level - all columns											
CTABGAN	03	$2.55\mathrm{e}{-2}$	03	$3.18\mathrm{e}{-2}$	03	$8.17\mathrm{e}{-1}$	03	$1.97\mathrm{e}{-1}$	04	$9.30\mathrm{e}{-1}$	3.2
CTGAN	05	$3.59\mathrm{e}{-2}$	05	$4.31\mathrm{e}{-2}$	04	$6.37\mathrm{e}{-1}$	04	$2.59\mathrm{e}{-1}$	05	$8.54\mathrm{e}{-1}$	4.6
DATGAN (WGAN)	01	$6.33\mathrm{e}{-3}$	01	$7.76\mathrm{e}{-3}$	01	$9.88\mathrm{e}{-1}$	01	$5.32\mathrm{e}{-2}$	01	$9.96\mathrm{e}{-1}$	1.0
TGAN	02	$1.16\mathrm{e}{-2}$	02	$1.50\mathrm{e}{-2}$	02	$9.49\mathrm{e}{-1}$	02	$1.14\mathrm{e}{-1}$	02	$9.81\mathrm{e}{-1}$	2.0
TVAE	04	$3.33\mathrm{e}{-2}$	04	$4.21\mathrm{e}{-2}$	05	$5.59\mathrm{e}{-1}$	05	$2.72\mathrm{e}{-1}$	03	$9.37\mathrm{e}{-1}$	4.2
First aggregation level - continuous columns											
CTABGAN	02	$1.23\mathrm{e}{-2}$	02	$1.71\mathrm{e}{-2}$	02	$9.37\mathrm{e}{-1}$	02	$1.71\mathrm{e}{-1}$	03	$9.73\mathrm{e}{-1}$	2.2
CTGAN	04	$2.10\mathrm{e}{-2}$	04	$2.87\mathrm{e}{-2}$	04	$8.27\mathrm{e}{-1}$	04	$2.87\mathrm{e}{-1}$	04	$9.24\mathrm{e}{-1}$	4.0
DATGAN (WGAN)	01	$7.98\mathrm{e}{-3}$	01	$1.05\mathrm{e}{-2}$	01	$9.70\mathrm{e}{-1}$	01	$1.05\mathrm{e}{-1}$	01	$9.86\mathrm{e}{-1}$	1.0
TGAN	05	$2.21\mathrm{e}{-2}$	05	$3.07\mathrm{e}{-2}$	05	$7.98\mathrm{e}{-1}$	05	$3.07\mathrm{e}{-1}$	05	$9.18\mathrm{e}{-1}$	5.0
TVAE	03	$1.32\mathrm{e}{-2}$	03	$1.72\mathrm{e}{-2}$	03	$9.32\mathrm{e}{-1}$	03	$1.72\mathrm{e}{-1}$	02	$9.80\mathrm{e}{-1}$	2.8
First aggregation level - categorical columns											
CTABGAN	03	$2.88\mathrm{e}{-2}$	03	$3.54\mathrm{e}{-2}$	03	$7.87\mathrm{e}{-1}$	03	$2.03\mathrm{e}{-1}$	04	$9.19\mathrm{e}{-1}$	3.2
CTGAN	05	$3.97\mathrm{e}{-2}$	04	$4.67\mathrm{e}{-2}$	04	$5.90\mathrm{e}{-1}$	04	$2.52\mathrm{e}{-1}$	05	$8.36\mathrm{e}{-1}$	4.4
DATGAN (WGAN)	01	$5.92\mathrm{e}{-3}$	01	$7.06\mathrm{e}{-3}$	01	$9.92\mathrm{e}{-1}$	01	$4.01\mathrm{e}{-2}$	01	$9.98\mathrm{e}{-1}$	1.0
TGAN	02	$9.01\mathrm{e}{-3}$	02	$1.10\mathrm{e}{-2}$	02	$9.87\mathrm{e}{-1}$	02	$6.63\mathrm{e}{-2}$	02	$9.96\mathrm{e}{-1}$	2.0
TVAE	04	$3.83\mathrm{e}{-2}$	05	$4.84\mathrm{e}{-2}$	05	$4.66\mathrm{e}{-1}$	05	$2.97\mathrm{e}{-1}$	03	$9.27\mathrm{e}{-1}$	4.4
Second aggregation level											
CTABGAN	03	$8.17\mathrm{e}{-3}$	03	$1.32\mathrm{e}{-2}$	03	$8.61\mathrm{e}{-1}$	03	$4.39\mathrm{e}{-1}$	03	$9.43\mathrm{e}{-1}$	3.0
CTGAN	04	$1.04\mathrm{e}{-2}$	04	$1.68\mathrm{e}{-2}$	04	$7.79\mathrm{e}{-1}$	04	$5.53\mathrm{e}{-1}$	05	$9.03\mathrm{e}{-1}$	4.2
DATGAN (WGAN)	01	$2.83\mathrm{e}{-3}$	01	$4.27\mathrm{e}{-3}$	01	$9.83\mathrm{e}{-1}$	01	$1.56\mathrm{e}{-1}$	01	$9.92\mathrm{e}{-1}$	1.0
TGAN	02	$4.73\mathrm{e}{-3}$	02	$7.66\mathrm{e}{-3}$	02	$9.29\mathrm{e}{-1}$	02	$2.92\mathrm{e}{-1}$	02	$9.71\mathrm{e}{-1}$	2.0
TVAE	05	$1.15\mathrm{e}{-2}$	05	$1.96\mathrm{e}{-2}$	05	$5.92\mathrm{e}{-1}$	05	$6.64\mathrm{e}{-1}$	04	$9.13\mathrm{e}{-1}$	4.8

Table 24 – continued from previous page

Name		MAE		RMSE		R^2		SRMSE		ρ_{Pearson}	rank
Third aggregation level											
CTABGAN	03	2.36e − 3	03	4.74e − 3	03	8.30e − 1	03	7.47e − 1	03	9.26e − 1	3.0
CTGAN	04	2.86e − 3	04	5.81e − 3	04	7.51e − 1	04	9.15e − 1	04	8.85e − 1	4.0
DATGAN (WGAN)	01	1.09e − 3	01	1.92e − 3	01	9.65e − 1	01	3.31e − 1	01	9.83e − 1	1.0
TGAN	02	1.63e − 3	02	3.24e − 3	02	8.93e − 1	02	5.43e − 1	02	9.57e − 1	2.0
TVAE	05	3.47e − 3	05	7.79e − 3	05	4.60e − 1	05	1.18	05	8.80e − 1	5.0

Table 25: Results of the Machine Learning efficacy between the best DATGAN version and the state-of-the-art models for the CMAP dataset. Lighter grey tone corresponds to better results compared to darker ones.

Name		Continuous		Categorical		rank
CTABGAN	03	3.33	02	1.43		2.5
CTGAN	05	3.45	03	1.49		4.0
DATGAN (WGAN)	01	3.05	01	7.56e − 1		1.0
TGAN	02	3.24	04	8.10e1		3.0
TVAE	04	3.36	05	8.04e2		4.5

5.2.2 LPMC case study

Table 26: Results of the statistical assessments between the best DATGAN version and the state-of-the-art models for the LPMC dataset. Lighter grey tone corresponds to better results compared to darker ones.

Name		MAE		RMSE		R^2		SRMSE		ρ_{Pearson}	rank
First aggregation level - all columns											
CTABGAN	04	2.72e − 2	04	3.47e − 2	05	−3.97	04	2.60e − 1	05	8.22e − 1	4.4
CTGAN	03	2.62e − 2	03	3.28e − 2	04	−2.92	03	2.27e − 1	04	8.71e − 1	3.4
DATGAN (WGGP)	01	7.64e − 3	01	1.02e − 2	01	9.63e − 1	01	8.13e − 2	01	9.85e − 1	1.0
TGAN	02	1.19e − 2	02	1.62e − 2	02	5.88e − 1	02	1.48e − 1	02	9.45e − 1	2.0
TVAE	05	2.79e − 2	05	3.71e − 2	03	−2.24	05	2.76e − 1	03	8.96e − 1	4.2
First aggregation level - continuous columns											
CTABGAN	04	1.68e − 2	04	2.60e − 2	02	9.44e − 1	04	2.60e − 1	02	9.80e − 1	3.2
CTGAN	02	1.57e − 2	02	2.35e − 2	03	9.25e − 1	02	2.35e − 1	03	9.70e − 1	2.4
DATGAN (WGGP)	01	8.93e − 3	01	1.31e − 2	01	9.69e − 1	01	1.31e − 1	01	9.86e − 1	1.0
TGAN	03	1.68e − 2	03	2.46e − 2	05	8.72e − 1	03	2.46e − 1	05	9.50e − 1	3.8
TVAE	05	1.72e − 2	05	2.79e − 2	04	8.98e − 1	05	2.79e − 1	04	9.58e − 1	4.6
First aggregation level - categorical columns											
CTABGAN	04	3.68e − 2	04	4.28e − 2	05	−8.54	04	2.59e − 1	05	6.76e − 1	4.4
CTGAN	03	3.60e − 2	03	4.14e − 2	04	−6.48	03	2.18e − 1	04	7.79e − 1	3.4
DATGAN (WGGP)	01	6.44e − 3	01	7.47e − 3	01	9.56e − 1	01	3.52e − 2	01	9.84e − 1	1.0
TGAN	02	7.39e − 3	02	8.45e − 3	02	3.24e − 1	02	5.69e − 2	02	9.40e − 1	2.0
TVAE	05	3.79e − 2	05	4.56e − 2	03	−5.16	05	2.74e − 1	03	8.39e − 1	4.2
Second aggregation level											
CTABGAN	04	8.63e − 3	04	1.50e − 2	05	3.11e − 2	04	6.13e − 1	05	8.93e − 1	4.4
CTGAN	03	8.30e − 3	03	1.42e − 2	03	4.28e − 1	03	5.39e − 1	03	9.07e − 1	3.0
DATGAN (WGGP)	01	3.52e − 3	01	5.91e − 3	01	9.51e − 1	01	2.26e − 1	01	9.78e − 1	1.0

Table 26 – continued from previous page

Name	MAE		RMSE		R^2		SRMSE		ρ_{Pearson}		rank
TGAN	02	4.83e−3	02	8.48e−3	02	8.19e−1	02	3.74e−1	02	9.47e−1	2.0
TVAE	05	9.77e−3	05	1.77e−2	04	1.34e−1	05	6.82e−1	04	8.95e−1	4.6
Third aggregation level											
CTABGAN	04	2.52e−3	04	5.82e−3	04	5.09e−1	04	1.10	04	8.75e−1	4.0
CTGAN	03	2.44e−3	03	5.54e−3	03	7.07e−1	03	9.67e−1	03	8.99e−1	3.0
DATGAN (WGGP)	01	1.32e−3	01	2.79e−3	01	9.35e−1	01	4.50e−1	01	9.69e−1	1.0
TGAN	02	1.71e−3	02	3.76e−3	02	8.30e−1	02	6.89e−1	02	9.34e−1	2.0
TVAE	05	3.15e−3	05	7.54e−3	05	4.07e−1	05	1.21	05	8.70e−1	5.0

Table 27: Results of the Machine Learning efficacy between the best DATGAN version and the state-of-the-art models for the LPMC dataset. Lighter grey tone corresponds to better results compared to darker ones.

Name	Continuous		Categorical		rank
CTABGAN	03	3.49e1	04	5.48	3.5
CTGAN	04	4.33e1	02	2.89	3.0
DATGAN (WGGP)	01	2.20e1	01	2.19	1.0
TGAN	02	2.82e1	03	2.91	2.5
TVAE	05	4.91e1	05	4.88e2	5.0

5.2.3 LPMC_half case study

Table 28: Results of the statistical assessments between the best DATGAN version and the state-of-the-art models for the LPMC_half dataset. Lighter grey tone corresponds to better results compared to darker ones.

Name	MAE		RMSE		R^2		SRMSE		ρ_{Pearson}		rank
First aggregation level - all columns											
CTABGAN	03	2.21e−2	03	2.79e−2	04	−2.46	03	2.06e−1	04	8.54e−1	3.4
CTGAN	04	2.44e−2	04	3.00e−2	03	−1.58	04	2.06e−1	05	8.24e−1	4.0
DATGAN (WGGP)	01	9.32e−3	01	1.25e−2	01	9.11e−1	01	1.03e−1	01	9.73e−1	1.0
TGAN	02	1.40e−2	02	1.88e−2	02	4.04e−1	02	1.65e−1	02	9.39e−1	2.0
TVAE	05	2.97e−2	05	3.83e−2	05	−2.69	05	2.68e−1	03	8.71e−1	4.6
First aggregation level - continuous columns											
CTABGAN	02	1.43e−2	03	2.21e−2	01	9.61e−1	03	2.21e−1	01	9.86e−1	2.0
CTGAN	03	1.51e−2	02	2.19e−2	03	9.15e−1	02	2.19e−1	03	9.66e−1	2.6
DATGAN (WGGP)	01	1.12e−2	01	1.65e−2	02	9.47e−1	01	1.65e−1	02	9.75e−1	1.4
TGAN	05	1.81e−2	05	2.64e−2	05	8.46e−1	05	2.64e−1	05	9.36e−1	5.0
TVAE	04	1.62e−2	04	2.57e−2	04	9.11e−1	04	2.57e−1	04	9.60e−1	4.0
First aggregation level - categorical columns											
CTABGAN	03	2.93e−2	03	3.33e−2	04	−5.63	03	1.92e−1	04	7.31e−1	3.4
CTGAN	04	3.30e−2	04	3.76e−2	03	−3.89	04	1.94e−1	05	6.92e−1	4.0
DATGAN (WGGP)	01	7.56e−3	01	8.80e−3	01	8.78e−1	01	4.57e−2	01	9.71e−1	1.0
TGAN	02	1.03e−2	02	1.19e−2	02	−5.40e−3	02	7.36e−2	02	9.42e−1	2.0
TVAE	05	4.22e−2	05	5.01e−2	05	−6.04	05	2.78e−1	03	7.89e−1	4.6
Second aggregation level											
CTABGAN	03	7.16e−3	03	1.24e−2	04	4.22e−1	03	5.06e−1	03	9.18e−1	3.2

Continues on next page...

Table 28 – continued from previous page

Name		MAE		RMSE		R^2		SRMSE		ρ_{Pearson}	rank
CTGAN	04	$8.05\text{e}-3$	04	$1.36\text{e}-2$	03	$5.59\text{e}-1$	04	$5.08\text{e}-1$	04	$9.09\text{e}-1$	3.8
DATGAN (WGGP)	01	$4.19\text{e}-3$	01	$7.12\text{e}-3$	01	$9.30\text{e}-1$	01	$2.79\text{e}-1$	01	$9.70\text{e}-1$	1.0
TGAN	02	$5.48\text{e}-3$	02	$9.52\text{e}-3$	02	$7.64\text{e}-1$	02	$4.13\text{e}-1$	02	$9.36\text{e}-1$	2.0
TVAE	05	$1.01\text{e}-2$	05	$1.81\text{e}-2$	05	$1.54\text{e}-1$	05	$6.54\text{e}-1$	05	$8.94\text{e}-1$	5.0
Third aggregation level											
CTABGAN	03	$2.21\text{e}-3$	03	$4.98\text{e}-3$	04	$6.85\text{e}-1$	03	$9.24\text{e}-1$	03	$9.04\text{e}-1$	3.2
CTGAN	04	$2.49\text{e}-3$	04	$5.52\text{e}-3$	03	$7.34\text{e}-1$	04	$9.24\text{e}-1$	04	$8.99\text{e}-1$	3.8
DATGAN (WGGP)	01	$1.57\text{e}-3$	01	$3.32\text{e}-3$	01	$9.11\text{e}-1$	01	$5.34\text{e}-1$	01	$9.60\text{e}-1$	1.0
TGAN	02	$1.94\text{e}-3$	02	$4.20\text{e}-3$	02	$7.85\text{e}-1$	02	$7.53\text{e}-1$	02	$9.20\text{e}-1$	2.0
TVAE	05	$3.24\text{e}-3$	05	$7.66\text{e}-3$	05	$4.22\text{e}-1$	05	1.16	05	$8.69\text{e}-1$	5.0

Table 29: Results of the Machine Learning efficacy between the best DATGAN version and the state-of-the-art models for the LPMC_half dataset. Lighter grey tone corresponds to better results compared to darker ones.

Name		Continuous			Categorical		rank
CTABGAN	04		4.25e1	04		4.14	4.0
CTGAN	05		5.13e1	02		3.09	3.5
DATGAN (WGGP)	01		2.90e1	01		2.54	1.0
TGAN	02		3.05e1	03		3.34	2.5
TVAE	03		4.24e1	05		3.93e3	4.0

5.2.4 ADULT case study

Table 30: Results of the statistical assessments between the best DATGAN version and the state-of-the-art models for the ADULT dataset. Lighter grey tone corresponds to better results compared to darker ones.

Name		MAE		RMSE		R^2		SRMSE		ρ_{Pearson}	rank
First aggregation level - all columns											
CTABGAN	06	$2.31\text{e}-2$	06	$3.04\text{e}-2$	06	$8.64\text{e}-1$	06	$2.79\text{e}-1$	06	$9.60\text{e}-1$	6.0
CTGAN	05	$1.98\text{e}-2$	05	$2.56\text{e}-2$	05	$9.40\text{e}-1$	05	$2.45\text{e}-1$	05	$9.79\text{e}-1$	5.0
DATGAN (WGAN)	01	$3.83\text{e}-3$	01	$4.99\text{e}-3$	01	$9.98\text{e}-1$	01	$4.12\text{e}-2$	01	$9.99\text{e}-1$	1.0
DATGAN (WGGP)	03	$1.01\text{e}-2$	03	$1.34\text{e}-2$	03	$9.81\text{e}-1$	03	$1.11\text{e}-1$	03	$9.96\text{e}-1$	3.0
TGAN	02	$5.01\text{e}-3$	02	$6.89\text{e}-3$	02	$9.94\text{e}-1$	02	$7.48\text{e}-2$	02	$9.98\text{e}-1$	2.0
TVAE	04	$1.06\text{e}-2$	04	$1.36\text{e}-2$	04	$9.64\text{e}-1$	04	$1.18\text{e}-1$	04	$9.84\text{e}-1$	4.0
First aggregation level - continuous columns											
CTABGAN	06	$1.56\text{e}-2$	06	$2.45\text{e}-2$	06	$9.26\text{e}-1$	06	$2.31\text{e}-1$	06	$9.77\text{e}-1$	6.0
CTGAN	04	$1.14\text{e}-2$	04	$1.70\text{e}-2$	05	$9.63\text{e}-1$	04	$1.66\text{e}-1$	05	$9.84\text{e}-1$	4.4
DATGAN (WGAN)	01	$5.88\text{e}-3$	01	$8.10\text{e}-3$	01	$9.96\text{e}-1$	01	$7.13\text{e}-2$	01	$9.98\text{e}-1$	1.0
DATGAN (WGGP)	05	$1.29\text{e}-2$	05	$2.03\text{e}-2$	04	$9.66\text{e}-1$	05	$1.85\text{e}-1$	04	$9.92\text{e}-1$	4.6
TGAN	02	$6.73\text{e}-3$	02	$1.00\text{e}-2$	02	$9.88\text{e}-1$	02	$9.62\text{e}-2$	02	$9.95\text{e}-1$	2.0
TVAE	03	$7.61\text{e}-3$	03	$1.09\text{e}-2$	03	$9.87\text{e}-1$	03	$1.04\text{e}-1$	03	$9.94\text{e}-1$	3.0
First aggregation level - categorical columns											
CTABGAN	06	$2.61\text{e}-2$	06	$3.28\text{e}-2$	06	$8.40\text{e}-1$	06	$2.99\text{e}-1$	06	$9.54\text{e}-1$	6.0
CTGAN	05	$2.32\text{e}-2$	05	$2.91\text{e}-2$	05	$9.31\text{e}-1$	05	$2.77\text{e}-1$	05	$9.78\text{e}-1$	5.0
DATGAN (WGAN)	01	$3.01\text{e}-3$	01	$3.74\text{e}-3$	01	$9.99\text{e}-1$	01	$2.91\text{e}-2$	01	1.00	1.0

Continues on next page...

Table 30 – continued from previous page

Name		MAE		RMSE		R^2		SRMSE		ρ_{Pearson}	rank
DATGAN (WGGP)	03	$8.93e-3$	03	$1.07e-2$	03	$9.87e-1$	03	$8.13e-2$	03	$9.98e-1$	3.0
TGAN	02	$4.32e-3$	02	$5.65e-3$	02	$9.97e-1$	02	$6.62e-2$	02	$9.99e-1$	2.0
TVAE	04	$1.18e-2$	04	$1.46e-2$	04	$9.55e-1$	04	$1.24e-1$	04	$9.80e-1$	4.0
Second aggregation level											
CTABGAN	06	$7.18e-3$	06	$1.47e-2$	06	$8.42e-1$	06	$9.00e-1$	06	$9.39e-1$	6.0
CTGAN	05	$5.94e-3$	05	$1.21e-2$	05	$9.25e-1$	05	$7.44e-1$	05	$9.70e-1$	5.0
DATGAN (WGAN)	02	$1.82e-3$	01	$3.23e-3$	01	$9.95e-1$	01	$1.69e-1$	01	$9.98e-1$	1.2
DATGAN (WGGP)	03	$3.22e-3$	03	$6.45e-3$	03	$9.78e-1$	03	$3.45e-1$	03	$9.93e-1$	3.0
TGAN	01	$1.76e-3$	02	$3.54e-3$	02	$9.91e-1$	02	$2.31e-1$	02	$9.96e-1$	1.8
TVAE	04	$3.46e-3$	04	$6.78e-3$	04	$9.60e-1$	04	$3.78e-1$	04	$9.81e-1$	4.0
Third aggregation level											
CTABGAN	06	$2.06e-3$	06	$6.43e-3$	06	$7.82e-1$	06	1.82	06	$9.12e-1$	6.0
CTGAN	05	$1.70e-3$	05	$5.26e-3$	05	$8.96e-1$	05	1.46	05	$9.56e-1$	5.0
DATGAN (WGAN)	02	$6.16e-4$	01	$1.57e-3$	01	$9.90e-1$	01	$4.18e-1$	01	$9.96e-1$	1.2
DATGAN (WGGP)	03	$9.61e-4$	03	$2.79e-3$	03	$9.68e-1$	03	$7.11e-1$	03	$9.89e-1$	3.0
TGAN	01	$5.90e-4$	02	$1.66e-3$	02	$9.87e-1$	02	$4.55e-1$	02	$9.94e-1$	1.8
TVAE	04	$1.09e-3$	04	$3.13e-3$	04	$9.45e-1$	04	$7.70e-1$	04	$9.73e-1$	4.0

Table 31: Results of the Machine Learning efficacy between the best DATGAN version and the state-of-the-art models for the ADULT dataset. Lighter grey tone corresponds to better results compared to darker ones.

Name		Continuous		Categorical		rank
CTABGAN	05	4.73	04	8.56e3		4.5
CTGAN	03	4.32	03	1.04e3		3.0
DATGAN (WGAN)	04	4.41	02	1.91		3.0
DATGAN (WGGP)	06	4.81	01	1.09		3.5
TGAN	01	4.13	06	1.00e4		3.5
TVAE	02	4.31	05	8.64e3		3.5

5.3 Sensitivity anaylsis of the DAG - Structure of the DAG

5.3.1 CMAP case study

Table 32: Results of the statistical assessments with the different DAGs for the CMAP dataset. Lighter grey tone corresponds to better results compared to darker ones.

Name		MAE		RMSE		R^2		SRMSE		ρ_{Pearson}	rank
First aggregation level - all columns											
full	05	$7.31e-3$	05	$9.45e-3$	03	$9.85e-1$	05	$6.49e-2$	03	$9.95e-1$	4.2
trans. red.	03	$6.70e-3$	04	$8.68e-3$	01	$9.88e-1$	03	$6.19e-2$	01	$9.95e-1$	2.4
linear	04	$6.71e-3$	03	$8.48e-3$	02	$9.86e-1$	02	$6.00e-2$	02	$9.95e-1$	2.6
prediction	02	$6.49e-3$	02	$8.01e-3$	05	$9.72e-1$	04	$6.25e-2$	05	$9.88e-1$	3.6
no links	01	$6.11e-3$	01	$7.57e-3$	04	$9.78e-1$	01	$5.90e-2$	04	$9.90e-1$	2.2
First aggregation level - continuous columns											
full	01	$8.75e-3$	01	$1.26e-2$	02	$9.61e-1$	01	$1.26e-1$	03	$9.81e-1$	1.6

Continues on next page...

Table 32 – continued from previous page

Name	MAE		RMSE		R^2		SRMSE		ρ_{Pearson}		rank
trans. red.	**02**	$9.34e-3$	**03**	$1.35e-2$	**01**	$9.63e-1$	**03**	$1.35e-1$	**01**	$9.83e-1$	**2.0**
linear	**03**	$9.61e-3$	**02**	$1.32e-2$	**03**	$9.61e-1$	**02**	$1.32e-1$	**02**	$9.83e-1$	**2.4**
prediction	**05**	$1.56e-2$	**05**	$1.96e-2$	**05**	$8.82e-1$	**05**	$1.96e-1$	**05**	$9.42e-1$	**5.0**
no links	**04**	$1.39e-2$	**04**	$1.77e-2$	**04**	$9.06e-1$	**04**	$1.77e-1$	**04**	$9.54e-1$	**4.0**
First aggregation level - categorical columns											
full	**05**	$6.94e-3$	**05**	$8.65e-3$	**05**	$9.91e-1$	**05**	$4.95e-2$	**04**	$9.98e-1$	**4.8**
trans. red.	**04**	$6.04e-3$	**04**	$7.47e-3$	**02**	$9.94e-1$	**04**	$4.36e-2$	**03**	$9.98e-1$	**3.4**
linear	**03**	$5.99e-3$	**03**	$7.30e-3$	**04**	$9.93e-1$	**03**	$4.20e-2$	**05**	$9.98e-1$	**3.6**
prediction	**02**	$4.20e-3$	**02**	$5.10e-3$	**03**	$9.94e-1$	**01**	$2.91e-2$	**01**	$9.99e-1$	**1.8**
no links	**01**	$4.16e-3$	**01**	$5.03e-3$	**01**	$9.96e-1$	**02**	$2.94e-2$	**02**	$9.99e-1$	**1.4**
Second aggregation level											
full	**03**	$3.22e-3$	**03**	$5.08e-3$	**02**	$9.77e-1$	**03**	$1.85e-1$	**02**	$9.89e-1$	**2.6**
trans. red.	**01**	$3.13e-3$	**01**	$4.93e-3$	**01**	$9.78e-1$	**01**	$1.81e-1$	**01**	$9.90e-1$	**1.0**
linear	**02**	$3.21e-3$	**02**	$4.95e-3$	**03**	$9.76e-1$	**02**	$1.84e-1$	**03**	$9.89e-1$	**2.4**
prediction	**04**	$5.87e-3$	**04**	$9.27e-3$	**05**	$9.14e-1$	**05**	$3.48e-1$	**05**	$9.56e-1$	**4.6**
no links	**05**	$6.03e-3$	**05**	$9.49e-3$	**04**	$9.16e-1$	**04**	$3.48e-1$	**04**	$9.57e-1$	**4.4**
Third aggregation level											
full	**02**	$1.19e-3$	**02**	$2.20e-3$	**02**	$9.57e-1$	**02**	$3.80e-1$	**02**	$9.79e-1$	**2.0**
trans. red.	**01**	$1.19e-3$	**01**	$2.19e-3$	**01**	$9.58e-1$	**01**	$3.76e-1$	**01**	$9.80e-1$	**1.0**
linear	**03**	$1.23e-3$	**03**	$2.24e-3$	**03**	$9.54e-1$	**03**	$3.90e-1$	**03**	$9.78e-1$	**3.0**
prediction	**04**	$2.36e-3$	**04**	$4.55e-3$	**04**	$8.31e-1$	**04**	$7.85e-1$	**04**	$9.11e-1$	**4.0**
no links	**05**	$2.45e-3$	**05**	$4.70e-3$	**05**	$8.31e-1$	**05**	$7.91e-1$	**05**	$9.11e-1$	**5.0**

Table 33: Results of the Machine Learning efficacy with the different DAGs for the CMAP dataset. Lighter grey tone corresponds to better results compared to darker ones.

Name	Continuous		Categorical		rank
full	**01**	3.13	**01**	$8.69e-1$	**1.0**
trans. red.	**02**	3.13	**02**	$9.17e-1$	**2.0**
linear	**03**	3.20	**03**	1.11	**3.0**
prediction	**04**	6.08	**04**	3.62	**4.0**
no links	**05**	6.22	**05**	3.95	**5.0**

5.3.2 LPMC case study

Table 34: Results of the statistical assessments with the different DAGs for the LPMC dataset. Lighter grey tone corresponds to better results compared to darker ones.

Name	MAE		RMSE		R^2		SRMSE		ρ_{Pearson}		rank
First aggregation level - all columns											
full	**02**	$7.74e-3$	**03**	$1.03e-2$	**02**	$9.54e-1$	**03**	$8.29e-2$	**02**	$9.83e-1$	**2.4**
trans. red.	**01**	$7.04e-3$	**01**	$9.50e-3$	**01**	$9.55e-1$	**02**	$7.73e-2$	**01**	$9.83e-1$	**1.2**
linear	**03**	$7.99e-3$	**02**	$1.03e-2$	**03**	$9.20e-1$	**01**	$7.60e-2$	**03**	$9.72e-1$	**2.4**
prediction	**04**	$1.59e-2$	**04**	$2.21e-2$	**05**	$8.71e-1$	**04**	$2.06e-1$	**05**	$9.37e-1$	**4.4**
no links	**05**	$1.60e-2$	**05**	$2.27e-2$	**04**	$8.79e-1$	**05**	$2.12e-1$	**04**	$9.49e-1$	**4.6**

Table 34 – continued from previous page

Name		MAE		RMSE		R^2		SRMSE		ρ_{Pearson}		rank
First aggregation level - continuous columns												
full	03	$9.34e-3$	03	$1.35e-2$	02	$9.55e-1$	03	$1.35e-1$	03	$9.80e-1$	2.8
trans. red.	02	$8.46e-3$	02	$1.26e-2$	03	$9.53e-1$	02	$1.26e-1$	02	$9.81e-1$	2.2
linear	01	$7.92e-3$	01	$1.15e-2$	01	$9.75e-1$	01	$1.15e-1$	01	$9.88e-1$	1.0
prediction	04	$2.79e-2$	04	$4.01e-2$	05	$7.84e-1$	04	$4.01e-1$	05	$8.93e-1$	4.4
no links	05	$2.80e-2$	05	$4.14e-2$	04	$7.92e-1$	05	$4.14e-1$	04	$9.06e-1$	4.6
First aggregation level - categorical columns												
full	04	$6.27e-3$	04	$7.34e-3$	03	$9.53e-1$	04	$3.41e-2$	03	$9.86e-1$	3.6
trans. red.	03	$5.72e-3$	03	$6.61e-3$	02	$9.57e-1$	03	$3.20e-2$	02	$9.86e-1$	2.6
linear	05	$8.05e-3$	05	$9.10e-3$	05	$8.69e-1$	05	$3.94e-2$	05	$9.57e-1$	5.0
prediction	01	$4.70e-3$	02	$5.39e-3$	04	$9.52e-1$	02	$2.57e-2$	04	$9.77e-1$	2.6
no links	02	$4.74e-3$	01	$5.37e-3$	01	$9.59e-1$	01	$2.47e-2$	01	$9.88e-1$	1.2
Second aggregation level												
full	03	$3.53e-3$	03	$5.94e-3$	02	$9.52e-1$	03	$2.28e-1$	02	$9.78e-1$	2.6
trans. red.	02	$3.36e-3$	02	$5.75e-3$	03	$9.51e-1$	02	$2.23e-1$	03	$9.78e-1$	2.4
linear	01	$2.95e-3$	01	$4.90e-3$	01	$9.60e-1$	01	$1.87e-1$	01	$9.83e-1$	1.0
prediction	04	$9.08e-3$	04	$1.58e-2$	04	$8.16e-1$	04	$6.64e-1$	05	$9.06e-1$	4.2
no links	05	$9.18e-3$	05	$1.63e-2$	05	$8.14e-1$	05	$6.74e-1$	04	$9.11e-1$	4.8
Third aggregation level												
full	03	$1.33e-3$	03	$2.78e-3$	02	$9.37e-1$	03	$4.47e-1$	02	$9.70e-1$	2.6
trans. red.	02	$1.29e-3$	02	$2.76e-3$	03	$9.36e-1$	02	$4.43e-1$	03	$9.70e-1$	2.4
linear	01	$1.06e-3$	01	$2.14e-3$	01	$9.55e-1$	01	$3.53e-1$	01	$9.79e-1$	1.0
prediction	04	$3.39e-3$	04	$7.64e-3$	04	$7.39e-1$	05	1.38	05	$8.64e-1$	4.4
no links	05	$3.45e-3$	05	$7.92e-3$	05	$7.29e-1$	04	1.37	04	$8.66e-1$	4.6

Table 35: Results of the Machine Learning efficacy with the different DAGs for the LPMC dataset. Lighter grey tone corresponds to better results compared to darker ones.

Name		Continuous		Categorical		rank
full	01	2.14e1	02	2.06	1.5
trans. red.	02	2.16e1	03	2.09	2.5
linear	03	2.18e1	01	1.96	2.0
prediction	04	4.94e2	04	6.14	4.0
no links	05	5.06e2	05	6.45	5.0

5.3.3 LPMC_half case study

Table 36: Results of the statistical assessments with the different DAGs for the LPMC_half dataset. Lighter grey tone corresponds to better results compared to darker ones.

Name		MAE		RMSE		R^2		SRMSE		ρ_{Pearson}		rank
First aggregation level - all columns												
full	01	$9.29e-3$	01	$1.22e-2$	01	$9.24e-1$	02	$9.85e-2$	02	$9.67e-1$	1.4
trans. red.	03	$1.38e-2$	05	$1.98e-2$	05	$7.75e-1$	03	$1.71e-1$	04	$9.45e-1$	4.0
linear	02	$9.74e-3$	02	$1.26e-2$	02	$8.85e-1$	01	$9.79e-2$	01	$9.72e-1$	1.6

Table 36 – continued from previous page

Name	MAE		RMSE		R^2		SRMSE		ρ_{Pearson}		rank
prediction	05	1.47e−2	04	1.97e−2	04	8.60e−1	05	1.78e−1	05	9.41e−1	4.6
no links	04	1.42e−2	03	1.90e−2	03	8.62e−1	04	1.72e−1	03	9.45e−1	3.4
First aggregation level - continuous columns											
full	02	1.10e−2	02	1.60e−2	02	9.45e−1	02	1.60e−1	02	9.73e−1	2.0
trans. red.	03	1.90e−2	03	2.97e−2	05	7.12e−1	03	2.97e−1	03	9.29e−1	3.4
linear	01	1.06e−2	01	1.53e−2	01	9.47e−1	01	1.53e−1	01	9.79e−1	1.0
prediction	05	2.39e−2	05	3.34e−2	04	7.67e−1	05	3.34e−1	05	8.96e−1	4.8
no links	04	2.34e−2	04	3.25e−2	03	7.69e−1	04	3.25e−1	04	9.02e−1	3.8
First aggregation level - categorical columns											
full	03	7.66e−3	03	8.69e−3	03	9.06e−1	03	4.11e−2	04	9.61e−1	3.2
trans. red.	04	8.91e−3	05	1.06e−2	04	8.34e−1	05	5.43e−2	05	9.61e−1	4.6
linear	05	8.92e−3	04	1.01e−2	05	8.26e−1	04	4.70e−2	03	9.66e−1	4.2
prediction	02	6.07e−3	02	7.00e−3	02	9.45e−1	02	3.20e−2	02	9.83e−1	2.0
no links	01	5.65e−3	01	6.46e−3	01	9.48e−1	01	2.93e−2	01	9.86e−1	1.0
Second aggregation level											
full	02	4.16e−3	02	6.98e−3	01	9.37e−1	02	2.69e−1	02	9.71e−1	1.8
trans. red.	03	5.90e−3	03	1.11e−2	05	7.68e−1	03	4.58e−1	03	9.36e−1	3.4
linear	01	3.88e−3	01	6.51e−3	02	9.29e−1	01	2.54e−1	01	9.73e−1	1.2
prediction	05	8.40e−3	05	1.46e−2	03	8.17e−1	05	6.10e−1	05	9.10e−1	4.6
no links	04	8.38e−3	04	1.45e−2	04	8.17e−1	04	6.03e−1	04	9.12e−1	4.0
Third aggregation level											
full	02	1.52e−3	02	3.21e−3	01	9.22e−1	02	5.19e−1	02	9.63e−1	1.8
trans. red.	03	2.05e−3	03	5.03e−3	05	6.95e−1	03	8.69e−1	03	9.19e−1	3.4
linear	01	1.38e−3	01	2.90e−3	02	9.18e−1	01	4.87e−1	01	9.65e−1	1.2
prediction	04	3.26e−3	05	7.36e−3	03	7.44e−1	05	1.28	05	8.69e−1	4.4
no links	05	3.27e−3	04	7.35e−3	04	7.43e−1	04	1.28	04	8.70e−1	4.2

Table 37: Results of the Machine Learning efficacy with the different DAGs for the LPMC_half dataset. Lighter grey tone corresponds to better results compared to darker ones.

Name	Continuous		Categorical		rank
full	02	2.86e1	02	2.55	2.0
trans. red.	03	3.67e1	03	2.68	3.0
linear	01	2.81e1	01	2.44	1.0
prediction	04	4.90e2	04	6.07	4.0
no links	05	4.99e2	05	6.45	5.0

References

Ba, Jimmy Lei, Kiros, Jamie Ryan, and Hinton, Geoffrey E. Layer Normalization. *arXiv:1607.06450 [cs, stat]*, July 2016. URL http://arxiv.org/abs/1607.06450. arXiv: 1607.06450.

Salimans, Tim, Goodfellow, Ian, Zaremba, Wojciech, Cheung, Vicki, Radford, Alec, and Chen, Xi. Improved Techniques for Training GANs. *arXiv:1606.03498 [cs]*, June 2016. URL http://arxiv.org/abs/1606.03498. arXiv: 1606.03498.